OPTIMIZATION AND LEARNING ALGORITHMS FOR ORTHOGONAL FREQUENCY DIVISION MULTIPLEXING-BASED DYNAMIC SPECTRUM ACCESS

HAMED AHMADI

A THESIS SUBMITTED

FOR THE DEGREE OF DOCTOR OF PHILOSOPHY

DEPARTMENT OF ELECTRICAL AND COMPUTER ENGINEERING

NATIONAL UNIVERSITY OF SINGAPORE

2012

DECLARATION

I hereby declare that this thesis is my original work and it has been written by me in its entirety. I have duly acknowledged all the sources of information which have been used in the thesis. This thesis has also not been submitted for any degree in any university previously.

....

Date HAMED AHMADI

Acknowledgments

I would like to take this opportunity to express my heartfelt gratitude to all those who have contributed in one way or another to the completion of this thesis. Firstly, I gratefully acknowledge the support provided by the Agency of Science, Technology and Research (A*STAR). The completion of this thesis is possible due to the funding provided by the Singapore International Graduate Award (SINGA).

Special thanks to my supervisors, Dr. Yong Huat CHEW and Dr. Chin Choy CHAI, who are both from the Institute for Infocomm Research (I^2R). I am especially indebted to them for their supervision and guidance throughout the candidature, without which, the completion of this thesis would not have been possible. I have benefited tremendously from them in terms of research skill developed and also in choosing research as a future career. I also greatly appreciate the meticulous effort put in by Dr. Chew in going through and refining my writings, as well as the enthusiasm shown during in-depth discussions which sometimes extend beyond office hours. I also wish to thank my thesis advisory committee members, Professor Chua and Professor Kam for their invaluable comments.

I would not have been here today if it were not for the love and support of my family. I want to express my deepest thanks to my parents for their unconditional love, devotion and support. Finally, my most special thanks to my wife, Mahnaz, for her love, support, patience, encouragement through my academic experience, and more importantly, for always being by my side through this journey of my life.

Summary

In this thesis, several algorithms to improve the performance of OFDM-based dynamic spectrum access (DSA) are proposed. In the first part of this thesis, we consider the centralized approach where the spectrum, in term of subcarriers, is assigned to the cognitive radios (CRs) through a central spectrum moderator (CSM). Two situations, with and without reuse of the subcarriers, are separately studied. Without frequency reuse, the objective of the problem is to minimize the total power consumption of the system. The assignment of subcarriers, power and bits is formulated as a mixed integer nonlinear programming (MINLP) problem which is inherently NP-hard. Using the piecewise convex transformations, the MINLP is reformulated to an integer linear programming problem, which enables us to obtain the optimal solution. While the solution to the integer linear programming problem still has high complexity, two novel evolutionary algorithms which efficiently provide desirable suboptimal solutions are proposed next. If frequency reuse is permitted, the subcarrier, power and bit assignment problem becomes more challenging due to the presence of interference introduced by the co-channel CRs. We propose a framework that converts the new NP-hard MINLP into a mixed binary linear programming (MBLP) problem without making any approximations.

In the second part of the thesis, learning algorithms are proposed for the CRs to further improve their decision making capability, and to decentralize the decision making process in DSA. First, an auction-based approach is proposed, where the CRs may either simply bid on the channels that have the best quality at each time, or learn the bidding behavior of their competitors, and then bid on the channels which are predicted to have the highest capacity per unit of cost.

Two nonparametric learning algorithms are proposed which significantly improve the CRs' bidding efficiency and increase their capacity per unit of cost. Finally, we study distributed DSA where the CRs have to sense the subcarriers in order to look for transmission opportunities. We also propose a low complexity HMM-based learning algorithm which is able to order the subcarriers to be sensed according to the predicted probability of being unoccupied. The proposed learning algorithm ensures a much higher chance of obtaining an unoccupied channel at the first attempt, and thus, reduces the sensing overheads.

Table of Contents

List of Figures

List of Tables

Acronyms

ACO	Ant colony optimization
AWGN	Additive white Gaussian noise
BER	Bit-error rate
BS	Base station
BWA	Baum-Welch algorithm
CR	Cognitive radio
CSI	Channel state information
CSM	Central spectrum moderator
DCA	Dynamic channel allocation
DEU	Dynamic exclusive use
DP	Dirichlet process
DSA	Dynamic spectrum access
EA	Evolutionary algorithm
FDMA	Frequency division multiple access
GA	Genetic algorithm
GP	Gaussian process
HMM	Hidden Markov model
HMP	Hidden Markov process
ICI	Inter-cell interference
ISI	Inter-symbol interference
ISM band	Industrial, scientific, and medical band
MAC	Medium access control
MBLP	Mixed binary linear programming

MINLP	Mixed integer nonlinear programming
MS	Mobile station
OFDM	Orthogonal frequency division multiplexing
OFDMA	Orthogonal frequency division multiple access
OSA	Opportunistic spectrum access
PN	Primary network
PSO	Particle swarm optimization
PU	Primary user
QoS	Quality of service
RAN	Radio access network
RF	Radio frequency
RNC	Radio network controller
SIND	Signal to interference-plus-noise difference
SINR	Signal to interference-plus-noise ratio
SNR	Signal to noise ratio
SU	Secondary user
TDMA	Time Division Multiple Access
WRAN	Wireless Regional Area Networks

List of Notations

a, A, α	Scalar constants, variables or sets (all normal font letters).
$\mathbf{a}$, $\boldsymbol{\alpha}$	Vector constants or variables (all bold-faced lowercase letters).
$\mathbf{A}$, $\boldsymbol{\Delta}$	Matrix constants or variables (all bold-faced uppercase letters).
$\mathbb{N}$ and $\mathbb{R}$	Set of all natural and real numbers, respectively.
$\mathcal{N}$ and N	The set of subcarriers and the number of subcarriers, respectively. So, $\mathcal{N} = \{1, \ldots, N\}$ and $\lvert\mathcal{N}\rvert = N$.
$\mathcal{K}$ and K	The set of cognitive radio pairs and the number of cognitive radio pairs, respectively.
$G_{n,k}$	Channel gain from transmitter k to its designated receiver on subcarrier n.
$G^n_{j,k}$	Channel gain from transmitter j to the receiver k on subcarrier n.
$p_{n,k}$	The transmit power of transmitter k on subcarrier n.
$r_{n,k}$	The bit rate of cognitive radio pair k on subcarrier n.

Chapter 1

Introduction

Traditionally, the regulators apply the static exclusive spectrum management approach when assigning spectrum to the service providers. The ability to avoid interference among various co-located wireless systems made this approach remain a dominant spectrum management model for a long period of time. Recently, the tremendous growth in the number of wireless devices and the increase in the demand for wireless services have challenged the traditional way in which radio spectrum resource is managed [2]. The traditional method is unable to reallocate the spectrum in a sufficiently dynamic manner to accommodate new emerging radio systems.

Many of the best usable radio frequency (RF) bands have already been allocated in advance to designated applications in most countries. However, spectrum occupancy measurements performed in the United States [3], Germany [4], China [5], and Singapore [6] indicate that at any given location, the scarce spectrum remains unused most of the time. This means that the traditional static spectrum assignment approach results in an inefficient use of spectrum, and it is actually a cause of the spectrum scarcity. Dynamic spectrum access (DSA) targets to im-

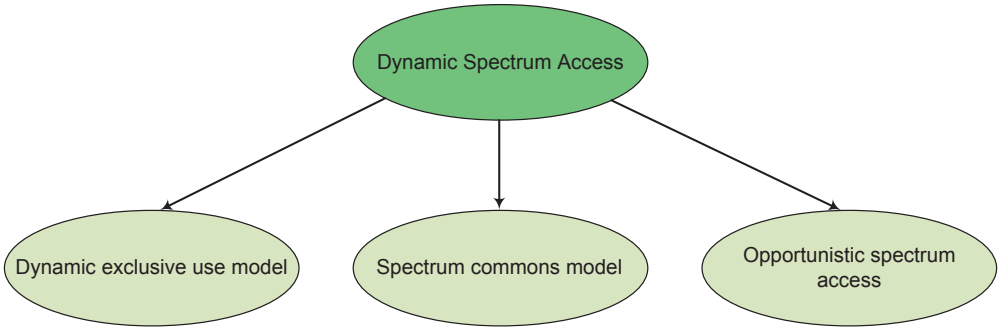

Figure 1.1: Categorization of DSA models

prove the spectrum utilization efficiency by enabling dynamic access of different services to the spectrum. Cognitive radio (CR) technology is the key technology that enables networks to use spectrum in a dynamic manner [7]. In specific, a CR is a radio that can change its transmitter parameters based on the interaction with the environment in which it operates [7]. In other words, DSA is a promising approach to increase the efficiency of the spectrum usage with the development of the CR technologies. For instance, this technology allows unlicensed secondary users (SU) to dynamically access the licensed bands from legacy spectrum holders (primary users (PU)) on a negotiated or an opportunistic basis.

DSA encompasses various approaches to the spectrum reform [8], and not just opportunistic transmission. We can broadly categorize DSA under three main models, namely the dynamic exclusive use model, the spectrum commons model, and the opportunistic spectrum access model. This categorization is shown in Fig.1.1.

1.1 Dynamic spectrum access models

Next, we give a brief introduction on the spectrum access models.

1.1.1 Dynamic exclusive use model

The dynamic exclusive use (DEU) model maintains the basis of the current spectrum regulation policy, where the spectrum bands are licensed to services for exclusive use. However, this model aims to improve spectrum efficiency by making the exclusive spectrum assignment flexible. Two approaches of spectrum property rights and dynamic spectrum allocation are classified under DEU model.

The spectrum property rights approach enables the licensee to sell/lease spectrum and also to freely choose the technology to operate in the licensed spectrum [9]. As a result, the economy and market will play a more important role in driving the system toward profitable use of the limited spectrum resources. However, the spectrum property rights approach has its own technical and legal challenges, e.g. unlike real property, radio spectrum does not allow for clear spatial boundaries, as radio waves propagate in varying ways depending on a variety of circumstances.

The European DRiVE project [10] introduced the dynamic spectrum allocation approach, and aimed to improve spectrum efficiency through dynamic spectrum assignment by exploiting the spatial and temporal traffic statistics of different radio access networks (RAN). In other words, in a given region and at a given time, spectrum is dynamically allocated to RANs for exclusive use. The dynamic spectrum allocation approach assigns the spectrum to RANs in either a contiguous or a fragmented manner. Fig.1.2 illustrates contiguous and fragmented dynamic spectrum allocation, and compares them with the fixed model. The contiguous assignment uses contiguous blocks of spectrum allocated to different RANs, and these are separated by suitable guard bands. However, the width of the spectrum block assigned to a RAN varies in order to allow for changing demands. The fragmented dynamic spectrum allocation treats the given spectrum as a single shared block, and any RAN can be assigned an arbitrary piece of spectrum anywhere

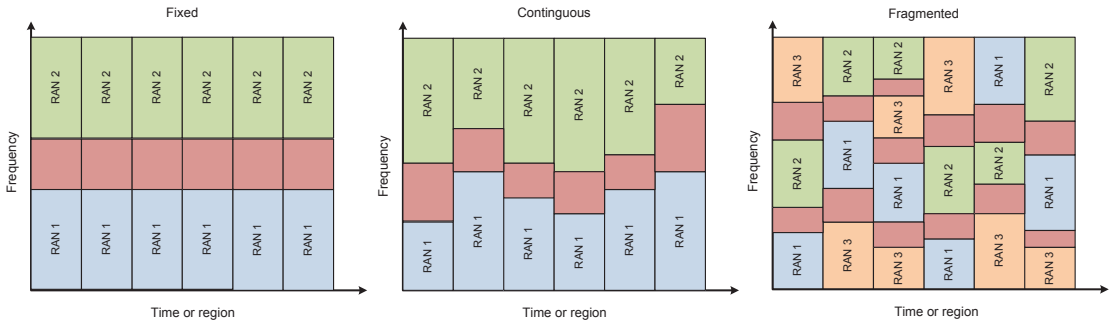

Figure 1.2: Fixed spectrum allocation compared to contiguous and fragmented dynamic spectrum allocation [1].

in this block. In the dynamic spectrum allocation approach, coordination has a key role, and the networks may have distributed and/or centralized coordination [11]. If dynamic spectrum allocation is only applied to one RAN it is called dynamic channel allocation (DCA). The DCA dynamically assigns the available radio resources to the base stations of a RAN [12].

1.1.2 Spectrum commons model

This framework eliminates the exclusive use of frequency spectrum, and radio devices are free to access any portion of the spectrum bands. To some extent we can claim that the idea of a spectrum commons originates from unlicensed industrial, scientific, and medical (ISM) bands, and advocates of this model draw support from the phenomenal success of wireless services operating in the unlicensed ISM radio bands (e.g., WiFi). However, radio systems operating in the spectrum commons model are required to comply with certain technical regulations, such as the transmission power level [13]. The imposed restriction (rule) is to ensure that the amount of interference generated by each radio can be tolerated by the other coexistent radio systems.

The radio systems in a spectrum commons model should also adopt vari-

ous rules, known as etiquettes, for medium access control (MAC) to mitigate interference. For example, the carrier sense multiple access/collision avoidance (CSMA/CA) protocol is implemented in WLAN devices, while Bluetooth devices adopt frequency-hopping, spread-spectrum technology in ISM bands. These etiquettes can greatly improve efficiency if and only if designed appropriately for the applications in the band [14]. However, the quality of service (QoS) is still degraded in the populated areas due to the high inter-system interference. In the spectrum commons model, we would expect next generation spectrum sharing devices to be more intelligent to perform negotiations or to cooperate, in order to obtain a more efficient solution to the resource sharing problem.

The spectrum commons model has been studied from its economic [15] and technical aspects. Centralized [16] and distributed [17] spectrum sharing strategies have been also investigated to address technological challenges under this spectrum management model like power control, efficiency and fairness.

We can also categorize the spectrum underlay approach under this model because the spectrum underlay model imposes severe constraints on the transmission power of the SUs [13]. In the spectrum underlay model, the SUs operate below the noise floor of the PUs. However, by spreading transmitted signals over a wide frequency band, the SUs can potentially achieve short-range high data rate with extremely low transmission power. Some studies [11] classified the spectrum underlay approach together with the opportunistic spectrum access model, creating a group named hierarchical access model, due to the presence of hierarchy among users. In other words, the spectrum underlay approach can be classified into either the spectrum commons model or the hierarchical access model, depending on the classification criterion.

1.1.3 Opportunistic spectrum access model

The opportunistic spectrum access (OSA) model maintains a hierarchy where the PUs have the exclusive access rights to the allocated spectrum within the specified geographical area, and the SUs opportunistically access and utilize the spatially and temporary unused frequency bands known as "white spaces" or "spectrum holes" [18].

The SUs usually sense the spectrum to detect white spaces, and utilize them. In this framework SUs must avoid collision with PUs, or in other words, they should not degrade the PUs' throughput. Therefore, SUs must constantly sense the spectrum and leave the band as soon as the PU returns, which means that the SU should either stop its transmission, or switch to a new detected white space. Fig.1.3 shows an example of an OSA scheme. The SU starts its transmission on channel 2, because initially only channel 2 and 3 are available. Then at T_1 a PU arrives at channel 2 and the SU which has to leave the channel, switches to channel 1, but after a short while, at T_2, a PU becomes active on channel 1. The SU has to stop its transmission at this moment, because there is no white space. At T_3, the SU detects a white space on channel 3, and restarts its transmission. At T_4, a PU arrives to channel 3, and the SU again has to switch.

Under the OSA model, SUs may operate based on a centralized or distributed architecture. In the distributed architecture, SUs operate without having a central controller/coordinator. Some literature used the term *"xG ad hoc access"* for the distributed OSA [7]. Distributed SUs may sense the spectrum to detect the white spaces individually and make the decision based on their own sensing outcomes, or they can perform cooperative sensing [19]. Moreover, a separate fixed sensor network may be provided by a secondary service provider to sense and detect the white spaces for SUs [20, 21]. In the latter case, the SUs may delegate the sensing

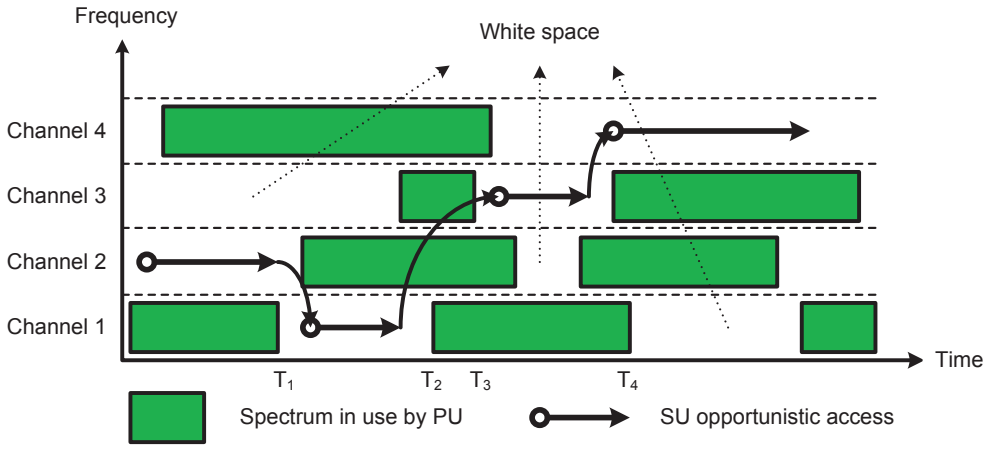

Figure 1.3: OSA model and white space

procedure to the provided sensor network.

The centralized architecture consists of a secondary base station (BS) and the SUs. In this model, if there is no information exchange between the primary and secondary systems, like in distributed OSA, the operation of the primary network (PN) is unaffected by the operation of the secondary system. The SUs must perform the spectrum sensing and detect white spaces. Then they feedback the information to the secondary BS through a common control channel. Medium access control is performed by the secondary BS, which allocates the available white spaces to the requesting SUs. This system model is adopted in the IEEE 802.22 Wireless Regional Area Networks (WRAN) [22]. As mentioned before, the secondary BS may also maintain a sensor network and delegate the sensing to it. PU and SU systems may exchange information for cooperative OSA. In this scenario, the PU assists the SU system to determine secondary spectrum access opportunities in the time and frequency domains. However, cooperative OSA faces some challenges due to the need to modify the PU systems.

1.2 Cognitive radio

In [23], Haykin provides a comprehensive definition of CR, which was first introduced by J. Mitola III [24]:

Cognitive radio is an intelligent wireless communication system that is aware of its surrounding environment (i.e., outside world), and uses the methodology of understanding-by-building to learn from the environment and adapt its internal states to statistical variations in the incoming RF stimuli by making corresponding changes in certain operating parameters (e.g., transmit-power, carrier-frequency, and modulation strategy) in real-time, with two primary objectives in mind: 1) highly reliable communications whenever and wherever needed; 2) efficient utilization of the radio spectrum.

There are some important key words in the definition which highlight the characteristics and desired capabilities of CRs. The key words are intelligence, learning, adaptivity, reliability, and efficiency. Two main characteristics of a CR are (1) cognitive capability and (2) reconfigurability, which are explained as follows.

1.2.1 Cognitive capability

The real time interaction between a CR and its environment is enabled by its cognitive capability. The cognitive capability of a CR determines its transmission parameters and adapts it to the dynamic radio environment. The cognitive cycle [23, 25] in Fig.1.4 shows the main steps of the adaptive behavior of a CR. The cognitive cycle of a CR consists of the following steps:

(1) Spectrum sensing: To detect the presence of white spaces, CRs have to frequently monitor the channels in the spectrum band under consideration.

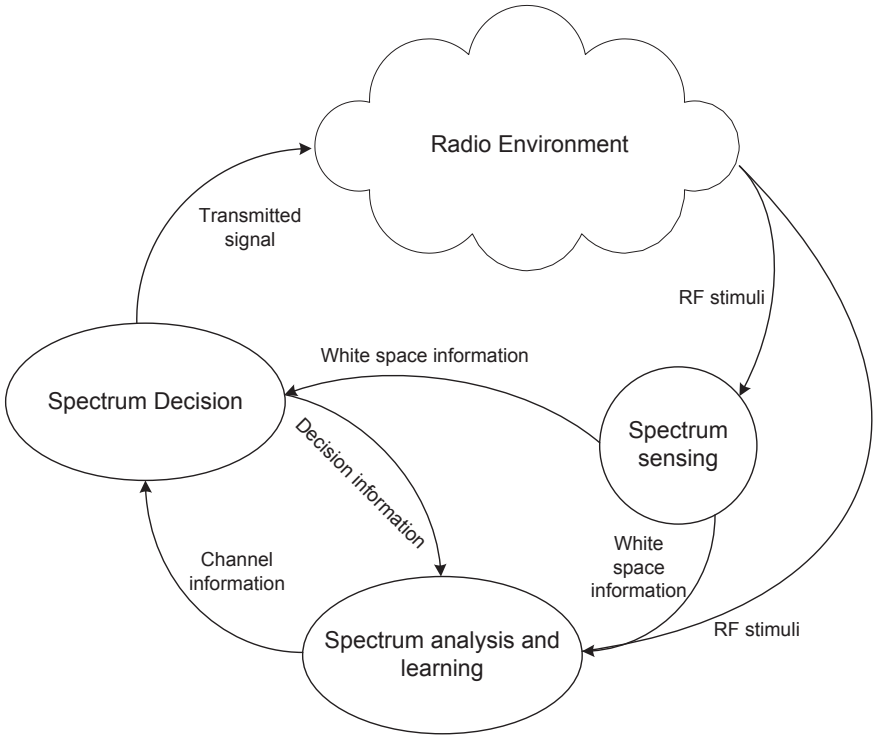

Figure 1.4: Cognitive cycle

Some commonly known sensing techniques include energy detection, matched filter and the cyclostationary feature detection [18].

(2) Spectrum analysis and learning: These are done to extract more information from the sensing results, e.g. the expected time duration that the CR can occupy the band before the PU arrives. Learning techniques enable CRs to gather knowledge about the radio environment from their observations and past decisions, so as to improve their future decisions.

(3) Spectrum decision: The CRs decide the white space that they want to access, the transmission power and other transmission parameters. In order to improve their access quality, the CRs can apply decision making techniques.

1.2.2 Reconfigurability

Reconfigurability enables a CR to adjust its transmission parameters in real time without the need to modify the hardware components. In other words, a CR must be able to adapt to the radio environment by adjusting its transmission parameters, which is achievable through reconfigurability. A CR is reconfigurable if it has the following functionalities [26]:

(1) Frequency agility: It is the capability that enables a CR to change its operating frequency. A CR must be able to adapt its operating frequency to the frequency that is selected based on the channel availability.

(2) Adaptive modulation/coding: A CR must be able to adapt its modulation and coding technique due to the application type and/or network conditions.

(3) Transmit power control: Transmit power constraints may or may not exist in different networks. Thus, a CR must have the transmission power control ability to dynamically configure its transmission power within the permitted limit.

(4) Dynamic network access: It is necessary for a CR to be able to access different networks which run different protocols.

1.3 Orthogonal frequency division multiplexing-based CR

A CR requires a flexible and adaptive physical layer in order to efficiently perform its required tasks. Orthogonal frequency division multiplexing (OFDM) is a widely used technology in the existing communication systems. OFDM has

the potential of fulfilling CR requirements inherently or with minor modifications. In this section we briefly introduce OFDM and then discuss OFDM-based CR.

1.3.1 OFDM

OFDM is a multi-carrier modulation scheme which can achieve high spectral efficiency. In OFDM, a broad bandwidth is divided into tens or hundreds of narrowband subcarriers [27]. As a result, OFDM transforms the whole channel, which is subject to frequency-selective fading, into subcarriers where each of them is subject to flat-fading, so that the transmitted data symbols can be recovered more easily.

In single-carrier systems, the duration of symbols decreases as the data rate increases, and therefore, single-carrier systems are very sensitive to inter-symbol interference (ISI), especially when the data rate is high. ISI occurs when the duration of data symbols is comparable to the channel delay spread. OFDM inherently overcomes this problem by transmitting data symbols over parallel subcarriers whose symbol durations are sufficiently long. In addition, OFDM extends the symbol duration with a cyclic prefix to completely abolish the remaining ISI [28].

Modulation and demodulation of OFDM signals can be easily and efficiently implemented by inverse fast Fourier transform and fast Fourier transform blocks, respectively. Moreover, the receiver of OFDM signals does not need to have a complex equalizer. As a result, with the technological advancement in digital signal processing and emergence of low cost digital signal processing components, OFDM has become a popular technology for wireless communications.

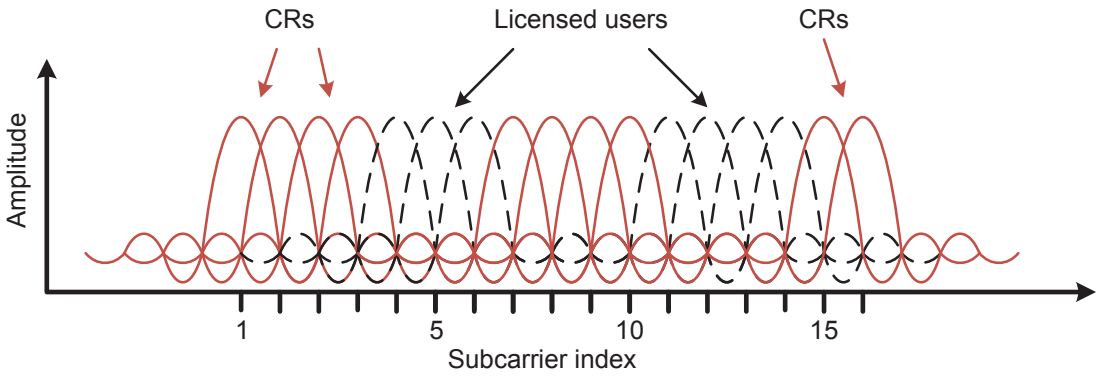

Figure 1.5: Spectrum shaping in OFDM

1.3.2 OFDM-based CR systems

The spectrum shaping capability, flexibility and adaptivity of OFDM make it a promising technology for CR systems. Here, we discuss some of the important OFDM properties which make it a suitable technology for CR systems.

Spectrum shaping capability

After the white spaces are identified, the next step is spectrum shaping. It is desirable for CRs to have a flexible spectrum mask and control over waveform parameters such as signal bandwidth, power level, and center frequency. OFDM systems can provide such flexibility due to the unique nature of OFDM signaling. By disabling a set of subcarriers, the spectrum of OFDM signals can be shaped adaptively to fit into the required spectrum mask. An example of spectrum shaping in OFDM-based CR systems is presented in Fig.1.5.

Adaptivity

An OFDM-based system can adaptively change the modulation order, coding, and transmit power of each individual subcarrier based on the user requirements

or the channel quality [29]. The subcarriers of an OFDM-based system generally experience different channel conditions, as long as their spacing in frequency is larger than the coherence bandwidth. Assuming that such a frequency selective behavior remains constant for some time span, for instance some OFDM symbol periods, we can use the channel state information (CSI) to dynamically assign resources. The water-filling algorithm [30]optimally assigns the resources for (the single user) OFDM-based systems. Practical OFDM systems are only able to transmit the data using a fixed number of modulation types. In these systems, the number of bits to be transmitted on a subcarrier can be defined by choosing the most suitable modulation type, based on the CSI and from the finite set of possible modulation types. This process is called bit loading, and the process of defining the corresponding transmission power is called power loading.

Multiple access

The resources available in a CR system must be shared among the radios. OFDM supports several multiple access techniques. In Frequency Division Multiple Access (FDMA), subcarriers are divided into several groups and each group is assigned to a user. As a result each portion of frequency band is given to a user, and if the allocation of subcarriers to the user is fixed, when the subcarriers are experiencing deep fades the corresponding subcarriers are wasted. An example of OFDM with FDMA is illustrated in Fig.1.6a. In contrast with FDMA, Time Division Multiple Access (TDMA) divides the spectrum in time domain. An example of TDMA-OFDM is shown in Fig.1.6b. With division of time into many intervals called time slots, the whole OFDM symbol consisting of all subcarriers is assigned to one user at a time, and the users take turns to gain access to the channel by transmitting at different OFDM symbols. Similar to FDMA-OFDM, fixed and exclusive allocation of a time slot to a single user in TDMA-OFDM results

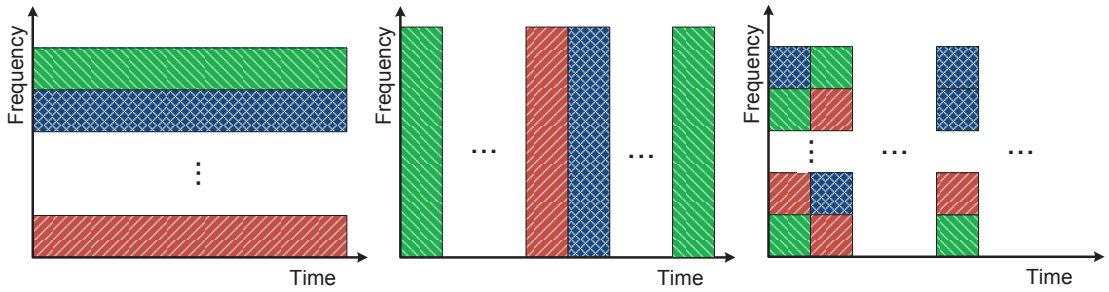

(a) FDMA-OFDM (b) TDMA-OFDM (c) OFDMA

Figure 1.6: Different multiple access techniques in OFDM systems.

in under-utilization of those subcarriers which are in deep fades. To combine the advantages and overcome the shortcomings of FDMA and TDMA, a combinatorial multiple access scheme was invented for OFDM systems known as orthogonal frequency division multiple access (OFDMA). OFDMA partitions both frequency and time dimensions, and assigns slots to users along the OFDM subcarrier index as well as the OFDM symbol index. In OFDMA, by assigning different numbers of subcarriers to different users, various data rates can be supported in view of fulfilling differentiated QoS requirements. Moreover, adaptive and dynamic subcarrier assignment to different users can be implemented more easily in OFDMA. Fig.1.6c shows an example of an OFDMA system.

1.4 Research motivation

In this section, the motivation behind the works in this thesis is presented for (i) optimization algorithms for DSA, and (ii) learning algorithms for DSA.

1.4.1 Optimization algorithms for DSA

In centralized DSA, there is a need for an optimization algorithm to dynamically and efficiently assign the frequency bands to the users. Consider a centralized CR system which can dynamically assign its available spectrum and/or power resources to the radios in the system. This centralized CR system may target at different objectives, such as maximizing its total throughput, minimizing its power consumption, or increasing the fairness, e.g. by maximizing the rate of the CR which has the minimum rate [31, 32, 33, 34]. To achieve any of these objectives, the central spectrum moderator (CSM) of the system should optimally assign the spectrum to the CRs. The CSM may also need to define the transmission power of the CRs to minimize the total power consumption of the system or to control the interference that the co-channel CRs impose on each other. Therefore, the CSM should perform an optimization algorithm which optimizes the objective of the system while satisfying all constraints.

Since realistic OFDM systems are only able to transmit the data using a fixed number of modulation types, it is important to involve the bit loading process in the joint spectrum and power assignment process. However, existing works did not consider the effect of bit loading procedure on the joint spectrum and power assignment process [35, 36]. Considering the bit loading process together with the power and subcarrier assignment makes the problem more complex, and the water-filling algorithm is unable to meet these design criteria [37]. Moreover, the water-filling algorithm does not provide the optimum power and subcarrier assignment for systems with more than one user. Satisfying the minimum required number of bits for the CRs, in a centralized OFDM-based CR system, while minimizing the total power consumption by optimally assigning the subcarriers, power and bits results in a mixed integer nonlinear programming (MINLP) problem, which is inherently

NP-hard. Introducing additional constraints usually makes the optimization problems more complex. Assume that we let the system further improve its spectrum utilization by assigning the same subcarrier to multiple CRs in order to perform data transmission simultaneously. Here, the CSM should also consider the interference that co-channel CRs impose on each other as new constraints in the optimization problem. These additional constraints make the problem even more complex.

In the majority of existing works, the problem is simplified by making some assumptions. These works either do not consider the bit loading process in the spectrum assignment problem, or do not guarantee a minimum bit rate for each CR [34, 38, 39, 40]. Only few works consider both bit loading process and guarantee the minimum required bit rate. However, these works use a sort of exhaustive search and have very high complexity [41]. These research gaps motivated us to overcome such shortcomings.

As a result, we are motivated to improve the spectrum utilization by dynamically assigning the subcarriers, power and bits to the CRs, designing low complexity heuristic algorithms. These low complexity heuristic algorithms should be able to achieve optimal or near optimal solutions. For complex optimization problems, heuristic approaches that can achieve high quality suboptimal solutions in real time are very favorable. In addition, we also need to find methods to solve these dynamic spectrum allocation problems optimally, in order to benchmark the results of the heuristic approaches against them. The goal is for the CSM to be able to minimize the power consumption or maximize the total bit rate of the system by efficiently utilizing its available spectrum and power resources.

1.4.2 Learning algorithms for DSA

In the discussed centralized systems, the computational load on the CSM will be reduced if the CRs also contribute in the decision making process. In other words, to overcome the high computational load on the CSM, we can decentralize these systems. Auction-based systems are good examples of decentralization. In auction-based systems, the CSM usually needs to perform a much simpler optimization algorithm to select the winners of the auctions [42, 43]. However, the CRs in the auction-based systems should be intelligent enough to make efficient decisions. Spectrum auctions become more popular recently [44]. In such distributed systems, the CRs are autonomous, and each CR makes its own spectrum decisions.

Auction-based systems with intelligent bidders are classified under games with incomplete information [45]. The players (bidders) maintain a belief vector which includes their belief about the type and/or strategy of other players. Depending on the game, different learning algorithms are applied [46]. Reinforcement learning [47] and regret minimization algorithms [48] are the popular learning methods in games with incomplete information [49].

Intelligent CRs should learn from their past experiences to improve their future decisions. However, the CRs should know what to learn, what information to learn from and how to learn. The CRs may need to learn the availability of the subcarriers, the channel quality and the number of the CRs in the system. In auction-based DSA, the CRs may also need to learn the bidding behavior of the other CRs. The CRs can achieve the required information by sensing the spectrum or by cooperating with the other CRs. As mentioned, the results of the past actions are also a good feedback which can be used in learning algorithms. In auction-based DSA, the CSM can also broadcast some information for the CRs, e.g. the available subcarriers, or the winning bid for each subcarrier.

After deciding about what the CRs should learn and finding a way for obtaining the required information, we have to propose a proper learning approach. In DSA, the learning is mostly involved in the prediction of future events, given the past information. Therefore, the problem takes the form of learning a time series. Normally, the time series learning algorithms need long training sequences and complex computations [50, 51].

In real time systems, the applied learning algorithm in the auction-based and distributed DSA should not require a long training sequence and complex computations. Thus, designing a proper learning algorithm, which has a high prediction accuracy and a low complexity, for auction-based and distributed DSA is a challenging task.

The CRs which are equipped with the learning algorithms will be able to predict the channel quality and/or the bidding behavior of other CRs in auction-based systems. In distributed DSA, the CRs which are equipped with the learning algorithms can predict the channel availability and quality. Therefore, each CR will be able to utilize the available frequency spectrum more efficiently, which results in higher spectrum efficiency for the system.

The above issues motivated us to propose practical optimization and learning algorithms for OFDM-based DSA to improve the spectrum utilization efficiency.

1.5 Contributions of the thesis

In the first part of the thesis, we study centralized DSA in OFDM-based CR systems, and we propose efficient optimization approaches to maximize the spectrum utilization. Initially, we investigate the problem of transmission power

minimization in a centralized OFDM-based CR system. To minimize the power consumption of the system, unlike existing works which do not consider bit loading, we have to optimally assign the subcarriers to CRs and define the number of bits to be transmitted. This problem is a MINLP problem which is NP-hard. Therefore, we make some assumptions and apply piecewise convex methods to remove the nonlinearity. As a result, we are able to optimally solve the problem. However, due to the presence of integer decision variables, the complexity of the approach is still high, but it provides us a benchmark for heuristic approaches. Then, we propose a novel genetic algorithm (GA) and a modified ant colony optimization (ACO) algorithm which are able to solve the aforementioned resource allocation problem efficiently.

We further generalize the system model and consider a centralized OFDM-based CR system, where the CSM aims to improve the system's total throughput by optimally assigning the subcarriers to CRs and defining their transmit power. In this system, the CSM is able to assign a subcarrier to the CRs which do not impose sever interference on each other. Initially, we formulate this problem as a MINLP problem. Then, we propose a framework which converts the problem into a mixed binary linear programming (MBLP) problem without making any assumptions or approximations. The MBLP is easily solvable with available commercial solver packages. Moreover, in our simulations we compare a CR system which assigns only one CR to each subcarrier with a CR system which assigns each subcarrier to multiple CRs. Here, our contributions provides a method for achieving optimal subcarrier and bit assignment in centralized OFDM-based CR systems with frequency reuse. This provides us a benchmark for comparing the performance of heuristic algorithms like the one proposed in [52, 53].

In the second part of this thesis, we study auction-based and distributed DSA. In this part, we investigate the problem of efficiently bidding by CRs in an auction-

based system. In order to bid efficiently, CRs need to predict the bids of the other CRs. We propose two nonparametric learning algorithms for the problem of learning the bidding behaviors of the other CRs, which enable each CR to predict the bids of the other CRs. We apply the proposed learning algorithms to auction-based systems with and without an entry fee, and evaluate their performance. Simulation results show that the CRs that are equipped with learning algorithms achieve significantly higher capacity per unit of cost, comparing with those CRs which do not have any learning capability. Our contributions highlight the importance of learning algorithms in such auctions, and shows the performance of nonparametric learning algorithms where the number and type of competitors are unknown.

In addition, we study distributed DSA for a CR system where the CRs have to sense the spectrum and find white spaces to transmit their data. The throughput of the CRs will be improved if we reduce the time that they are searching for a white space. In [54], the authors analyze the real spectrum measurement data and by using a simple Q-learning algorithm show that realtime learning of the primary users activities improves the performance of CRs. Therefore, we propose a low complexity HMM-based learning algorithm which computes the probability that a subcarrier is unoccupied. The searching time for a white space will be reduced significantly if the CR senses the channels according to their probability of being unoccupied. Our simulation results show that the probability of detecting a white space at the first attempt for a CR which is using our proposed HMM-based learning algorithm is more than 0.85.

1.6 Organization of the thesis

The thesis is organized as follows: Centralized DSA algorithms are presented in Chapter 2. In Chapter 3, we study centralized DSA algorithms for systems with frequency reuse. Non-parametric learning algorithms for auction-based DSA are introduced in Chapter 4. In Chapter 5, a novel HMM-based learning algorithm for distributed DSA is presented. Lastly, concluding remarks and future works are discussed in Chapter 6.

Chapter 2

Centralized dynamic spectrum access algorithms

In the previous chapter we discussed that in OFDMA networks, multiuser diversity gain can be achieved by allowing each user to exploit the differences in the channel gains of all available subcarriers and select only the appropriate subcarriers for transmission. The aforementioned OFDMA technology also gives a suitable transmission platform to perform DSA for CR systems. Thus, novel adaptive subcarrier, power and bit allocation algorithms, which can obtain optimal or near optimal solutions, are very important to realize DSA in OFDM-based CR systems. The algorithm is actually assigning white spaces to the CRs. In other words, the spectrum allocation algorithm in OFDM-based DSA must consider the availability of subcarriers, because some/all subcarriers may be unavailable due to the presence of the PUs.

In the literature some works proposed subcarrier, power and bit allocation algorithms for OFDMA systems. However, in the context of DSA, there are very limited works. In those efficient resource allocation algorithms which have been

developed for OFDMA systems, the objective function to be optimized falls under two major criteria. In the margin adaptive optimization, the objective is to minimize the total power consumption while satisfying either the system or the individual user minimum bit rate. In the rate adaptive optimization, the objective is to maximize the overall system bit rate under a given power constraint [55].

In [56], an approach has been proposed to compute the optimal margin adaptive solution by converting the MINLP problem into a MBLP problem. Unfortunately, the complexity is still high and the problem is NP-hard. Heuristic solutions are more commonly developed, and their approaches can be classified into two main groups. Algorithms in the first group look for heuristic solutions through programming methods; for example, two heuristic algorithms are proposed in [57] to minimize the total transmit power for a two-class OFDMA system. The first approach is approximating the exponential function when computing the power consumption by a polynomial function to reduce the computation complexity. The second approach takes two steps: at first relaxes the variables to real number solutions and then truncates the results to integers by using minimum square error fitting. In [58], Wong et al. relax the integer constraints and propose a Lagrangian-based algorithm to solve the problem. Liu et al., in [59], propose an optimum method and a low complexity algorithm to allocate subcarriers and power to multiple users. In their work, they maximize the system throughput under a given transmit power constraint with no guarantee on the individuals' minimum bit rate.

The second group applies EAs to obtain an acceptable heuristic solution to the problem. EAs are methods which are inspired by the nature. Evolutionary methods are very popular for resource allocation in telecommunication engineering [60]. Genetic Algorithm (GA) is one of the most popular EAs which has been used in optimizing radio resource usage [61]. In [39], the authors use a GA with a binary chromosome for subcarrier assignment, and apply a discrete water-filling

method for bit allocation. The authors minimize the total power consumption while satisfying a total bit rate constraint; however, the minimum number of bits for each user is not guaranteed. In [38], the total bit rate was maximized under a total transmit power constraint, while a GA is applied for subcarrier and power allocation. In [62], the authors maximized the minimum rate user's bit rate to achieve better fairness within a specific total power constraint. Despite a better fairness, the algorithm does not guarantee any minimum number of transmitted bits for each user.

Spectrum allocation for OFDM-based DSA has been proposed and studied recently. In [63], the authors aim to maximize the minimum achieved downlink rate for each CR under the power constraint of the secondary BS. Two heuristics have been proposed and compared with the optimum solution. In [31], a knapsack heuristic algorithm has been presented; however the problem is formulated for only one SU and with no minimum bit rate guarantee. In, [64] the authors formulate the problem as a reward maximization problem, and propose a novel GA. By assigning a subcarrier to a user, the secondary BS receives a reward, and its aim is to maximize the reward by optimally allocating the subcarriers rather than satisfying the individual data rate demand. An interference table is used to identify those users who impose interference on each other and should not share any subcarrier for transmission.

Here, we consider OFDM-based network which has a group of distributed transmit/receive CR pairs. A CSM dynamically assigns the available subcarriers (white spaces) to the CR pairs at each time slot. To achieve better radio resource utilization, the CSM jointly considers the type of modulation which can be used by each CR pair when deciding the number of available subcarriers (white spaces) to be assigned. Our objective is to minimize the total power consumption of the network while satisfying a minimum required bit rate for every CR pair. For

such an OFDM-based CR system, a critical design challenge is maintaining the orthogonality and handling the timing misalignments among the distributed CR pairs. Here, we assume the ideal situation where the time misalignment has been dealt with, and an example can be found in [65]. Our contributions are as follows. Firstly, a programming method is introduced to solve the problem optimally. Secondly, we present two EAs to optimize the subcarrier (white space) allocation of the DSA system, in the way that the total power consumption is minimized while the minimum required bit rate for each CR pair is satisfied. The ability to solve for multiple CR pairs and to satisfy their minimum demanded bit rate makes our proposed algorithms unique. In the proposed GA, we illustrate how to handle the invalid chromosomes resulting from the crossover and mutation processes so that it can be used to improve the optimality in the solution. We also modify the ant colony optimization (ACO) algorithm so that it is suitable to solve the DSA problem under service rate constraints. Finally, the performance of the two EAs are benchmarked against the optimal solution.

2.1 System model and problem formulation

There are altogether K CR pairs competing for bandwidth to transmit. Here a pair of CRs refers to the transmitter of a link together with its designated receiver. The function of the CSM is to assign frequency bands to all CR pairs for transmission. The CSM is assumed to have full channel state information (CSI) between the transmitters and their designated receivers. All information exchange and control between the CSM and the CRs are through a common control channel. We further assume no spatial reuse is allowed due to interference. The algorithms developed here do not make any pre-requisite on the CRs – the pairs could be all of equal or hierarchical (opportunistic) access rights. For the latter, those frequency

bands which are detected to be occupied by PUs have to be excluded from the algorithm. We assume that PUs' occupancy and all channel gains vary in a larger time scale than the spectrum allocation period. We also assume the applied spectrum sensing technique is reliable, or equivalently, that the CSM gets full knowledge about the subcarrier occupancy by communicating with PUs.

We consider that the available spectrum B is equally divided into N orthogonal subcarriers, such that each subcarrier has a bandwidth of $b = B/N$. In practice, each CR has an OFDM transceiver to select the subcarriers designated for its transmission. Due to different channel gains for different subcarriers between CRs, different ways of allocating subcarriers and bits to the CR pairs affect the total power consumption of the network. Our objective therefore is to allocate subcarriers to all transmitting CRs so that the total power consumption in the network is minimized. To achieve this, the CSM has to jointly consider the modulation level used by each transmitter based on the available CSI, which is similar to the bit loading process in OFDMA, except that some subcarriers may be unavailable due to the presence of PUs.

Although each subcarrier can be used only by one transmitter, a CR pair can occupy more than one subcarrier for transmission. The CSM assigns subcarriers based on a few considerations. Firstly, the minimum demanded bit rate of each connection must be satisfied. For instance, pair k may have an application which needs to transmit with at least R_k bits in one OFDM symbol. The second essential consideration is that the transmission power should be sufficient to achieve the BER requirement. If the network can support multiclass services, then each CR pair may demand a service which has a different BER and a different bit rate.

Transmission can be made using one of three modulation techniques: QPSK, 16QAM and 64QAM. A subcarrier which has been assigned to a radio by CSM

can be left unused. Thus the number of transmitted bits on a subcarrier can only be either 0, 2, 4 or 6. We use $c_{n,k}$ to denote the number of bits transmitted on subcarrier n by CR pair k, where $c_{n,k} \in \{0, 2, 4, 6\}$. The total number of bits transmitted by CR pair k over an OFDM symbol duration is given by:

$$r_k = \sum_{n=1}^{N} \rho_{n,k}.c_{n,k}, \tag{2.1}$$

where ρ is the subcarrier assignment variable defined as

$$\rho_{n,k} = \begin{cases} 0 & c_{n,k} = 0 \\ 1 & \text{otherwise,} \end{cases} \tag{2.2}$$

and to prevent the allocation of a subcarrier to more than one CR pair, it is constrained by

$$\sum_{k=1}^{K} \rho_{n,k} \leq 1 \qquad \forall n \in \{1, .., N\}. \tag{2.3}$$

We introduce the vector $\mathbf{v}$, with dimension equal to the number of subcarriers, to indicate whether the subcarriers have been occupied by PUs. For example, if $N = 10$, and if subcarriers 3,4,10 are occupied by PUs, then $\mathbf{v} = [0, 0, 1, 1, 0, 0, 0, 0, 0, 1]$. This vector is stored and updated at the CSM after the subcarrier occupancy model is known (either by sensing or communicating with PU). The following constraint is used, to ensure that no occupied subcarrier is assigned to CRs.

$$v_n \sum_{k=1}^{K} \rho_{n,k} = 0 \qquad \forall n \in \{1, .., N\}. \tag{2.4}$$

Under the dynamic exclusive use or spectrum commons model, $\mathbf{v} = \mathbf{0}$, which means that all subcarriers are available.

The required received power to achieve BER P_e with a constellation of c

bit/symbol can be approximately computed from [58]:

$$f(c) = \frac{N_0}{3}\left[Q^{-1}(\frac{P_e}{4})\right]^2.(2^c - 1), \tag{2.5}$$

where

$$Q(x) = \frac{1}{\sqrt{2\pi}}\int_x^\infty e^{-t^2/2}dt, \tag{2.6}$$

and $\frac{N_0}{2}$ represents the double-sided power spectrum density of additive white Gaussian noise (AWGN). Given the subcarrier channel gain $G_{n,k}$ and the desired received power, the minimum power to fulfill the QoS requirements at the transmitter of the k^{th} pair on the n^{th} subcarrier is given by

$$P_{n,k} = \frac{f(c_{n,k})}{G_{n,k}}. \tag{2.7}$$

The total power consumed by the access network is given by

$$P_T = \sum_{n=1}^{N}\sum_{k=1}^{K}\frac{f(c_{n,k})\cdot\rho_{n,k}}{G_{n,k}}. \tag{2.8}$$

The DSA problem to minimize the total transmission power is therefore given by

$$\min_{\rho_{n,k},c_{n,k}} \sum_{n=1}^{N}\sum_{k=1}^{K}\frac{f(c_{n,k})\cdot\rho_{n,k}}{G_{n,k}} \tag{2.9}$$

subject to

$$\sum_{k=1}^{K}\rho_{n,k} \leq 1 \qquad \forall n \in \{1,2,...,N\} \tag{2.10}$$

$$v_n \sum_{k=1}^{K} \rho_{n,k} = 0 \qquad \forall n \in \{1,..,N\} \tag{2.11}$$

$$r_k = \sum_{n=1}^{N} \rho_{n,k}.c_{n,k} \geq R_k \qquad \forall k \in \{1,2,...,K\} \tag{2.12}$$

$$\rho_{n,k} \in \{0,1\} \qquad \forall n \in \{1,...,N\}, \forall k \in \{1,...,K\} \tag{2.13}$$

$$c_{n,k} \in \{0,2,4,6\} \qquad \forall n \in \{1,...,N\}, \forall k \in \{1,...,K\}. \tag{2.14}$$

2.2 Optimum subcarrier and bit allocation

The optimization problem which is formulated in Section 2.1 has a nonlinear objective function and nonlinear constraints. The problem is indeed difficult to solve mathematically. Fortunately, under some specific assumptions, it is possible to transform the objective function to a piecewise linear function and the constraints to linear form [66]. Assume that the power spectrum density of AWGN is the same for all receivers, and the BER requirement is the same for all services. As a result of these assumptions, P_e and N_0 in (2.5) become constants, and the remaining nonlinear component is simply $2^{c_{n,k}} - 1$. Since $c_{n,k}$ can only take four values, it is not difficult to show that

$$2^{c_{n,k}} - 1 = \max\{0,\ 2 \times c_{n,k} - 1,\ 6 \times c_{n,k} - 9,\ 24 \times c_{n,k} - 81\}. \quad \forall c_{n,k} \in \{0,2,4,6\} \tag{2.15}$$

Using (2.15), it is possible to express $2^{c_{n,k}} - 1$ as a piecewise linear [67] function of $c_{n,k}$, as will be seen shortly. We also need to linearize the way that ρ takes its value that is given in (2.2). The need to define ρ is to ensure no two CR pairs use the same subcarrier. Since ρ can only take either zero or one, we have to find a linear expression to force it taking only one of the two values. Since the maximum

value which $c_{n,k}$ can take is 6, a possible way is to rewrite (2.2) as

$$c_{n,k} \leq 6 \times \rho_{n,k} \tag{2.16}$$

After making all these transformations and substituting $d_{n,k} = c_{n,k}/2$, the final linearized problem can be written as follows:

$$\min \frac{N_0}{3} \left[Q^{-1} \left(\tfrac{P_e}{4} \right) \right]^2 . \sum_{n=1}^{N} \sum_{k=1}^{K} \frac{F_{n,k}}{G_{n,k}} \tag{2.17}$$

subject to

$$\sum_{n=1}^{N} 2d_{n,k} \geq R_k \qquad \forall k \in \{1, ..., K\} \tag{2.18}$$

$$d_{n,k} - 3\rho_{n,k} \leq 0 \qquad \forall n \in \{1, ..., N\}, \forall k \in \{1, ..., K\} \tag{2.19}$$

$$\sum_{k=1}^{K} \rho_{n,k} \leq 1 \qquad \forall n \in \{1, ..., N\} \tag{2.20}$$

$$v_n \sum_{k=1}^{K} \rho_{n,k} = 0 \qquad \forall n \in \{1, .., N\} \tag{2.21}$$

$$-F_{n,k} \leq 0 \qquad \forall n \in \{1, ..., N\}, \forall k \in \{1, ..., K\} \tag{2.22}$$

$$4d_{n,k} - F_{n,k} \leq 1 \quad \forall n \in \{1, ..., N\}, \forall k \in \{1, ..., K\} \tag{2.23}$$

$$12d_{n,k} - F_{n,k} \leq 9 \quad \forall n \in \{1, ..., N\}, \forall k \in \{1, ..., K\} \tag{2.24}$$

$$48d_{n,k} - F_{n,k} \leq 81 \quad \forall n \in \{1, ..., N\}, \forall k \in \{1, ..., K\} \tag{2.25}$$

$$\rho_{n,k} \in \{0, 1\} \qquad \forall n \in \{1, ..., N\}, \forall k \in \{1, ..., K\} \tag{2.26}$$

$$d_{n,k} \in \{0, 1, 2, 3\} \qquad \forall n \in \{1, ..., N\}, \forall k \in \{1, ..., K\} \tag{2.27}$$

where $F_{n,k}$ $(\forall n, k)$ introduced in (2.22) to (2.25) are the auxiliary variables used to define the linear form of $2^{c_{n,k}} - 1$, with their values exactly matched at $c_{n,k} \in$

$\{0, 2, 4, 6\}$ (or $d_{n,k} \in \{0, 1, 2, 3\}$). Now this integer linear programming problem can be solved by commercial software packages like TOMLAB/MIPsolve [68].

2.3 Genetic algorithm (GA)

Although we are able to compute the optimal solution through linearizing the objective function and constraints, the computational complexity increases significantly with the increase in the numbers of subcarriers or CR pairs due to the tremendous growth in the number of unknowns. Moreover, the original problem, which has different BER requirements for different CR pairs, is an NP hard problem that could not be linearized and solved optimally. Since the problem is NP hard, looking for heuristic algorithms to solve the problem becomes necessary.

The feasible search space for the problem is usually very large. We therefore prefer to have a method which can obtain the solution without searching through the entire feasible solution space. Moreover, the developed algorithm should avoid being trapped at local optimums. In general, GAs use their powerful tools of crossover, mutation, and selection to improve the initial solution [69]. A possible assignment is first coded into a chromosome (also known as individual) and the optimality of the solution is evaluated using a fitness function. Crossover combines fragments of two chromosomes, and creates two new chromosomes which are other solutions in the feasible area. Mutation changes a gene randomly with the hope of reaching better solutions, and it is the tool used to overcome the local optimums. Finally, fitter solutions are selected for the next generation [70].

Subcarrier 1		Subcarrier 2		...	Subcarrier N	
CR pair *i*	q_1	CR pair *j*	q_2	...	CR pair *k*	q_N
0010	01	0110	00	...	1011	11

Figure 2.1: Chromosome structure

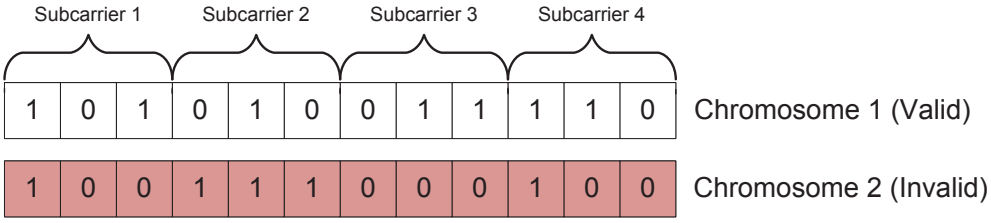

Figure 2.2: Example of valid and invalid chromosomes

2.3.1 Defining the chromosome

In our approach, CR identity and modulation type are both coded into a binary chromosome. Each chromosome has N blocks, and each block represents one of the subcarriers. Each block consists of two parts; the first part uses $\lceil \log_2 K \rceil$ bits to identify the CR pair which is assigned to the subcarrier, and the second part uses two bits to represent the modulation used, as shown in Fig.2.1. For instance "01" stands for QPSK, "10" presents 16QAM, "11" indicates 64QAM and finally "00" shows no bit is transmitted on the subcarrier for the specified CR pair. In our approach, the designed GA must satisfy the constraint (2.12). Unfortunately, this complicates the regeneration process, since it is likely that generated chromosomes do not satisfy the CR's (or CRs') rate constraint. The challenge therefore is how the algorithm should handle this situation.

Fig.2.2 presents an example of two chromosomes designed for a simple system with four subcarriers and two CR pairs. There are four blocks that each represents a subcarrier and each block consists of 3 bits. For a given block, the first bit is used to represent the CR index, and the next two bits are used to represent the modulation used in the subcarrier. Supposing in this example, CR one and

two need 4 and 6 bits per OFDM symbol, respectively. The first chromosome indicates that CR 1 transmits using 16QAM and 64QAM on subcarriers 2 and 3, respectively, and CR 2 transmits using QPSK and 16QAM on subcarriers 1 and 4, respectively. The second chromosome indicates that CR 1 is assigned to subcarrier 3 but is not transmitting, and CR 2 is assigned to subcarriers 1, 2 and 4 but only transmits using 64QAM on subcarrier 2. The first chromosome is a *valid* chromosome because it satisfies the rate constraint given in (2.12), whilst the second chromosome is an *invalid* chromosome since CR 1 could not satisfy (2.12).

Although a straightforward way is to reject the invalid chromosomes generated by the crossover and mutation processes, we let both valid and invalid chromosomes go to the next generation. In this way, the diversity for constructing new chromosomes will not be restricted. However, a penalty will be given to any invalid chromosome. This idea is taken from the invisible walls in particle swarm optimization (PSO) [71], but here the fitness of those chromosomes which exceed the boundaries is calculated with a penalty – in this way they are forced to return to the feasible boundaries. In our algorithm, the fitness of a chromosome is given by the negative of the total consumed power given in (2.8). Valid and invalid chromosomes are classified into two separate lists in the population, and the best result is chosen from the valid list. This approach applies the elitism technique [72] to ensure faster convergence, where elites are chosen only from the valid list.

2.3.2 Proposed GA

Initialization

An initial population of valid chromosomes is generated. As the algorithm proceeds, the number of chromosomes in the population remains unchanged, even

though invalid chromosomes may sometimes appear. The length of each chromosome is given by $N \times (\lceil \log_2 K \rceil + \log_2 Q)$, where $\lceil \log_2 K \rceil$ is the number of bits required to uniquely distinguish the CRs and $\log_2 Q$ is the number of bits required to represent the possible modulation levels. Various modulation levels have different binary representations.

Evaluation and parent selection

The fitness of each individual is evaluated by the negative of (2.8). Furthermore, chromosomes which satisfy (2.12) receive full fitness, whilst invalid chromosomes receive a fitness-related penalty. After this, all chromosomes take part in a binary tournament to be selected as parents of the next generation. For the binary tournament, two random chromosomes are selected, and their fitness is compared. The one with the higher fitness is copied to the mating pool. The tournament continues until the mating pool has filled up. The size of the mating pool is the same as the population size. Some chromosomes, especially those with better fitness, may appear multiple times in the mating pool.

Crossover and mutation

Selected chromosomes in the mating pool are taking part in crossover and mutation processes to form the chromosomes of the next generation. A two-point crossover between two selected chromosomes is used in the algorithm to construct two new chromosomes (child chromosomes), as shown in Fig.2.3. In a two-point crossover process, initially two crossover points (fraction points) are randomly selected in the parent chromosomes (both parents have same fraction points). The first child is a duplication of the first parent except for its genes between the fraction points. These genes are copied from the respective genes of the second

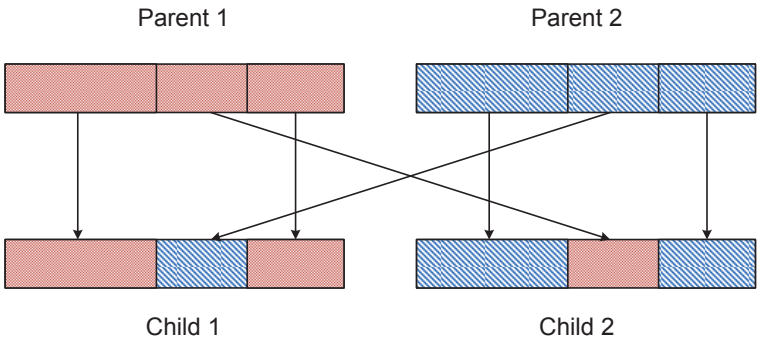

Figure 2.3: Two-point crossover

parent. The same process is applied to generate the second child, but the role of the parents is swapped. A few chromosomes will go through a mutation process – a randomly selected bit of these selected chromosomes will be swapped. For instance, if the fifth bit of the chromosome is selected for mutation and its value is a one, the value of this bit after the mutation process is replaced by a zero.

Survivor selection

Our GA also aims at developing elitism. The top five chromosomes from the valid list of the previous generation replace the worst five of the new generations.

Repetition

The above three steps will be repeated until the maximum number of generations is reached.

2.3.3 Special features of the proposed GA

Like most GAs, we are unable to claim that the algorithm will finally reach the global optimum. Furthermore, an efficient GA should avoid being trapped at local

optimums. Several measures are taken in our algorithm to achieve this objective. Firstly, the new generation lets the algorithm try new chromosomes, while elitism keeps the best individuals of previous generations, and in this way we ensure that the solution always improves. Secondly, during the crossover or mutation process, newly generated chromosomes do not necessarily satisfy the constraint (2.12). We do not reject these chromosomes, but rather employ the idea of invisible walls used in the PSO to ensure that the diversity in generating new chromosomes remains. We keep these chromosomes in an invalid list, and introduce a penalty in their fitness so as to force the chromosomes which have crossed the feasible boundaries to return. By letting those fit genes in the invalid chromosomes to be involved in generating new chromosomes, we ensure that a larger landscape can be searched. This, to some extent, helps to avoid the solution from being trapped at local optimums. Poor diversity in constructing new chromosomes will increase the probability that the solution is being trapped at a local optimum.

The main features that distinguish our algorithm from other efforts are how we evaluate the chromosomes and how we select the survivors. They are presented in detail below.

Evaluation

To evaluate each chromosome we use the fitness function. First, the total power consumption of a chromosome is calculated by (2.8) and then the feasibility of the solution is checked by (2.12). If the chromosome satisfies the constraint it will be added to the valid list, otherwise, the chromosome is placed in the invalid chromosomes list. Invalid chromosomes will receive a penalty related to their total power, given by

$$P_T \longleftarrow (1+\gamma)P_T. \tag{2.28}$$

In (2.28), $0 \leq \gamma < 1$ is the penalty factor. The lower the total power consumption, the higher fitness the chromosome will receive. With the use of this penalty, we can influence the diversity and the convergence rate. As mentioned before, we keep the invalid chromosomes because of the possibility that they can produce high quality valid chromosomes in combination with other valid or invalid chromosomes. In other words, there is a possibility that some valuable parts of the feasible region can be reached much faster by an offspring of chromosomes from outside feasible boundaries. For example, consider a chromosome which is invalid but it has a useful combination of genes. This chromosome would be eliminated if we just care about the valid solutions, but now a combination of a chromosome like this with other chromosomes may sometimes lead us to a fitter solution.

We illustrate this using a simple example with two subcarriers and two CR pairs, which minimum bit rate for the first and second CR pairs are given by 4 and 2 bits, respectively. Each chromosome consists of two blocks of length 3 bits – the first bit identifies the CR pairs and the next two bits represent the adopted modulation level. A sample population is shown in Fig.2.4a. From the given channel gains shown in Fig.2.4b, we realize that if subcarrier one is allocated to radio 1 with 16QAM, and radio 2 takes subcarrier two with QPSK, the power consumption is minimum. None of the chromosomes in the population present the optimum solution; however, a combination of them can be the optimum. Chromosome 1 in Fig.2.4a is an invalid chromosome, but by replacing its fourth gene with the fourth gene from chromosome 3 gives the optimum solution. On the other hand, if we discard invalid chromosomes, it may take us more generations to reach the optimum

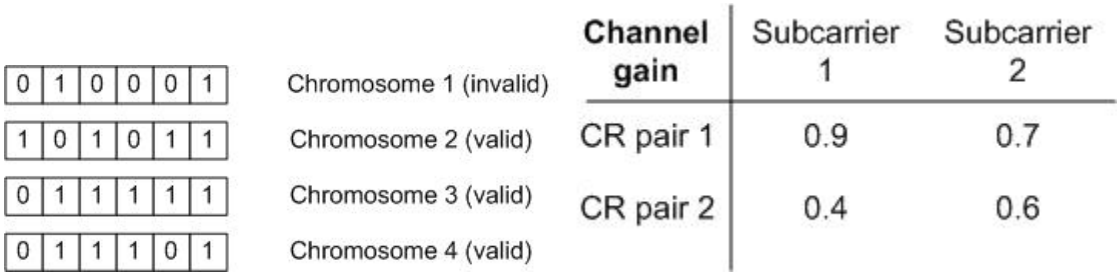

(a) Population (b) Channel gain table

Figure 2.4: Example of useful genes

solution, or in some occasions the algorithm may be trapped at a local optimum. Keeping the diversity becomes more important when the numbers of subcarriers and CRs increase as the chromosome length becomes longer.

Selection

In every GA, selection of the chromosomes for the next generation is vital. Another difference between our method and other reported methods is that we do not just combine the parent and offspring generations to select the survivors according to their fitness. Elitism is added to our method to force the GA to retain a number of the best chromosomes at each generation [69]. Our method takes the five elites of each parent generation to the next generation, while all other chromosomes are taken from the offspring generation. The replacement with elitism to form the new generation leads to fitter generations without losing the fittest chromosomes – keeping children (even those which have low fitness) enables our search to proceed in a vaster area, and will not lose the best chromosomes from the parent generation by keeping the elites. The populations of all generations are of equal and fixed size.

2.4 Ant colony optimization (ACO)

Similar to swarm intelligence, which is developed from observing the behavior of swarms of birds, fish, etc., ACO is inspired by the way ants find the shortest path between their nest and a food source. Ants deposit some amount of a liquid called *pheromone* on the path where they found the food upon their return. When there are more ants using a path to the food source, that path will receive a higher amount of pheromone. The longer way will have a lower amount of pheromone because of evaporation. Therefore, the number of ants selecting these ways will decrease with time. On the other hand, the shortest path clearly will have the strongest amount of pheromone after some time. A metaheuristic approach known as ant colony optimization [73] applies this idea to look for the optimal path. In most of the ACO algorithms developed, all the possible paths from the nest to the food source are represented using a complete graph. The solution to the problem would be a list of edges and vertices which are most commonly chosen by the ants to complete the tour.

Virtual ants choose their paths by considering two factors: visibility and trail intensity [74]. Visibility (n) is what an ant can see, and usually it is taken as the inverse of the edge length. Trail intensity (T) is indicated by the amount of pheromone, and it is related to the number of ants which have passed through the edge and completed the tour. Trail intensity is the factor that helps the algorithm to learn from previous successful attempts. A virtual ant selects its own path randomly from edges which have different probabilities of being selected. The search for edges will continue until the food source is found. During the path selection process, the path with higher visibility and trail intensity will have higher probability of being selected.

2.4.1 Proposed ACO-based algorithm

We find that with some modifications, it is possible to model the dynamic resource allocation problem for the centralized OFDM-based CR systems using the aforementioned ACO algorithm. The details are presented below.

Vertex and edge selection

Since subcarriers can be assigned only to one CR pair, if they are represented by the vertices of the graph, geometrically it means that each vertex can only be visited once. We use edges to represent combinations of CR pairs and modulation levels. Unlike existing ACO algorithms where there is only one edge to each vertex, our proposed ACO has multiple edges available to a vertex due to the fact that different modulation levels and radios can be assigned to that subcarrier. With a *pseudograph* (multigraph: a graph which has vertices connected to each other with more than one edge), the solution using ACO is possible if a suitable path (k, q) to a vertex (subcarrier) can be identified. This corresponds to the situation where CR k is assigned to transmit using modulation level q in that particular subcarrier.

We illustrate the process using the example shown in Fig.2.5a where there are two available CR pairs and two subcarriers. It is not difficult to figure out that there is a total of six ways to allocate every subcarrier to one of the two CR pairs together with a suggested modulation level. All edges have a probability to be selected, but those edges with relatively higher visibility or trail intensity will have higher probabilities. In our algorithm, the order in assigning subcarriers is not important, e.g. if we assign subcarrier 2 to CR 1 with 16QAM and then assign subcarrier 1 to CR 2 with QPSK, physically this is the same as the case when we assign subcarrier 1 to CR 2 with QPSK and then assign subcarrier 2 to CR 1 with

16QAM. Furthermore, the starting point of an edge does not carry any information. For example, in Fig.2.5b, after the path (CR 2, 16QAM) to subcarrier 2 is selected by the ant, it can consider all paths to subcarrier 1 are originated from subcarrier 2, so that there is continuation in its visit (despite that they are actually originated from the initial point, the ant can assume that physically these two points are interchangeable so that there is a continuation on the path it has chosen). This helps to reduce the trail intensity computing complexity. Moreover, visibility is just calculated once for all cycles and regardless of the edge origin.

To optimize (2.9), the conventional ACO has to be modified. In conventional ACO, the ant must visit all vertices to complete its tour, but in our proposed ACO algorithm, an ant finishes its tour as soon as it satisfies the constraint (2.12). When all constraints are satisfied, the selected paths are saved. The process repeats for a chosen number of ants which is also known as the *colony size*. Finally, when all ants of a colony completed their tours, the trail intensity matrix will be updated.

Ants cannot visit a vertex more than once. Two reasons can be given for this restriction. Firstly, visiting a vertex more than once shows that there is a loop inside the tour made by an ant, which indicates a redundancy of some edges and vertices in the tour. Secondly, by visiting a vertex more than once, constraint (2.10) will not be satisfied. To add this restriction to the proposed method, like all ACOs, a tabu list is used in the algorithm. After visiting a vertex, the tabu list will be updated by adding that vertex and all its entering edges. They will be removed from the list of available vertices and edges to prevent them from being selected again. Another feature is the removal of the satisfied CR pairs, as soon as the minimum required bit rate of the respective pair is satisfied. This helps to speed up the search for the solution by forcing the ant to satisfy the minimum bit rate requirement of the remaining CR pairs. Moreover, it reduces the complexity in computing the path selection probability.

We define P_{ij}^{kq} as the probability of moving from vertex i to vertex j through edge (k,q). Therefore, in the DSA problem, P_{ij}^{kq} means the probability of assigning subcarrier j to CR pair k with modulation level q after subcarrier i has been assigned. In our algorithm, since the order of assigning subcarriers is not important, it is sufficient to simply denote P_{ij}^{kq} as P_{j}^{kq}, which is the probability of assigning subcarrier j to CR pair k with modulation level q. This probability is calculated by the following formula:

$$P_j^{kq} = \begin{cases} \frac{[T_j^{kq}]^\alpha . [n_j^{kq}]^\beta}{\sum_{i \in C} [T_i^{kq}]^\alpha . [n_i^{kq}]^\beta} & j \in C \\ 0 & \text{otherwise,} \end{cases} \tag{2.29}$$

where n_j^{kq} is the visibility of edge (k,q) to vertex j, and T_j^{kq} is the trail intensity of the same edge. C is the list of available (not visited) vertices. As mentioned before, n_j^{kq} is the visibility, and is assumed to be one over the edge length. In this problem, the consumed power is taken to be the length of the selected edge. Since visibility of an edge is not changing by increasing the number of iterations, the visibility of each edge is calculated once, and saved in a table for further operations. In the proposed ACO, the size of the visibility table is [number of subcarriers $\times$ number of CRs $\times$ available modulation levels], while the conventional ACO in the similar case needs a 4D table of size [number of subcarriers $\times$ number of subcarriers $\times$ number of CRs $\times$ available modulation levels].

Updating trail intensity

A 3D table is created. Each cell in this table stores the trail intensity of an edge, and the initial value is one for all edges. A cycle or iteration is completed when all ants in the colony have completed their tours. All trail intensities will be

updated at the end of each cycle. A tour of an ant is considered to be completed only when (2.12) is satisfied. There is a possibility that an ant visits all the vertices and yet still unable to satisfy (2.12). The tour is considered incomplete, and the result will be discarded. This is similar to those ants that lose their way to the food place. This situation may happen especially when the system load is high.

Trail intensity shows the popularity of an edge. If more ants visit an edge and complete the trail, the edge will receive a higher trail intensity. On the other hand, if the edge is not used during each cycle, its trail intensity will be reduced by a factor ρ (to be explained shortly). This property is similar to the evaporation of pheromone in the real world. The following formulas are used to update the trail intensity after each cycle t.

$$T_j^{kq}(t+1) = (1-\rho).T_j^{kq}(t) + \Delta T_j^{kq}, \tag{2.30}$$

$$\Delta T_j^{kq} = \sum_{\forall a \in A} \Delta T_{aj}^{kq}, \tag{2.31}$$

$$\Delta T_{aj}^{kq} = \begin{cases} \frac{Q}{L_a} & a^{th}\text{ant select } (k,q) \text{ to vertex } j \\ 0 & \text{otherwise,} \end{cases} \tag{2.32}$$

where Q is a constant, ρ is the evaporation coefficient which is between 0 and 1, and finally, L_a is the tour length of the a^{th} ant, which corresponds to the total consumed power. At the beginning of algorithm, the trail intensities for all edges are assumed to be equal to one. After each cycle this matrix will be updated. As mentioned before, only ants which have satisfied the constraint (2.12) are included in computing (2.31).

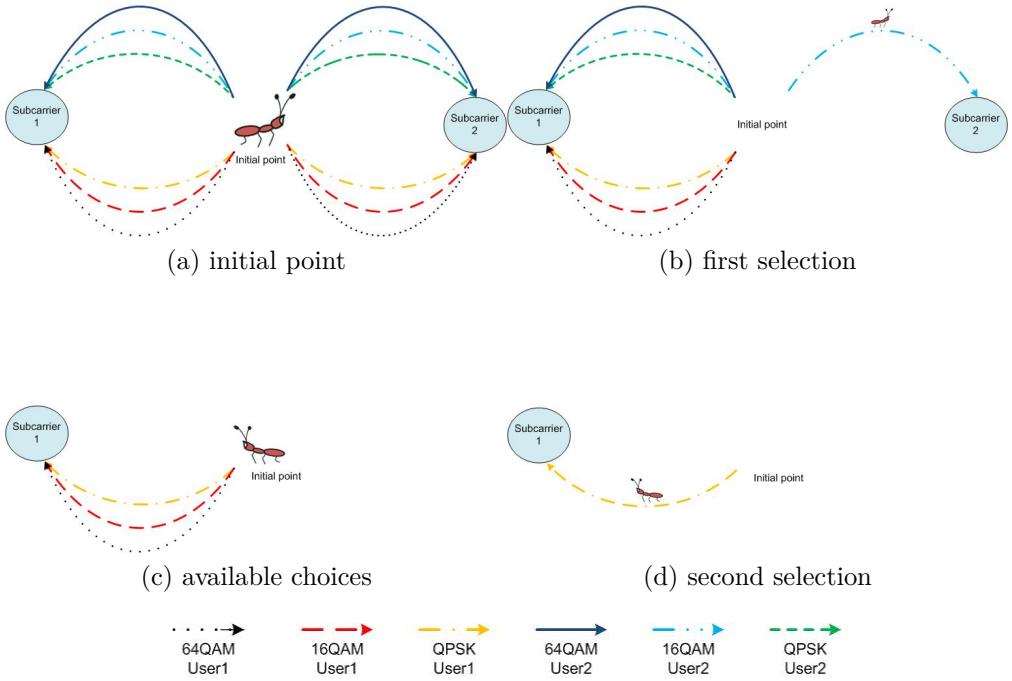

(a) initial point (b) first selection

(c) available choices (d) second selection

Figure 2.5: Example of ACO

2.4.2 The algorithm

The proposed ACO algorithm for spectrum access is summarized as shown in Algorithm 2.4.1.

Algorithm 2.4.1 Modified ACO algorithm for subcarrier and bit allocation

for t=1 to number of cycles **do**
  for a=1 to number of ants in the colony **do**
    while constraint (2.12) is not satisfied, and unallocated subcarriers are available **do**
      Select an edge to visit a new vertex with probability P_j^{kq}
      Add the selected vertex and its connected edges to the Tabu list (remove them from the available list)
    end while
    Calculate the tour length (Total power)
  end for
  Save the best solution found so far
  Update the pheromone trail levels T on paths
end for

Fig.2.5 presents a simple illustrative example where there are two CR with two available subcarriers. The first and second CRs demand a minimum bit rate

of 2 and 4 bits, respectively. Since the order of selection is not important, the ant will choose an edge randomly with the probabilities given by (2.29). Fig.2.5a shows all the available choices of the ant. In Fig.2.5b, the ant selected the edge which represents that subcarrier 2 is allocated to CR 2 to transmit using 16-QAM. Since subcarrier 2 has been selected, all other paths to vertex 2 will be removed. In addition, since this allocation has satisfied the minimum bit rate requirement of CR 2, all the edges representing CR 2 will be removed from the pseudograph, and the result is shown in Fig.2.5c. Fig.2.5d shows that the ant chose the edge which represents CR 1 with QPSK. This allocation satisfies the 2 bits requirement for CR 1. The ant finally completed the tour and satisfied the bit rate requirement of both CRs.

2.5 Simulation results

In this section, simulation results of the three proposed methods are compared. In our simulations, the channel gain between transmitter-receiver pair k in subcarrier n is denoted by $G_{n,k}$. To be able to calculate the channel gains we consider a coverage area of 100 square meters. A propagation model consisting of path loss, shadowing effect and fast fading is considered. The channel gain is given by [75]:

$$G_{n,k} = \frac{c_0 F_g |H|^2}{d_k^\theta} \tag{2.33}$$

where $|\cdot|^2$ is the norm square. The d_k is the distance between the k^{th} transmitter/receiver pair in meters, and $\theta = 3.5$ is the path loss coefficient in an urban area. The path loss coefficient at the reference point is given by $c_0 = d_0^\theta 10^{\frac{-L_0}{10}}$, where the reference distance from the transmitter is $d_0 = 1$ meter, and the path loss at the

reference distance is $L_0 = 0$. The $F_g = 10^{\frac{-X_g}{10}}$ gives the shadowing component where X_g is an independent log-normal random variable with standard deviation equal to 8dB. For the small scale fading component, we use $H = \frac{1}{\sqrt{2}}(X_1 + jX_2)$ to generate the Rayleigh fading gain, where $X_1, X_2 \sim \mathcal{N}(0,1)$ [76], and $\mathcal{N}(0,1)$ denotes a zero mean Gaussian distribution with variance 1.

GA and ACO have some parameters which may affect the simulation results. After some preliminary runs, we have selected the best values for these parameters to be as follows:

The general parameters of GA are:

- Population: 100 chromosomes;
- Generation number: 100 generations;
- Crossover probability: 0.9;
- Mutation probability: 0.05; and
- Penalty: 0.2.

The general parameters of ACO are:

- Number of ants: 100 ants;
- Number of cycles: 100 iterations;
- α (effect of trail intensity): 1;
- β (effect of visibility): 1;
- Q (constant): 100; and
- ρ (evaporation coefficient): 0.2.

To solve the problem optimally, it is necessary to define a constant BER level. In the simulations we set $P_e = 0.0001$. A test was conducted for 1000 realizations of a system having two CR pairs and 10 available subcarriers. Numerical results show that ACO can obtain the optimal value for more than 64% of the realizations, whilst GA reaches the optimum results only in 5% of the realizations. The difference between the two EA methods and the optimal solution for each realization is collected, sorted according to the percentage difference and presented in Fig.2.6. When the curve stays at zero, it indicates that GA or ACO algorithm obtained the optimal solutions. During the 1000 realizations, it can be seen that ACO gives very good estimations with less than 1% difference from the optimum result for nearly 700 realizations, whilst GA has the same accuracy for only about 5% of the realizations. The difference between the average total power by using ACO and the optimum solution was 1.41%, whilst the average GA-based CR system consumed 21.46% more power than the optimum allocation. Fig.2.7 gives the unsorted comparison of the total power consumption for the first 100 channel realizations.

The algorithms are next applied to a system in OSA model, where there are changing number of available subcarriers due to the arrival or leaving of PUs. We simulated 50 allocation cycles with two CR pairs respectively demand for 10 and 12 bits per OFDM duration for transmission. The system has 14 subcarriers, but some of these subcarriers are unavailable in some specific time. Fig.2.8 shows the results of this scenario where the availability of subcarriers varies in a step of 10 allocation cycles. We can see that the power consumption generally becomes higher when the number of available subcarriers decreases. For instance, between 20^{th} and 30^{th} time slot, since only 8 subcarriers are available, the increase in the network total power consumption is caused by the reduction of the available subcarriers. With fewer subcarriers, most CR pairs need to transmit at higher power by using

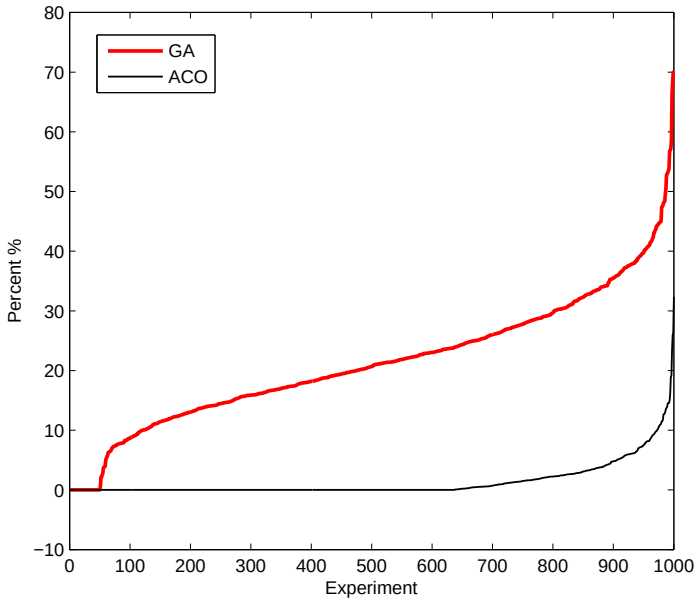

Figure 2.6: Difference in performance (sorted) between GA and ACO with optimum for 1000 network realizations

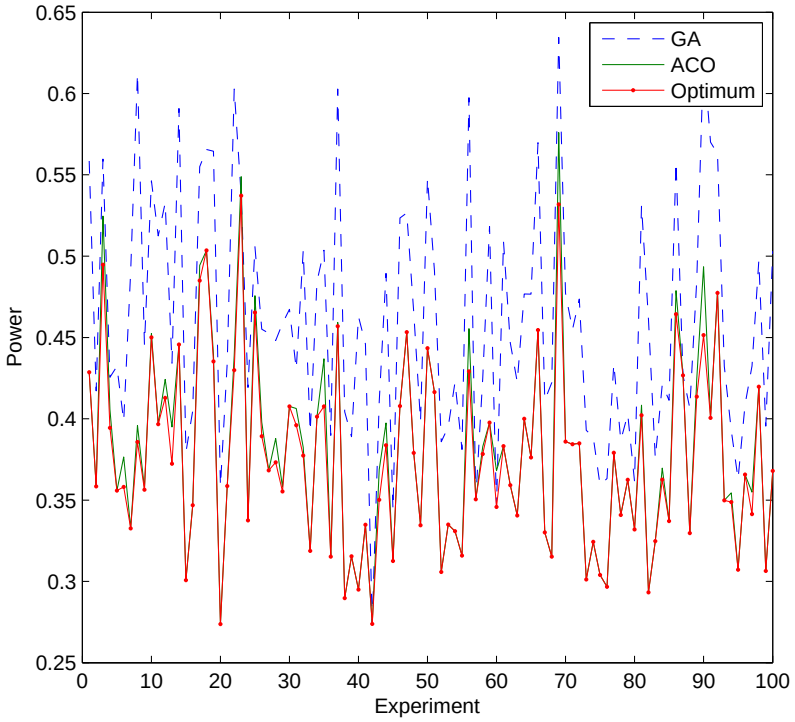

Figure 2.7: Performance comparison in 100 network realizations for optimum, ACO and GA approaches

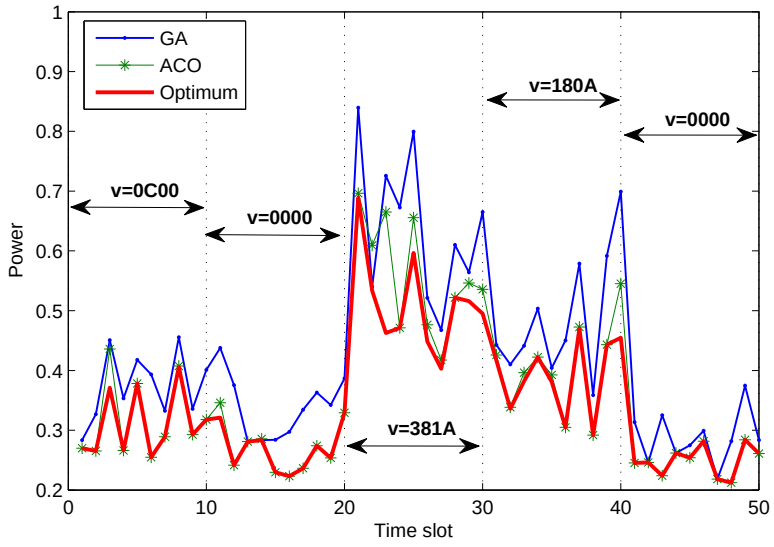

Figure 2.8: Proposed methods performance in an environment with varying number of subcarriers. For simplicity of presentation, vector $\mathbf{v}$ is shown in hexadecimal form. For example $\mathbf{v} = 0C00$ stands for $\mathbf{v} = [0,0,1,1,0,0,0,0,0,0,0,0,0,0]$

higher order of signal constellation, in order to achieve their expected throughput.

2.5.1 Convergence of the proposed algorithms

Convergence is a major concern when designing any heuristic algorithm. It is generally difficult to prove that an EA will always converge, and many practically implemented algorithms stop the iteration when one of the following conditions is met [70]:

- No improvement: The algorithm stops if the GA continues with the same best chromosome for a certain number of iterations, In this case, either the algorithm found the optimal, or it is stuck in a local minimum.
- Number of iterations: The algorithm stops after it reaches the maximum number of iterations and still could not achieve the above condition.

Table 2.1: Average convergence of proposed EAs in iterations

Method	ACO			GA		
Subcarrier No → Radio Pairs No ↓	10	12	14	10	12	14
2	11.15	15.56	15.06	7.15	9.58	11.77
4	24.8	30.53	29.92	4.87	6.61	10.51

We simulated the system with different number of subcarriers and CR pairs to investigate their convergence property. Table.2.1 summarizes the average convergence time (iterations) of the two algorithms over 1000 snapshots. As it is illustrated in the table, the GA converges much faster than ACO. On average GA converged after 12 iterations while ACO converges between 10 and 30 iterations. From the table we can also conclude that the convergence time does not change significantly by changing the number of available subcarriers. On the other hand, the change in convergence time is more noticeable when the number of CR pairs changes.

2.5.2 Complexity of the proposed algorithms

Run time complexity is another concern in designing algorithms for real time applications. Generally, algorithms with polynomial time complexity are believed to be suitable for applying to real time problems [77].

The developed GA must run for a certain number of generations, where each generation approximately has the complexity of $\mathcal{O}(P(N+K))$, where P represents the population size. So the overall complexity of the proposed GA will be $\mathcal{O}(GP(N+K))$, where G is the number of generations to be performed [78]. The complexity for ACO is approximately $\mathcal{O}(AN.log_2(NK))$ per iteration, where A refers to the number of ants. Therefore, the overall complexity of ACO is

$\mathcal{O}(IAN.log_2(NK))$, where I indicates the number of iterations. Hence, both GA and ACO are polynomial-time algorithms.

2.6 Conclusions

In this chapter, we proposed a novel GA algorithm and a modified ACO algorithm to solve the subcarrier, power and bit allocation problem for the centralized OFDMA-based DSA. We obtained the performance of the two EAs through simulations, and benchmarked them against the optimal solution. Our studies showed that ACO gives better solutions most of the time. While the solution to the integer linear programming problem is NP-hard, the proposed EAs provide useful suboptimal solutions when the number of CRs and/or the number of subcarriers are large.

Chapter 3

Centralized dynamic spectrum access algorithms for systems with frequency reuse

In this chapter, we extend the presented system model in the last chapter to a more general case. In the previous chapter, the allocation of subcarriers to CR pairs through CSM is addressed. However, frequency reuse is not considered in the model, i.e. no subcarrier can be used by more than one CR pair at a time even if they impose very low interference on each other. If frequency reuse is to be considered, the resulting problem will involve multiple nonlinear constraints which make the problem even more difficult to solve.

We model an OFDM-based CR network that supports multiple transmit/receive CR pairs. The CSM dynamically assigns the available subcarriers (white spaces) to each of the CR pairs by jointly taking into consideration the impact of interference resulting from spatial reuse of frequency, so as to maximize the total network bit rate while satisfying the minimum bit rate requirement and transmit power

constraints of each CR pair. The algorithm is capable of obtaining the optimal transmission power and modulation to be used by each transmitter. Each CR pair therefore should transmit at the power and modulation level assigned by the CSM to obtain the social optimum once the subcarriers have been allocated by the CSM.

Multicell OFDMA resource allocation problems also consider frequency reuse. Since we can consider multicell OFDMA resource allocation as a special case of our DSA problem (where the transmitters have a predefined distance from each other), we review the multicell OFDMA resource allocation literature. A two-stage heuristic algorithm has been proposed in [79] for subcarrier and power allocation. The authors referred to the transmission opportunity at each time slot on each subcarrier as a traffic bearer. A certain amount of power is given to each traffic bearer. At the higher level, the radio network controller (RNC) suggests a possible way to partition the total number of subcarriers to each BS, aiming at reducing the inter-cell interference (ICI) through increasing the reuse distance. The second algorithm runs at the BS level. Based on the RNC suggestions and the traffic demands, the BS allocates the subcarriers to users. It is possible that a user does not have any traffic to transmit, or/and other users need more bandwidth to transmit. In [80], the authors consider that all the mobile stations (MS) are divided into two groups: cell center users and cell edge users. The paper reformulates the problem into two parts. They first reduced the ICI by using a weighted graph subcarrier allocation model based on the geographical locations of the MSs. A method which maximizes the signal to noise ratio (SNR) for each cell is then applied. Finally, the paper proposed two heuristic algorithms to solve the formulated problem. An ant colony-based heuristic algorithm for jointly subcarrier and power allocation is proposed in [53]. The algorithm sub-optimally assigns the subcarriers and power to radio users on multicell OFDMA systems with reuse. A utility-based optimal approach for multicell OFDMA is reported in [41]. However, the approach requires

an exhaustive search within a feasible solution space, which is very time consuming. In [81], the authors considered OFDM-based links between an access point and distributed users. They proposed a greedy water filling approach to efficiently allocate subcarrier, power and rate with no spatial frequency reuse. In [52], Choi et al. decomposed the joint subcarrier and power allocation problem into multiple subproblems. They obtained an efficient solution to the problem. However, there is no guarantee on the optimality of the solution.

In summary, almost all of the proposed algorithms in the literature are based on heuristic approaches, and do not guarantee the optimal subcarrier and power assignment for such OFDM-based multiuser CR systems. The CSM proposed in this work maximizes the network total bit rate, subject to a power constraint for each CR transmitter and a minimum bit rate guarantee for each CR pair. The main contributions of this work are as follows. We first introduce the notion of signal-to-interference plus noise difference (SIND), and then convert the original problem into a mixed binary linear programming problem that can be solved optimally using available standard optimization algorithms in commercial software. Thus, the proposed linearization method enables us to achieve the maximum possible total bit rate in an OFDM-based multiuser CR system, by optimally assigning the subcarriers and power. The proposed linearization method can similarly be applied to other similar OFDMA resource allocation problems.

3.1 System and channel models

The OFDM-based network studied in this work is shown in Fig.3.1. The given total spectrum B is equally divided into N orthogonal subcarriers denoted by the set of indices $\mathcal{N} = \{1, 2, \ldots, N\}$, where each subcarrier has a bandwidth given by

B/N. There are K CR pairs denoted as $\mathcal{K} = \{1, 2, \ldots, K\}$ being admitted to transmit using the assigned subcarriers, where each CR pair consists of a transmitter and a designated receiver. The network has a CSM which allocates subcarriers to these distributed CR pairs. It is assumed that the CSM has full CSI about all CR pairs. The system follows time slots, and all the channel gains vary relatively much more slowly than the spectrum allocation period. We assume that the CSM has the full knowledge of subcarrier occupancies either by communicating with the PU, or by performing accurate sensing.

The k^{th} CR transmitter would request to transmit at some given minimum bit rate $\tilde{R}_k$ (bits per second) with their maximum acceptable BER (P_{e_k}). Given that there are J OFDM symbols per second transmitted in the system, the rate requirement can be converted to R_k, given by $R_k = \frac{\tilde{R}_k}{J}$, where R_k is the number of bits transmitted by the k^{th} transmitter per OFDM symbol.

Each transmitter may occupy more than one subcarrier for its data transmission, i.e., the CSM can allocate more than one subcarrier to each CR pair. In Fig.3.1, *Tx3* uses two subcarriers to transmit its data to *Rx3*. Also, the CSM can assign more than one CR pair to use the same subcarrier provided that, in the presence of interference, all co-channel pairs can still meet their respective BER requirement. Such frequency reuse is illustrated in Fig.3.1 for subcarrier one, where both the 1^{st} and 3^{rd} CR pairs use the first subcarrier simultaneously. Each of the transmitters can only use one of QPSK, 16QAM and 64QAM modulation levels on a subcarrier.

Each CR transmitter should request a certain bandwidth from CSM so as to be able to transmit at some given minimum guaranteed data rate. The service level is measured in term of the BER (P_e) and rate requirement. In other words, the CSM should assign subcarriers and power to CR pairs such that the minimum

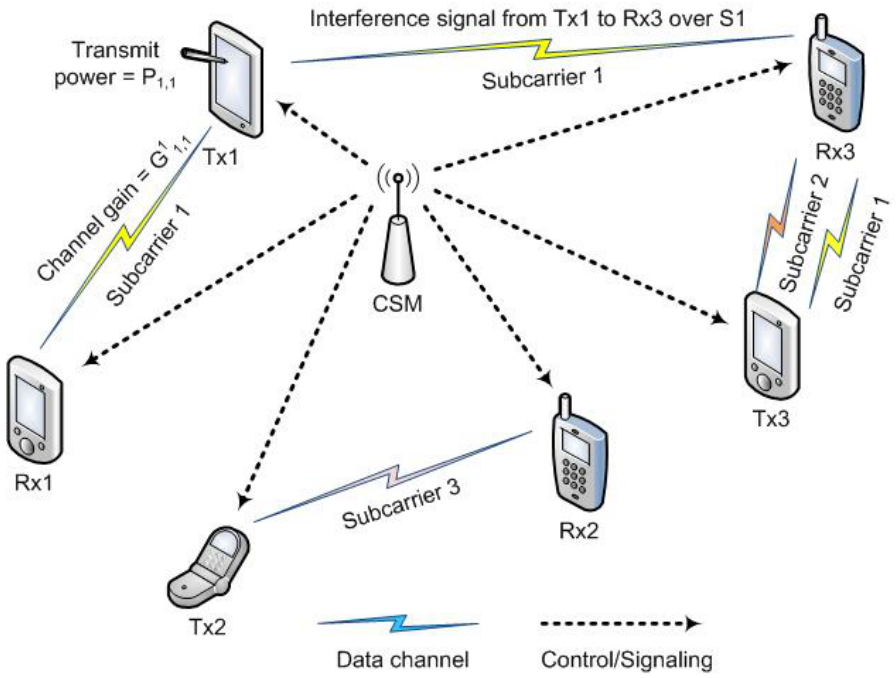

Figure 3.1: System model

bit rate and BER requirements are satisfied. The BER and bit rate depend on the signal to interference-plus-noise ratio (SINR), which is given by:

$$SINR_{n,k} = \frac{p_{n,k} G^n_{k,k}}{I_{n,k} + N_0}, \tag{3.1}$$

where $p_{n,k}$ is the transmission power of the k^{th} transmitter on the n^{th} subcarrier; $G^n_{j,k}$ indicates the subcarrier gain on the n^{th} subcarrier between the j^{th} transmitter and the k^{th} receiver, which takes into account the effects of path loss, lognormal shadowing and small scale fading components. N_0 denotes the average power of the AWGN. The interference to the k^{th} CR receiver by other co-channel CR transmitters, on the n^{th} subcarrier, is given by:

$$I_{n,k} = \sum_{j=1, j \neq k}^{K} G^n_{j,k} p_{n,j}. \tag{3.2}$$

The objective is to maximize the total number of bits per OFDM symbol,

$$C = \sum_{k=1}^{K} \sum_{n=1}^{N} r_{n,k}, \tag{3.3}$$

where $r_{n,k}$ is the number of modulated bits transmitted by the k^{th} transmitter on the n^{th} subcarrier. As stated previously, it can either be 2, 4, 6 or zero, which indicate QPSK, 16QAM, 64QAM and no transmission, respectively. We consider that the network rate maximization is also subject to the following constraints:

(1) *SINR constraint*: The minimum required SINR at each CR receiver to achieve the aforementioned modulation levels on OFDM subcarriers is given by [82]:

$$\gamma_{min}^{n,k,q} = (2^{2q} - 1) \times \left(\frac{1}{3} \left[Q^{-1} \left(\frac{P_{e_k}}{4} \right) \right]^2 \right), \tag{3.4}$$

where $2q, \forall q \in \{0, 1, 2, 3\}$ is the number of transmitted bits per OFDM symbol by the k^{th} CR pair on the n^{th} subcarrier, and P_{e_k} indicates the target BER of the k^{th} CR pair.

(2) *Transmit power constraint*: Each CR transmitter has a limited amount of power, and cannot consume more than the following over the subcarriers,

$$\sum_{n=1}^{N} p_{n,k} \leq P_k \qquad \forall k \in \mathcal{K}, \tag{3.5}$$

where P_k is the maximum available power of the k^{th} transmitter.

(3) *Minimum bit rate guarantee for each user*: The system meets a minimum rate guarantee for each CR pair as,

$$\sum_{n=1}^{N} r_{n,k} \geq R_k \qquad \forall k \in \mathcal{K}, \tag{3.6}$$

where R_k is the k^{th} CR pair's minimum required number of bits per OFDM symbol. There also might be some best effort CR pairs in the system, who wish to pay less, and do not request a guaranteed minimum bit rate. The CSM can assign subcarriers to these CR pairs based on their availability. For these best effort CR pairs, R_k is set to zero.

3.2 Optimization on transmit power and subcarrier assignment

3.2.1 Original problem formulation

We aim to maximize the total number of bits per OFDM symbol by optimally assigning the subcarriers and transmit power to K CR pairs. From the above discussions, the optimization problem can therefore be formulated as follows:

$$\max_{a,p} \sum_{k=1}^{K} \sum_{n=1}^{N} r_{n,k}, \tag{3.7}$$

subject to:

$$\sum_{n=1}^{N} p_{n,k} \leq P_k \qquad \forall k \in \mathcal{K}, \tag{3.8}$$

$$\sum_{n=1}^{N} r_{n,k} \geq R_k \qquad \forall k \in \mathcal{K}, \tag{3.9}$$

$$\frac{v_n p_{n,k} G^n_{k,k}}{\sum_{j=1,j\neq k}^{K} p_{n,j} G^n_{j,k} + N_0} \geq \sum_{q=1}^{3} a^q_{n,k} . \gamma^{n,k,q}_{min} \qquad \forall k \in \mathcal{K}, \forall n \in \mathcal{N}, \tag{3.10}$$

$$\sum_{q=1}^{3} a_{n,k}^{q} \leq 1 \qquad \forall k \in \mathcal{K}, \forall n \in \mathcal{K}, \tag{3.11}$$

$$r_{n,k} = \sum_{q=1}^{3} 2.q \times a_{n,k}^{q} \qquad \forall k \in \mathcal{K}, \forall n \in \mathcal{N}, \tag{3.12}$$

$$a_{n,k}^{q} \in \{0,1\}, \tag{3.13}$$

$$p_{n,k} \geq 0, \tag{3.14}$$

$$r_{n,k} \in \{0,2,4,6\}. \tag{3.15}$$

Equations (3.8) and (3.9), give the maximum transmit power and the minimum guaranteed rate constraints for each CR pair respectively. Equation (3.10) is the SINR constraint, which involves the modulation assignment, transmit power, interfering powers, and the subcarrier assignment, all of which affect the SINR. In (3.10), v_n shows the availability of n^{th} subcarrier. $v_n = 1$ means that the subcarrier is not occupied by the PU, and the CSM can allocate it to the CR pairs. On the other hand, if $v_n = 0$, the subcarrier is occupied by PUs, and it cannot be assigned to any CR pair. Thus, in (3.10) having $v_n = 0$ forces $a_{n,k}^{q}$, which is the assignment decision variable, to become zero. A CR pair cannot transmit on a subcarrier using more than one modulation level and this restriction is represented by (3.11). The $a_{n,k}^{q}$ is a binary variable, and $a_{n,k}^{q} = 1$ is used to indicate that the k^{th} CR pair transmits $2q$ bits on the n^{th} subcarrier. Equation (3.12) evaluates the number of bits transmitted on the n^{th} subcarrier by the k^{th} CR, and only one of the terms can be non-zero.

The above NP-hard mixed integer nonlinear optimization problem has nonlinear constraints due to the multiplication of two unknowns in (3.10). Next, we propose a new optimization framework by introducing a linearization method that converts the above problem into a MBLP problem that can be solved optimally.

3.2.2 Proposed linearization method

We reformulated the optimization problem to become a standard linear problem. The constraint that makes the optimization problem nonlinear is the SINR constraint in (3.10). We take the following steps to linearize the constraint. Firstly, in (3.16), we quantize the achievable SINR based on the $\gamma_{min}^{n,k,q}$ threshold levels, to determine the transmitted bits (per OFDM symbol) $r_{n,k}$ for each CR on every subcarrier as follows,

$$r_{n,k} = \begin{cases} 2 & \gamma_{min}^{n,k,2} > \dfrac{v_n p_{n,k} G_{k,k}^n}{\sum_{j=1,j\neq k}^{K} p_{n,j} G_{j,k}^n + N_0} \geq \gamma_{min}^{n,k,1} \\ 4 & \gamma_{min}^{n,k,3} > \dfrac{v_n p_{n,k} G_{k,k}^n}{\sum_{j=1,j\neq k}^{K} p_{n,j} G_{j,k}^n + N_0} \geq \gamma_{min}^{n,k,2} \\ 6 & \dfrac{v_n p_{n,k} G_{k,k}^n}{\sum_{j=1,j\neq k}^{K} p_{n,j} G_{j,k}^n + N_0} \geq \gamma_{min}^{n,k,3} \\ 0 & \texttt{otherwise} \end{cases} \quad \forall k \in \mathcal{K}, \forall n \in \mathcal{N} \quad (3.16)$$

In (3.16), the k^{th} CR is allowed to transmit on a subcarrier with only one selected modulation index; thus, $r_{n,k}$ is directly computed and allocated based on (3.16). Therefore, the auxiliary variable $a_{n,k}$ and constraint (3.12) become redundant, and can be removed without affecting the optimization process.

To facilitate the subsequent development of the algorithm, we introduce the notion of signal-and-interference plus noise difference (SIND) as follows:

$$\zeta_{n,k}^q = (v_n p_{n,k} G_{k,k}^n) - \gamma_{min}^{n,k,q} \times (\sum_{j=1,j\neq k}^{K} p_{n,j} G_{j,k}^n + N_0) \quad \forall k \in \mathcal{K}, \forall n \in \mathcal{N}, \forall q \in \{1,2,3\}, \quad (3.17)$$

where $\zeta_{n,k}^q$ is the SIND for the k^{th} CR pair to achieve $2q$ bits on the n^{th} subcarrier. Now $r_{n,k}$ can be redefined such that:

$$r_{n,k} = \sum_{q=1}^{3} 2b_{n,k}^{q}, \tag{3.18}$$

where

$$b_{n,k}^{q} = \begin{cases} 1 & \zeta_{n,k}^{q} \geq 0 \\ 0 & \texttt{otherwise} \end{cases} \qquad \forall k \in \mathcal{K}, \forall n \in \mathcal{N}, \forall q \in \{1,2,3\}, \tag{3.19}$$

which means that the k^{th} CR is allowed to transmit on the n^{th} subcarrier only if $\zeta_{n,k}^{q} \geq 0$. It can be seen that after the transformation, the new binary variables $b_{n,k}^{q} \in \{0,1\}(q = 1,2,3)$ have been used to replace the integer variable $r_{n,k}$. Furthermore, by introducing a sufficiently large positive number M (for example, $M = \max\{P_k\}$), we are able to write the following linear inequality:

$$M(b_{n,k}^{q} - 1) - \zeta_{n,k}^{q} \leq 0 \quad \forall k \in \mathcal{K}, \forall n \in \mathcal{N}, \forall q \in \{1,2,3\}. \tag{3.20}$$

Next, we prove that (3.20) behaves in the same way that (3.19) does in the original maximization problem.

For the same channel conditions, (3.19) and (3.20) must give exactly the same results. In (3.19), $\zeta_{n,k}^{q} < 0$ results in $b_{n,k}^{q} = 0$ while for $\zeta_{n,k}^{q} \geq 0$ the value of $b_{n,k}^{q}$ becomes unity. For (3.20), we explain the following two cases separately:

(1) $\zeta_{n,k}^{q} < 0$: the inequality is satisfied only when $b_{n,k}^{q} = 0$. Therefore, $b_{n,k}^{q}$ must set to zero.

(2) $\zeta_{n,k}^{q} \geq 0$: the inequality is satisfied regardless of the value of $b_{n,k}^{q}$. So, $b_{n,k}^{q}$ can be either 0 or 1. Since the optimization problem is to maximize the

summation of $b^q_{n,k}$, this will force $b^q_{n,k} = 1$ to be the only solution.

So in either situation, (3.19) and (3.20) result in the same solution for the binary variables for $b^q_{n,k}$, and we therefore can replace (3.19) by (3.20). As (3.20) is linear while (3.19) is not, such replacement allows the use of conventional linear programming solution algorithms.

3.2.3 Equivalent problem formulation and its optimal solution

By making use of the above transformations, the original problem formulation in (3.7) to (3.12) can now be written as:

$$\max_{b,p} \sum_{k=1}^{K} \sum_{n=1}^{N} \sum_{q=1}^{3} 2 \times b^q_{n,k}, \tag{3.21}$$

subject to:

$$\sum_{n=1}^{N} p_{n,k} \leq P_k \qquad \forall k \in \mathcal{K}, \tag{3.22}$$

$$\sum_{n=1}^{N} \sum_{q=1}^{3} 2 \times b^q_{n,k} \geq R_k \qquad \forall k \in \mathcal{K}, \tag{3.23}$$

$$M(b^q_{n,k} - 1) - \zeta^q_{n,k} \leq 0 \qquad \forall k \in \mathcal{K}, \forall n \in \mathcal{N}, \forall q \in \{1,2,3\}, \tag{3.24}$$

$$b^q_{n,k} \in \{0,1\}, \tag{3.25}$$

$$p_{n,k} \geq 0. \tag{3.26}$$

The problem is now transformed into a standard MBLP form which can be solved optimally with conventional methods [67]. From this step the MBLP problem can be solved with commercial software packages like TOMLAB/CPLEX [68]. The inputs to the optimization problem are the known optimization variables, such as: channel gains ($G^n_{j,k}$), maximum power of each pair (P_k), minimum required rate (R_k), AWGN power density (N_0), maximum acceptable BER (Pe), and the large positive number (M). The outputs of the optimization problem are the decision variables $p_{n,k}$ and $b^q_{n,k}$ as well as the maximum of the objective function.

The number of variables and constraints of the proposed linearization method is compared to the original mixed integer nonlinear programming problem in Table 4.1. The final linear problem has $4 \times N \times K$ decision variables, where $3 \times N \times K$ of the decision variables are binary and $N \times K$ of them are real numbers. As linearity and nonlinearity of the constraints determines the hardness of the problem, our modified problem with linear constraints is much easier to solve than problems with nonlinear constraints. The transformation and linearization processes proposed above impose no optimality loss, because no relaxation or approximation is made. Only the utility function is transformed from integer format to a summation of binary variables, and some constraints are replaced by linear constraints with exactly the same behavior. As a result of these modifications, we are able to maximize the system total achievable rate by optimally allocating the subcarriers and the transmit power to each CR pair.

In the next section, we focus our study on OFDM-based CR with frequency reuse, which is now made possible by the optimum framework proposed in this work.

Table 3.1: A comparison between the number of decision variables and constraints in original problem and the linearized problem.

Problem	Number of Decision Variables	Number of Constraints
Original Nonlinear	$4 \times N \times K$	$2 \times K + 2 \times N \times K$ (nonlinear)
Linearized	$4 \times N \times K$	$2 \times K + 3 \times N \times K$ (linear)

3.3 Numerical results

In this section, we present the simulation result on the DSA problem, by using the proposed formulation in Section 3.2.3. We consider a coverage area of 100 square meters. A propagation model consisting of path loss, shadowing effect and fast fading is considered. The channel gain is given by [75]:

$$G_{j,k}^{n} = \frac{c_0 F_g |H|^2}{d_{j,k}^{\theta}} \tag{3.27}$$

where $|\cdot|^2$ is the norm square. The $d_{j,k}$ is the distance between the j^{th} transmitter and the k^{th} receiver in meters, and $\theta = 3.5$ is the path loss coefficient in a urban area. The path loss coefficient at the reference point is given by $c_0 = d_0^{\theta} 10^{\frac{-L_0}{10}}$, where the reference distance from the transmitter is $d_0 = 1$ meter and the path loss at the reference distant is $L_0 = 0$. The $F_g = 10^{\frac{-X_g}{10}}$ gives the shadowing component where X_g is an independent log-normal random variable with standard deviation equal to 8dB. For the small scale fading component, we use $H = \frac{1}{\sqrt{2}}(X_1 + jX_2)$ to generate the Rayleigh fading gain, where $X_1, X_2 \sim \mathcal{N}(0,1)$ [76], and $\mathcal{N}(0,1)$ denotes a zero mean Gaussian distribution with variance 1. The maximum allowable transmission power of each radio is 33dBm (2000 mW).

Two service grades are provided by the CSM in our simulations. The higher service grade ensures radios are guaranteed to transmit at a minimum guarantee transmission rate of 6 bits per OFDM symbol at a BER of 10^{-6}. The lower service grade is for best effort users, and it guarantees a BER of 10^{-3}.

3.3.1 Effect of frequency reuse

In this simulation, we consider a system with 10 subcarriers and 4 CR pairs. We assume that the first two CR pairs have high service grade requests and other two pairs have low service grade requests. The following two scenarios are simulated.

(1) *Scenario 1*: The radio transmitters and receivers are randomly placed in the coverage area in this scenario. Therefore, it is possible that a transmitter and its designated receiver are located far apart. As a result, it is likely that the distance between any transmitter and its designated receiver is much larger than the distance between that receiver and other transmitters. Fig.3.2a shows a snapshot of this scenario. By knowing the location of radio pairs for this snapshot, we can compute the channel gain from (3.27). Then we can maximize the total system bit rate using (3.21)-(3.26). The optimum subcarrier, power and bit allocation of this system are presented in Table 3.2 and Table 3.3, respectively.

(2) *Scenario 2*: We randomly place the the transmitters. Then their respective receivers are randomly placed in a defined vicinity (5 meters) from their respective transmitter. Therefore, it is likely that the distances between different transceiver pairs are much larger than the distance within any transmitter and its designated receiver. A snapshot of this scenario is shown in Fig.3.2b. The optimum power, subcarrier and bit allocation results are presented in Table 3.4 and Table 3.5, respectively.

The presented values of $r_{n,k}$ and $p_{n,k}$ in Table 3.3 (Table 3.5) and Table 3.2 (Table 3.4) are the optimum results obtained using our proposed algorithm (3.21)-(3.26) for scenario 1 (scenario 2). Thus, any deviation of $r_{n,k}$ and $p_{n,k}$ from their

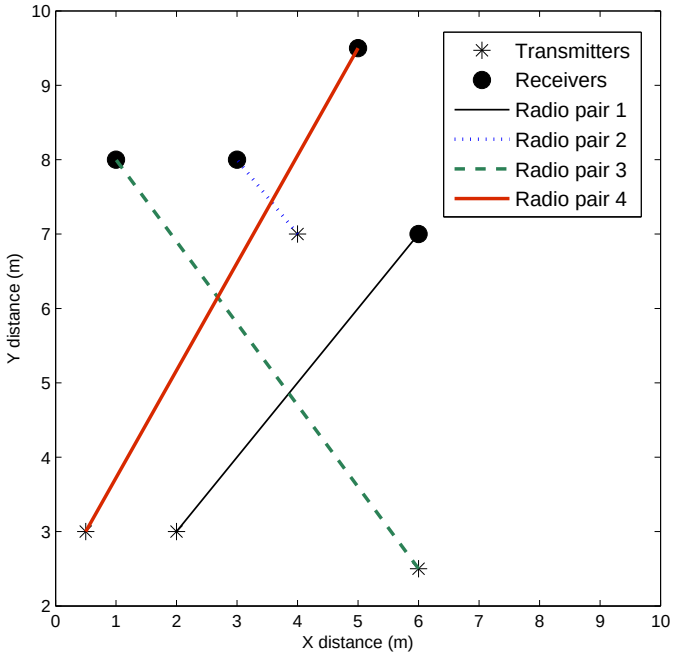

(a) Scenario 1

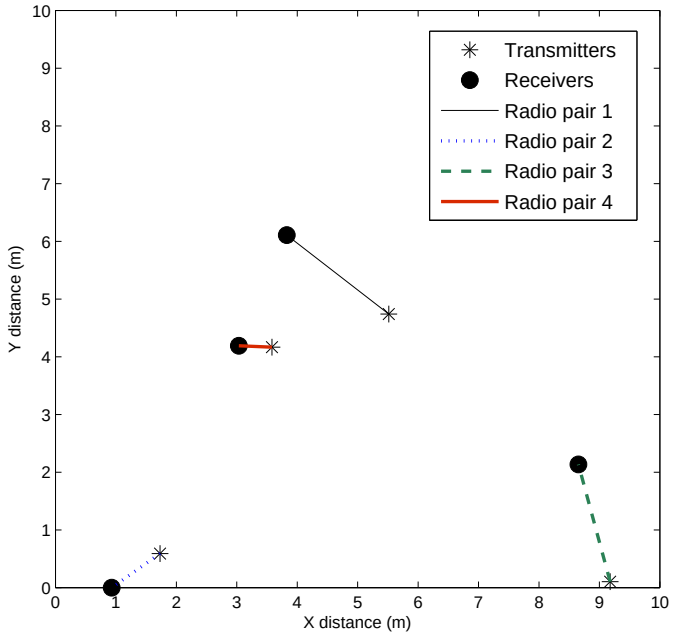

(b) Scenario 2

Figure 3.2: Locations of CR pairs in a snapshot of scenario 1 and scenario 2

Table 3.2: Scenario 1, comparison of the optimum subcarrier, power (mW) and bit assignment for systems with and without frequency reuse. Optimum subcarrier and power assignment. Numbers in the table denote the assigned power in milliwatts.

Subcarrier No	Reuse model	CR pair 1	CR pair 2	CR pair 3	CR pair 4
Subcarrier 1	reuse	0	20.2	0	0
	no reuse	0	20.2	0	0
Subcarrier 2	reuse	0	653.0	0	0
	no reuse	0	653.0	0	0
Subcarrier 3	reuse	0	935.2	0	0
	no reuse	0	0	0	985.1
Subcarrier 4	reuse	803.4	1.3	0	0
	no reuse	659.2	0	0	0
Subcarrier 5	reuse	0	75.9	0	0
	no reuse	0	75.9	0	0
Subcarrier 6	reuse	1196.6	0	0	0
	no reuse	1196.6	0	0	0
Subcarrier 7	reuse	0	51.8	0	0
	no reuse	0	51.8	0	0
Subcarrier 8	reuse	0	0	484.2	0
	no reuse	0	378.3	0	0
Subcarrier 9	reuse	0	134.7	0	0
	no reuse	0	566.4	0	0
Subcarrier 10	reuse	0	127.9	1389.3	0
	no reuse	0	0	1016.5	0
Pair Power	reuse	2000	2000	1873.5	0
	no reuse	1855.8	1745.6	1016.5	985.1

Table 3.3: Comparison of the number of bits per subcarrier and total bit rate for systems with and without frequency reuse in Scenario 1. Numbers in the table denote the number of transmitted bits.

Subcarrier No	Reuse model	CR pair 1	CR pair 2	CR pair 3	CR pair 4
Subcarrier 1	reuse	0	6	0	0
	no reuse	0	6	0	0
Subcarrier 2	reuse	0	6	0	0
	no reuse	0	6	0	0
Subcarrier 3	reuse	0	6	0	0
	no reuse	0	0	0	4
Subcarrier 4	reuse	2	2	0	0
	no reuse	4	0	0	0
Subcarrier 5	reuse	0	6	0	0
	no reuse	0	6	0	0
Subcarrier 6	reuse	4	0	0	0
	no reuse	4	0	0	0
Subcarrier 7	reuse	0	6	0	0
	no reuse	0	6	0	0
Subcarrier 8	reuse	0	0	2	0
	no reuse	0	6	0	0
Subcarrier 9	reuse	0	4	0	0
	no reuse	0	6	0	0
Subcarrier 10	reuse	0	6	6	0
	no reuse	0	0	6	0
Pair Rate	reuse	6	42	8	0
	no reuse	8	36	6	4
Total Rate	reuse	56			
	no reuse	54			

optimal values given in Table 3.3 (Table 3.5) and Table 3.2 (Table 3.4) will result in either a lower total bit rate or violation of power or rate constraints.

To illustrate the effect of frequency reuse on the network, we computed the optimum subcarrier and power assignment without frequency reuse by modifying the algorithm in [56]. This gives us the capability to compare the effect of frequency reuse in different snapshots of the network. In all cases, the minimum guaranteed bit rate for higher service grade users was satisfied. However, as the system did not guarantee any minimum bit rate for the best effort users, no subcarrier is assigned to the fourth CR pair in the first Scenario solution with frequency reuse.

Scenario 1: In Table 3.3, we observe that frequency reuse brings negligible improvement to the system total bit rate. The reason for such observation is due to the geographical positions of transmitters and receivers. As shown in Fig.3.2a, each radio transmitter is far from its receiver, and in some cases a receiver is nearer to another pairs' transmitter than its own designated transmitter, e.g. 1^{st} receiver is closer to the 2^{nd} transmitter than the 1^{st} transmitter (its paired transmitter). Due to the high co-channel interference between different transceiver pairs, frequency reuse has negligible advantage in improving the system total bit rate.

Scenario 2: Frequency reuse significantly improves the total bit rate of the system. Since receivers are located close to their designated transmitters, the effect of path loss from other transmitters is much higher, and this results in smaller co-channel interference among different transceiver pairs. Therefore, most of the subcarriers in Scenario 2 were reused by more than one radio pairs, each of which is able to achieve higher achievable rate than a radio pair in Scenario 1, as presented in Table 3.5.

Comparison on Scenario 1 and 2: The average achievable total bit rate in both scenarios for systems with and without frequency reuse are compared in Fig.3.3 by

Table 3.4: Scenario 2, comparison of the optimum subcarrier, power (mW) and bit assignment for systems with and without frequency reuse. Optimum subcarrier and power assignment. Numbers in the table denote the assigned power in milliwatts.

Subcarrier No	Reuse model	CR pair 1	CR pair 2	CR pair 3	CR pair 4
Subcarrier 1	reuse	0	0	0	29.9
	no reuse	0	0	0	17.0
Subcarrier 2	reuse	671.3	110.7	23.5	0
	no reuse	0	43.2	0	0
Subcarrier 3	reuse	0	204.1	0	28.0
	no reuse	1532.0	0	0	0
Subcarrier 4	reuse	0	849.3	874.9	10.5
	no reuse	0	0	0	22.6
Subcarrier 5	reuse	0	0	264.1	265.5
	no reuse	304.0	0	0	0
Subcarrier 6	reuse	0	0	0	106.9
	no reuse	0	0	631.5	0
Subcarrier 7	reuse	123.2	689.3	0	0
	no reuse	53.7	0	0	0
Subcarrier 8	reuse	0	43.1	0	1055.2
	no reuse	0	35.4	0	0
Subcarrier 9	reuse	0	103.5	803.9	67.5
	no reuse	0	271.7	0	0
Subcarrier 10	reuse	0	0	33.6	210.5
	no reuse	0	0	0	39
Pair power	reuse	794.5	2000	2000	1771.0
	no reuse	1898.7	350.3	631.5	78.6

Table 3.5: Comparison of the number of bits per subcarrier and total bit rate for systems with and without frequency reuse in Scenario 2. Numbers in the table denote the number of transmitted bits.

Subcarrier No	Reuse model	CR pair 1	CR pair 2	CR pair 3	CR pair 4
Subcarrier 1	reuse	0	0	0	6
	no reuse	0	0	0	6
Subcarrier 2	reuse	4	6	6	0
	no reuse	0	6	0	0
Subcarrier 3	reuse	0	6	0	4
	no reuse	6	0	0	0
Subcarrier 4	reuse	0	4	2	4
	no reuse	0	0	0	6
Subcarrier 5	reuse	0	0	6	6
	no reuse	6	0	0	0
Subcarrier 6	reuse	0	0	0	6
	no reuse	0	0	6	0
Subcarrier 7	reuse	6	6	0	0
	no reuse	6	0	0	0
Subcarrier 8	reuse	0	6	0	6
	no reuse	0	6	0	0
Subcarrier 9	reuse	0	2	4	6
	no reuse	0	6	0	0
Subcarrier 10	reuse	0	0	4	6
	no reuse	0	0	0	6
Pair Rate	reuse	10	30	22	44
	no reuse	18	18	6	18
Total Rate	reuse	106			
	no reuse	60			

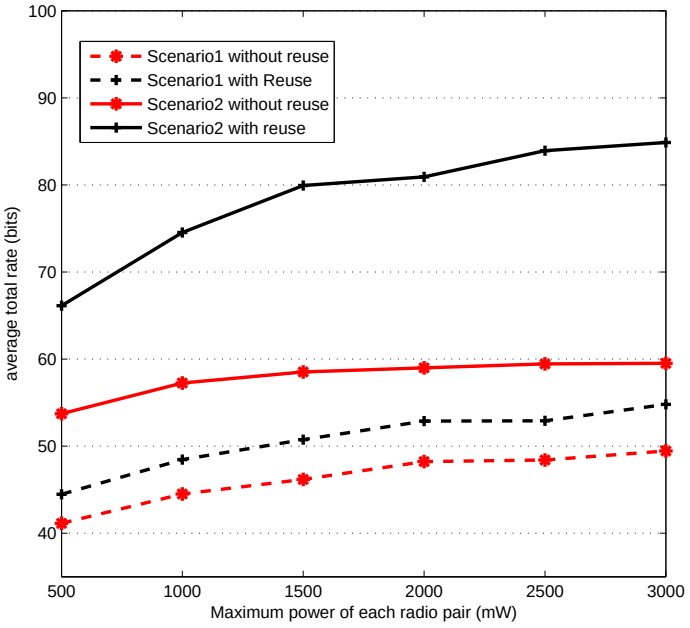

Figure 3.3: Average achieved rate over 1000 realizations of scenario 1 and scenario 2

averaging over 1000 system realizations. As expected, the average rate increases as power level increases. However, for the case of without frequency reuse the presented increase diminishes faster, as the maximum achievable bit rate for the case of without frequency reuse is 60 bits. On the other hand, increasing the power level on the CR pair with frequency reuse achieves a higher bit rate of 85.

3.3.2 Effect of increasing the number of CR pairs

Here, we consider that the number of subcarriers is fixed at 10 and the number of CR pairs is increasing. We consider that all transmitters are requesting a minimum bit rate of 8 bits per OFDM symbol. In Fig.3.4a and Fig.3.4b, we present the average rate per subcarrier and the average number of radio pairs per subcarrier, respectively. The results are for a particular snapshot of the position of the CR pairs, which is generated randomly. As it is shown in Fig3.4a, the average number

of bits per subcarrier increases when the number of CR pairs increases. However, further increase of the number of CR pairs will reduce the average number of bits per subcarrier due to the high interference imposed on each particular CR pair. If we further increase the number of CR pairs there might be no feasible solution, because high interference prevents CR pairs from satisfying their minimum required bit rate constraint.

Fig.3.4b shows the average number of CR pairs assigned to a subcarrier. When the number of CR pairs is increased the average number of CR pairs per subcarrier becomes large. This shows that on average more CR pairs impose interference on each other, degrading the performance of other CR pairs. Therefore, if the system increases its load by accepting more CR pairs, it will become unable to satisfy the rate requirement of the CR pairs due to higher interference.

3.3.3 Comparison with a heuristic method

Although we presented a MBLP solution to the problem of DSA with frequency reuse, there are some heuristics which provide suboptimal solutions with lower complexity. The presented MBLP solution provides a benchmark to all these heuristics against the optimum solution, and checks their validity. ACO is a popular evolutionary method for finding acceptable suboptimum solutions to the NP-hard problems. Here, we compare the achievable rate of the proposed ACO-based method in [53] with the optimum subcarrier and power assignment in this work. In Fig.3.5, we present the average bit rate by averaging over 100 realizations. In each realization, the CR pairs are positioned randomly, and as a result, the CR pairs face different channel gains. The network has 6 subcarriers and all the CR pairs are best effort users.

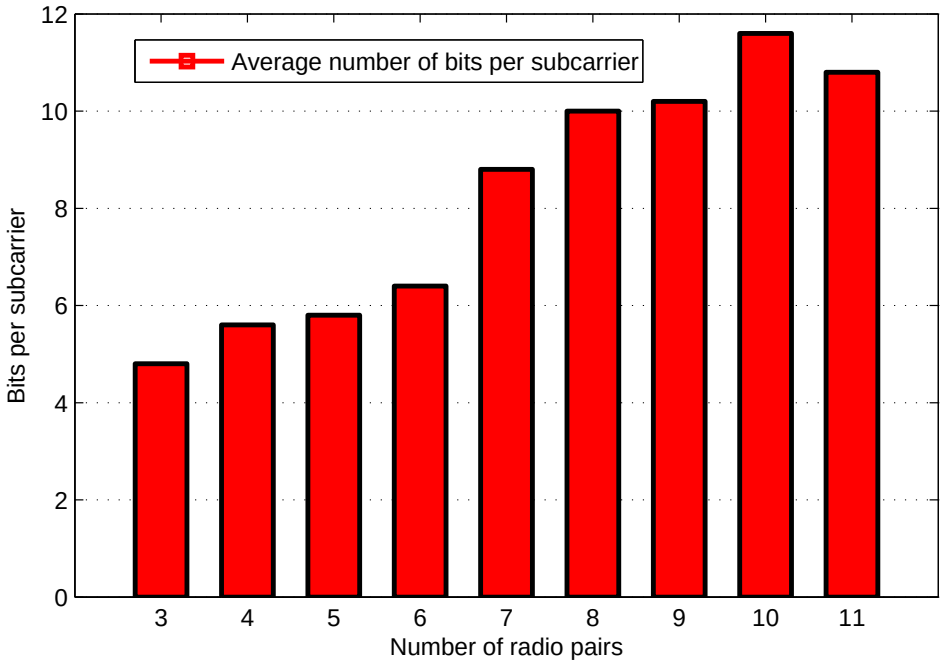

(a) Comparison on the subcarrier rate versus the number of users

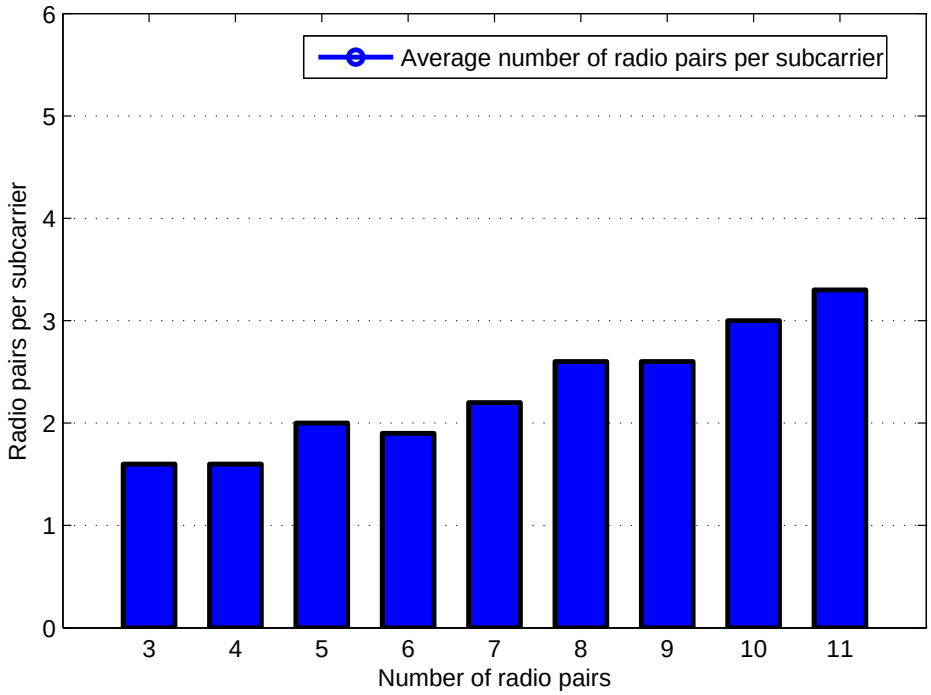

(b) Comparison on the number of CR pairs sharing a subcarrier versus the number of CRs

Figure 3.4: Effect of increasing system load

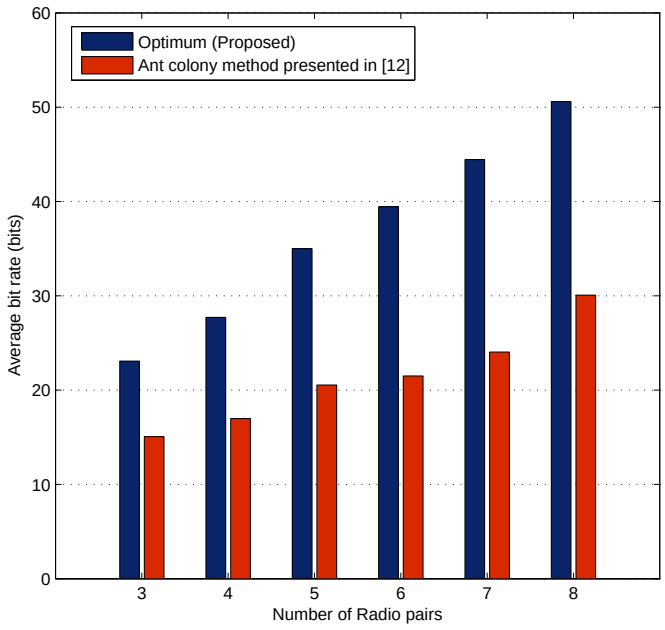

Figure 3.5: Average achievable rate, a comparison between the optimum solution and ACO-based suboptimum

Fig.3.5 shows that the results of ACO-based algorithm are indeed suboptimal, and about 30% less than the optimum bit rate. Moreover, the difference increases as the number of network users increases. The optimum solution by us provides a means to benchmark the optimality of solutions provided by ACO and other heuristic schemes.

3.4 Conclusions

We have proposed a novel framework that converts the DSA problem for multiuser OFDM-based CR system with frequency reuse to an equivalent MBLP problem, by introducing the notion of signal-to-interference plus noise difference and linearizing the nonlinear SINR constraint. The optimal solution for transmit power and subcarrier (white space) assignment can now be solved optimally and exactly without any relaxation and approximation. The equivalent problem can

then be optimally solved by using commercially available software. The optimal solution provides a benchmark for comparing the performance of the heuristic algorithms using ACO, GA or other methods.

Chapter 4

Nonparametric learning algorithms for auction-based dynamic spectrum access

Learning enables CRs to make more intelligent decisions by considering their past experiences. Depending on the available information, and to make better decisions, CRs can learn the channel availability, channel quality, and behavior of other CRs. In the next two chapters, we show how learning can be performed to improve the spectrum allocation process. Most recent studies about learning in CRs focus on learning the channel quality or the spectrum activities of PUs. In [83], the authors apply a hidden Markov model (HMM) to learn the PUs' traffic pattern so that while accessing the white space for transmission, the collision probability is kept under a certain limit. In [84], CRs learn the subcarrier availability by using an HMM. A CR ranks the subcarriers according to the likelihood that the subcarrier is unoccupied. Each CR then senses the subcarriers for transmission based on its order until the number of desired subcarriers has been achieved; as a result, there is

no necessity to sense all subcarriers before a decision is made. Partially observed Markov decision processes are applied to learn and exploit the white spaces in the channels in [85]. The authors derive an upper performance bound for the optimal policy when the probability distribution of channel availability is known. The authors also assume a parametric model for the unknown channel availability distribution, and propose a learning algorithm to learn the distribution.

Auction theory is an economics-originated method which has recently attracted attention, and has been applied to a wide range of spectrum management applications [86]. Spectrum regulators like FCC also propose auctions for selling or leasing spectrum. Other small operators like secondary operators can use auctions to dynamically purchase spectrum to provide services [87]. Double-sided auctions have also been proposed to allow the sellers to compete for the buyers who are able to select the best offer [88].

Channel allocation by an auction algorithm has been studied in [89]. The authors show the uniqueness in the Nash equilibrium for both uniform and exponential channel state distributions over $[0, 1]$. In [90], the authors consider auction-based spectrum sharing, where a PU assigns the spectrum to CR bidders according to the bandwidth requirement from CRs without degrading its own performance. The paper adopts OFDM framework, and applies Vickrey-Clarke-Groves (VCG) auction for bandwidth allocation. In [91], a spectrum manager allocates units of bandwidth to the demanding users by performing sequential VCG auctions, and the power auction applies to the situation in which a user wishes to acquire power by bidding against other users. In [92], the authors apply auction theory for scheduling CR transmissions. They perform a first price auction, and achieve a throughput performance which is very close to the optimum results given by centralized optimization.

A few works studied the effects of learning in DSA auctions. A single-carrier VCG auction with entry and monitoring fees is proposed in [93]. The CRs learn the valuation of other bidders for a channel with a nonparametric Bayesian learning algorithm. This enables the CRs to bid on a channel only if bidding on that channel improves the expected utility of the CR, where the utility is the capacity-to-cost ratio of a CR over time. With this strategy, the CRs reduce these participation costs by bidding on the channel only when they are likely to be successful, and therefore their utility will be improved. If the method is applied to the multi-carrier scenario, with the same predefined power is used in each channel: this means that all bids are treated equally with no prioritization. In [43], Fu et al. propose a reinforcement learning based algorithm for multi-carrier CR spectrum auctions. Each CR can bid for several channels, but it will only win one of them. Their proposed best response learning algorithm tracks the stochastic of channels and buffer, then values each channel based on the probable availability and quality of that channel. The authors show that their proposed best response learning algorithm improves the bidding strategy and the utility by increasing the number of transmitted packets and reducing the auction cost.

In this chapter, we present two nonparametric learning algorithms which aim to improve the total achieved capacity per unit of cost for autonomous CRs with multicarrier transmission. We consider a multi-carrier auction schema for assigning subcarriers to CRs which are able to learn their competitors' behavior and adjust their bids in order to maximize their individual utility, i.e. the achieved capacity per unit of cost. The CRs bid on a subcarrier based on their achievable capacity on that particular subcarrier. Unlike other studies, the CRs have the freedom to divide their power (and hence the achievable capacity) on the available subcarriers to increase or decrease their bid on these subcarriers. In other words, a CR is able to increase its bid on the high quality unoccupied subcarriers, which also

have relatively lower predicted cost, by increasing its power on that subcarriers. We formulate the bidding policy as a constrained convex maximization problem. Having an accurate estimation on others' valuation for subcarriers plays a critical role in this bidding policy. Due to the intractable state space of the learning problem, we adopt nonparametric learning models which are based on the Dirichlet process (DP) and Gaussian process (GP) regression. Both algorithms observe the highest bid of opponent CRs, and use it to learn the opponents' biding behavior and to predict the opponents' highest bid for the next time slot. Finally, we compare the total utility of the CRs equipped with DP-based and GP regression-based learning algorithms with that for CRs which do not use any learning algorithm.

4.1 System model

We consider a CR network with N equal OFDM subcarriers and K CR pairs which are trying to transmit their data over the subcarriers. Each CR pair consists of a CR transmitter and its designated receiver, and only the transmitting CRs will be involved in the bidding procedure, to bid for the unoccupied subcarriers for data transmission. The PUs are the license holders of these subcarriers and may become active on some or all of the subcarriers. We assume that a CSM has full and accurate information of all available subcarriers.

The CSM repeatedly and simultaneously leases the unoccupied time slots of subcarriers to CRs by running second price auctions. Fig.4.1 shows the system model and information exchange between a CR and the CSM. As it is shown in Fig.4.1, at the beginning of every time slot, the CSM broadcasts a binary vector ($\mathbf{v}$) with dimension equal to the number of subcarriers, to indicate whether the subcarriers have been occupied by PUs. The element which corresponds to an

unoccupied subcarrier in $\mathbf{v}$ will take the value of 1, otherwise it will have the value of 0. Under the DEU or spectrum commons model, we assume that all the subcarriers are available ($\mathbf{v} = \mathbf{1}$), and the CSM will not broadcast $\mathbf{v}$. The CSM also broadcasts the base price (R_0) which is equal for all the subcarriers. At time t, the k^{th} CR can estimate its achievable rate on the n^{th} subcarrier by:

$$\phi_{n,k}^t = B.\log_2\left(1 + \frac{p_{n,k}^t.G_{n,k}^t}{N_0}\right), \tag{4.1}$$

where B is the bandwidth, which is equal for all subcarriers, N_0 represents the double-sided power spectrum density of AWGN, and $p_{n,k}^t$ is the power that the k^{th} CR assigned to the n^{th} subcarrier at time t. The channel gain of the n^{th} subcarrier for the k^{th} CR is given by $G_{n,k}^t$, consisting of path loss, shadowing effect and fast fading components.

The CRs will then compute and submit their bid vectors ($\mathbf{b}_k^t$) based on their strategy. The CRs will bid for available subcarriers based on their achievable capacity and the predicted cost of the subcarrier. The details will be discussed in the next section. Each bid vector has the length of N, and the elements of the vectors are the bids of the CR for the respective subcarriers. After receiving the bid vectors, the CSM performs a second highest price auction for each subcarrier. Each subcarrier has only a single winner in the auction, and only the winner can use the subcarrier. However, it is possible for a CR to win more than one subcarrier.

The highest bid of a subcarrier will win the subcarrier, and the CSM creates the binary allocation matrix $\mathbf{A}^t$. The $(n,k)^{th}$ element of $\mathbf{A}^t$, $a_{n,k}^t = 1$, if the n^{th} subcarrier is allocated to the k^{th} CR; otherwise, its value will be zero. Moreover, it must satisfy the constraint:

$$\sum_{k=1}^{K} a_{n,k}^t \leq 1 \quad \forall n \in \mathcal{N}, \tag{4.2}$$

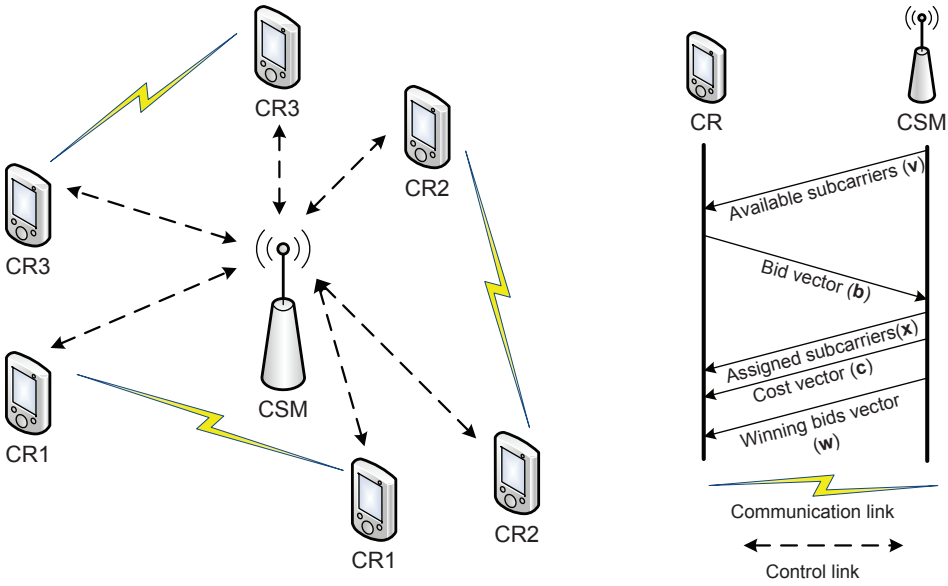

Figure 4.1: System model and information exchange.

which prevents the allocation of one subcarrier to more than one CR. The CSM will send each CR its respective allocation ($\mathbf{a}_k^t$) and cost ($\mathbf{c}_k^t$) vectors; therefore, the CRs will not be aware of other allocations. Moreover, the CSM will provide all CRs supplementary information, which is the vector that comprises the winning bids. The elements of the winning bids vector ($\mathbf{w}^t$) are the winning bids of the respective subcarriers. The $\mathbf{w}^t$ is the only information each CR can have about other CRs. If the auction requires an entry fee (ϵ) to bid for a subcarrier, the CSM will also broadcast the entry fee*, which is the cost that every CR must pay for bidding on each subcarrier regardless of the outcome in the auction.

In this model, all the CRs are assumed to have a common maximum transmit power (P_{max}), and have the freedom to assign a portion of this power to each preferred subcarrier with the objective to maximize their achievable rate, which differentiates our work from [93]. Here the CRs can prioritize the subcarriers to bid for. If a CR decides to bid higher by assigning more power on a subcarrier, it should reduce its bid on some other subcarriers.

*The CSM can broadcast a different entry fee at the beginning of each auction or keep a static entry fee. Here, we considered having the same entry fee for all auctions.

4.2 Problem formulation

In this section, we introduce the utility function and bidding policy for the auctions, with and without entry fee.

4.2.1 Auction without entry fee

Utility function

In a second highest price auction, the highest bidder wins the good and pays the second highest bid. It is proven that in this type of auction, the best strategy is to bid truthfully [94]. The k^{th} CR wins the n^{th} subcarrier if and only if $b^t_{n,k} > b^t_{n,-k}$, where $b^t_{n,-k}$ represents the bids for subcarrier n of all CRs except k. The winner has to pay the second highest bid which is given by $c^t_{n,k} = \max(b^t_{n,-k})$. The CR will be rewarded by the achieved rate. Thus, the utility of each CR can be considered as its reward (capacity) per unit of cost given by:

$$U^t_k = \sum_{n=1}^{N} a^t_{n,k} \frac{\phi^t_{n,k}}{c^t_{n,k}} \quad \forall k \in \mathcal{K}. \tag{4.3}$$

In (4.3), the utility not only depends on subcarrier allocation ($a^t_{n,k}$) and the cost ($c^t_{n,k}$) which are given by the auctioneer, it also depends on the achievable capacity ($\phi^t_{n,k}$), which changes based on the level of power allocated to each of the assigned subcarriers.

Bidding policy

Each CR will need to predict the cost of every subcarrier, based on the learning algorithm. In this subsection, we describe how CRs decide their bid on every subcarrier ($\phi_{n,k}$), based on the predicted cost which is denoted by $\check{c}_{n,k}$.

Without loss of generality, we assume that the predicted cost for all the subcarriers is known to the k^{th} CR. The determination of $\check{c}_{n,k}$ will be discussed in the next section. The predicted cost (others' highest bid) must be greater or equal to the base price (R_0).

$$\check{c}^t_{n,k} \geq R_0. \tag{4.4}$$

Thus, under the learned $\check{c}^t_{n,k}$, the optimal bidding policy for the k^{th} CR is given by:

$$\max_{p} \sum_{n=1}^{N} v^t_n \frac{\phi^t_{n,k}}{\check{c}^t_{n,k}}, \tag{4.5}$$

$$\text{subject to: } \sum_{n=1}^{N} p^t_{n,k} \leq P_{max}, \tag{4.6}$$

$$p^t_{n,k} \geq 0 \quad \forall n \in \mathcal{N}, \tag{4.7}$$

where v^t_n shows the availability of the n^{th} subcarrier at current time slot t. When the n^{th} subcarrier is occupied, $v^t_n = 0$, and therefore CRs will not bid on it. P_{max} is the maximum available power of the CR, and $p^t_{n,k}$ is the assigned power of the k^{th} CR to the n^{th} subcarrier.

The problem is convex and can be solved easily with convex programming methods. In (4.5), to maximize its instantaneous utility, the CR will place more power on the available subcarriers whose predicted costs and channel gains are

relatively lower and higher, respectively. Moreover, with this utility maximization, the subcarriers who suffer from a deep fade or predicted to have higher bids from other competitors are expected to receive no power, i.e. the CR will not bid on these subcarriers. This model allows the CR pairs with closer Tx-Rx distance and better channel qualities to compete for more subcarriers and achieve higher rate. On the other hand, it helps CR pairs with longer Tx-Rx distance to put their power only on the subcarriers with better quality and lower predicted bids in order to increase their winning probability. We will illustrate this using an example in our simulations in Section 4.4.

The total power consumption of the CR cannot be more than its maximum available power (4.6). The results of this optimization problem gives the optimum bid on every subcarrier ($b_{n,k} = \phi_{n,k}$) for each CR. However, these bids strongly depend on the CR's belief about the other CRs valuations (bids), for every subcarrier. In the next section, we will discuss about the learning of others' valuation.

Utility computation

As mentioned before, CRs' bids strongly depend on their belief about the other CRs' bids in which their statistics are usually unavailable. Therefore, the assigned subcarriers by the auctioneer might be only a subset of subcarriers that the CR has bid for. In other words, there is a probability of losing the auctions on some/all subcarriers. The CR will then recalculate its utility based on the assigned subcarriers, after the auctions outcomes are announced. At this step, the CR knows the exact value that it must pay for each assigned subcarrier ($c^t_{n,k}$) as well as the assigned subcarriers ($\mathbf{a}^t_k$). For the k^{th} CR at time t, this is given by:

$$\max_{p} \sum_{n=1}^{N} a_{n,k}^{t} \frac{\phi_{n,k}^{t}}{c_{n,k}^{t}}, \tag{4.8}$$

$$\text{subject to: } \sum_{n=1}^{N} p_{n,k}^{t} \leq P_{max}, \tag{4.9}$$

$$p_{n,k}^{t} \geq 0 \quad \forall n \in \{1 \dots N\}. \tag{4.10}$$

4.2.2 Auction with entry fee

In this section, we consider an auction which requires an entry fee of ϵ to bid for a subcarrier. This model of auction prevents CRs from bidding for those subcarriers for which their possibility of winning is not high [93, 95].

Utility function

Like other second price auctions, the bidder with the highest bid wins the good and pays the second highest bid. The cost for each subcarrier that has been assigned to a CR is given by $c_{n,k}^{t} = \max(b_{n,-k}^{t})$. Moreover, there is an additional entry fee (ϵ), which the CR has to pay for every subcarrier that it has bid for, regardless of the outcome on that particular subcarrier. Therefore, the total cost that the CR must pay is:

$$C_{total,k}^{t} = \sum_{n=1}^{N} a_{n,k}^{t} c_{n,k}^{t} + Q_k \epsilon \quad \forall k \in \mathcal{K}, \tag{4.11}$$

where Q_k is the total number of the subcarriers that the k^{th} CR has bid for. Similarly the total achievable capacity is:

$$\phi^t_{total,k} = \sum_{n=1}^{N} a^t_{n,k}\phi^t_{n,k} \quad \forall k \in \mathcal{K}. \tag{4.12}$$

The utility function for the auction with entry fee is different from that for the auction without entry fee. In the auction without entry fee, the utility is the total achieved capacity per unit of cost. Therefore, if a CR loses the auctions on all the subcarriers that it has bid for, it does not need to pay any cost, and its utility will be zero. On the other hand, in the auctions with entry fee, even if a CR loses all the auctions and obtains zero capacity, it must pay the entry fee for each subcarrier that it has bid for. Applying the utility function defined by (4.3) will not reflect this correctly as the utility remains zero regardless of the amount of the fee paid. Thus, for auctions with entry fee we adopt the following utility function which is defined in [93] :

$$U^t_k = \frac{\sum_{\tau=1}^{t-1}(1-\lambda)^{t-\tau}\phi^\tau_{total,k}+\phi^t_{total,k}}{\sum_{\tau=1}^{t-1}(1-\lambda)^{t-\tau}C^\tau_{total,k}+C^t_{total,k}} \quad \forall k \in \mathcal{K}, \tag{4.13}$$

where $0 \leq \lambda \leq 1$ is the forgetfulness factor. In (4.13), at time t, even if a CR does not get any subcarrier, it has to pay the entry fee, and it is accumulated to the previous costs.

Bidding policy

Finding the optimum bidding policy for (4.13), is an NP-hard problem, due to the nonlinear mixed integer utility function. Thus, in order to bid efficiently, we propose a heuristic method.

Based on the heuristic, we maximize the summation of the capacity to cost

plus entry fee ratio for every CR, because we know that a CR bids only for the subcarriers which are predicted to be successful. As a result, the heuristic bidding policy of the k^{th} CR is similar to the bidding policy for the auction without entry fee.

$$\max_{p} \sum_{n=1}^{N} v_n^t . \frac{\phi_{n,k}^t}{(\check{c}_{n,k}^t + \epsilon)}, \tag{4.14}$$

$$\text{subject to: } \sum_{n=1}^{N} p_{n,k}^t \leq P_{max}, \tag{4.15}$$

$$p_{n,k}^t \geq 0 \quad \forall n \in \mathcal{N}. \tag{4.16}$$

The CR will bid based on the results of (4.14). The effect of ϵ is similar to adding a value to the predicted cost before applying the water-filling algorithm.

Utility computation

After the auction, the CSM announces the assigned subcarriers and the costs that the CRs must pay. The CRs have the chance to redistribute their power on the assigned subcarriers in order to maximize their utility. The CRs already know the assigned subcarriers and their exact cost, as well as the entry costs that they have to pay. Therefore, at this stage, the problem of maximizing the utility given by (4.13) is not an NP-hard mixed integer nonlinear programming problem anymore. The utility is maximized only by maximizing the achievable capacity:

$$\max_{p} \sum_{n=1}^{N} a_{n,k}^{t} \phi_{n,k}^{t} \tag{4.17}$$

subject to: (4.15) and (4.16).

After we achieve the optimum power assignment to the allocated subcarriers, we can compute the utility from (4.13).

4.3 Learning and cost prediction

It is presented in the previous section that learning has a key role in the above formulations to decide $\check{c}_{n,k}^{t}$. Next, we propose suitable learning algorithms for the CRs in the auction-based system. We consider the system where the CSM informs each CR about its assigned subcarriers and the cost it must pay for every subcarrier. However, the CSM also broadcasts the winning bids ($\mathbf{w}$). Therefore, each CR is able to create a history of observations for every subcarrier ($\boldsymbol{o}_n$) which keeps the highest bid of other CRs on the previous time slots. Each CR updates its $\boldsymbol{O}$ by following the rule:

$$o_n^t = \begin{cases} w_n^t & a_{n,k}^t = 0 \\ c_{n,k}^t & a_{n,k}^t = 1, \end{cases} \tag{4.18}$$

where o_n^t is the highest bid of other CRs at time t on the n^{th} subcarrier. If the subcarrier is not assigned to the CR, o_n^t will be equal to the broadcasted w_n^t. On the other hand, if the subcarrier is assigned to the CR, then w_n^t shows its own bid. Thus, other CRs highest bid is the cost that the CR must pay for the assigned

subcarrier, and as a result, o_n^t equals to $c_{n,k}^t$.

In order to have an accurate prediction of the cost to transmit at the next time slot, the CRs must learn how the other CRs value the subcarriers from their past observations $\boldsymbol{O}$. A popular way of learning from the observed data is to use nonparametric approaches. Dirichlet process (DP) is a popular Bayesian nonparametric method due to its ease in updating the posterior distribution [96]. The Gaussian Process (GP) regression is a famous nonparametric regressive learning method in time series. Next we discuss about these nonparametric algorithms, and illustrate how they can be used to learn bidding behaviors of other CRs.

4.3.1 Using DP-based learning method for cost prediction

Dirichlet process

The Dirichlet distribution is a multivariate generalization of the Beta distribution. Consider an unfair coin with the probability of Heads to be q which is unknown. We represent the uncertainty about q with the Beta distribution:

$$f_q(q;\beta_1,\beta_2) = \frac{\Gamma(\beta_1+\beta_2)}{\Gamma(\beta_1)\Gamma(\beta_2)} q^{\beta_1-1}(1-q)^{\beta_2-1}, \tag{4.19}$$

where hyperparameters $\beta_1, \beta_2 > 0$ can be thought of as pseudocounts. So, a random variable q that is Beta-distributed with hyperparameters β_1, β_2 is denoted as: $q \sim Beta(\beta_1, \beta_2)$.

This concept can be extended to more than two events, for instance rolling a die. In this case, there are M possible events, and q_m represents the probability

of the m^{th} event. Thus, the Dirichlet distribution can be defined as:

$$f_{\mathbf{q}}(\mathbf{q};\beta) = \frac{\Gamma\left(\sum_{i=1}^{M}\beta_i\right)}{\prod_{i=1}^{M}\Gamma(\beta_i)}\prod_{i=1}^{M}q_i^{\beta_i-1}, \tag{4.20}$$

and denote as $\mathbf{q} = [q_1, q_2, ..., q_M] \sim Dir(\beta_1, \beta_2, \ldots, \beta_M)$ where $\mathbf{q} > 0$, $q_1 + q_2 + \cdots + q_{M-1} < 1$ and $q_M = 1 - q_1 - q_2 - \cdots - q_{M-1}$. The density is zero outside this $(M-1)$-simplex. $\boldsymbol{\beta} = (\beta_1, \beta_2, \ldots, \beta_M), \beta_i > 0$ is a set of parameters.

To define DP we should consider a probability space Θ and the probability distribution H on Θ. Let α and $\mathcal{G}$ be a positive number and a random distribution on Θ, respectively. For any finite measurable disjoint partition $(A_1, A_2, ..., A_M)$ of Θ, the probability vector $[\mathcal{G}(A_1), \mathcal{G}(A_2), ..., \mathcal{G}(A_M)]$ is random since $\mathcal{G}$ is random, where $\mathcal{G}(A_m)$ is the probability assigned to A_m and $\sum_{m=1}^{M}\mathcal{G}(A_m) = 1$.

According to [96], if

$$[\mathcal{G}(A_1), \mathcal{G}(A_2), ..., \mathcal{G}(A_M)] \sim Dir(\alpha H(A_1), \alpha H(A_2), ..., \alpha H(A_M)), \tag{4.21}$$

we say $\mathcal{G}$ is DP distributed with base distribution H and concentration parameter α, denoted as: $\mathcal{G} \sim DP(\alpha, H)$.

The parameters α and H play a very important role in the DP. The $H(A_m)$ is the mean of the DP. This means $\mathbb{E}(\mathcal{G}(A_m)) = H(A_m)$ for any measurable set $A_m \subset \Theta$. The parameter α, also known as strength parameter, is an inverse variance: $Var[\mathcal{G}(A_m)] = H(A_m)(1 - H(A_m))/(\alpha + 1)$. Thus, a larger α causes smaller variance and more concentration of the mass around the mean.

DP-based learning method

The DP-based learning method is used to calculate the posterior distribution of the bid values from the observation and the prior distribution of the bid values. In our discussions, we assume that a CR learns each subcarrier separately, and hence we illustrate using only one subcarrier. Therefore, without loss of generality, we drop the subscript of subcarriers from now on.

We assume that the CRs know the minimum and maximum possible bids. Therefore, it is possible to partition the bidding region (Θ) into M disjoint subsets, and denote them by $A_1, ..., A_M$. For instance, if the base price is set to unity and the maximum bid is 10, $A_1 = [1, 2)$ for $M = 9$. Assume that the observations until time t are denoted as $o^1, ..., o^t$, and let $h_m = \#\{i : o^t \in A_m\}$ be the number of observed values in A_m. Initially, we assume that the CRs do not have any prior information about the probability distribution of observations, and therefore, we let the prior distributions of observations, H, be a uniform distribution over the bidding region (Θ). For subsequent updates, given the prior distribution of observations, the posterior distribution can be updated as:

$$[\mathcal{G}(A_1), \mathcal{G}(A_2), ..., \mathcal{G}(A_M)]|o^1, o^2 ... o^t \sim Dir(\alpha H(A_1) + h_1, ..., \alpha H(A_M) + h_M). \tag{4.22}$$

In (4.22), the strength parameter and the base distribution are updated to $\alpha + t$ and $\frac{\alpha H + \sum_{i=1}^{t} \delta_i(A_m)}{\alpha + t}$, respectively, where δ_i is a point located at o^t and $h_m = \sum_{i=1}^{t} \delta_i(A_m)$. By adopting our notation used earlier, the posterior distribution in (4.22) can be written as:

$$\mathcal{G}|o^1, o^2 ... o^t \sim DP(\alpha + t, \frac{\alpha}{\alpha + t} H + \frac{\alpha}{\alpha + t} \frac{h_m}{t}). \tag{4.23}$$

As a result, the posterior distribution is a weighted average between the prior base distribution (H) and the empirical distribution ($\frac{h_m}{t}$), and as the number of observations increases, the weight of empirical distribution increases accordingly.

Cost prediction

To predict the cost, we should obtain the probability distribution of the other CRs possible bids. Having the past observations $(o^1, o^2..., o^t)$ and their prior distribution, from (4.23), we can compute the posterior probability distribution of observations, and use it to predict the cost for the next time slot.

Let F be the CDF of the distribution in (4.23). We define the parameter $0 < \gamma \leq 1$ as the probability that the predicted cost, $\check{c}^{t+1}$, is higher than the actual observation, o^{t+1} (either cost or winning bid), then the predicted cost is given by:

$$\check{c}^{t+1} = F^{-1}(\gamma). \tag{4.24}$$

A higher value of γ brings a higher probability of winning the subcarrier; however, it can also causes over bidding on some subcarriers or not bidding on a subcarrier because of the high predicted cost. In practical implementation, the CRs can be made to change their γ value adaptively according to consecutive success or failure in bidding. A CR which continuously loses the auctions can increase its γ value to bid at a higher value on fewer subcarriers. In vice a versa, a CR which has won most of the previous auctions can bid lower on more subcarriers by reducing its γ to avoid over bidding.

4.3.2 GP regressive learning method for cost prediction

Gaussian process regression

Let us assume that given the sample set $\mathcal{S}_t = \{(\boldsymbol{x}_i, y_i)_{i=1}^t\}$, where $\boldsymbol{x}_i \in \mathcal{X} \subset \mathbb{R}^L, y_i \in \mathbb{R}$, where $\mathbb{R}$ represents the set of all real numbers, and $y_i = g(\boldsymbol{x}_i), \forall \boldsymbol{x}_i \in \mathcal{X}$, $g : \mathcal{X} \to \mathbb{R}$ is an unknown smooth function. Here, t denotes the sample size, and L denotes the number of covariates. Let us denote a multivariate Gaussian with mean $\boldsymbol{m}$ and covariance Σ by $\mathcal{N}(\boldsymbol{m}, \Sigma)$. We are interested in estimating the function g at a new point $\boldsymbol{x}_{t+1}$, denoted by $\check{g}(\boldsymbol{x}_{t+1})$. This is a non-linear regression problem.

In GP regression, we assume that the process $\{y_i, \boldsymbol{x}_i \in \mathcal{X}\}$ is a GP. Here, a GP is a collection of random variables such that any finite number of them are jointly Gaussian [97]. A Gaussian variable is fully characterized by its mean and covariance. Therefore, in order to construct a GP regression, let us assume that $\mathbb{E}(y_i) = 0$, and that the covariance function is defined as $\mathbb{E}(y_i, y_j) = k(\boldsymbol{x}_i, \boldsymbol{x}_j)$, where $k(\cdot, \cdot) : \mathcal{X} \times \mathcal{X} \to \mathbb{R}$ is an smooth positive definite function. In our experiment, we use the Radial basis function (RBF) kernel function for covariance function that is defined by [98]

$$k(\boldsymbol{x}_i, \boldsymbol{x}_j) = \exp\left(-\frac{1}{\rho^2}\|\boldsymbol{x}_i - \boldsymbol{x}_j\|_2^2\right), \tag{4.25}$$

where $\|\boldsymbol{x}\|_2 = \sqrt{x_1^2 + \cdots + x_L^2}$. The parameter ρ is the kernel parameter that can be estimated using cross-validation or other selection techniques [98].

By assumption, we have $y_{t+1} = g(\boldsymbol{x}_{t+1}) \sim \mathcal{N}(0, k(\boldsymbol{x}_{t+1}, \boldsymbol{x}_{t+1}))$. Now, given the

samples $\mathcal{S}_t$, we obtain

$$[\boldsymbol{y}, y_{t+1}] \sim \mathcal{N}\left(0, \begin{pmatrix} \mathbf{K}_{\mathcal{S}_t} & \mathbf{k}_{\mathcal{S}_t, \boldsymbol{x}_{t+1}} \\ \mathbf{k}_{\boldsymbol{x}_{t+1}, \mathcal{S}_t} & k(\boldsymbol{x}_{t+1}, \boldsymbol{x}_{t+1}) \end{pmatrix}\right), \tag{4.26}$$

where

$$\mathbf{K}_{\mathcal{S}_t} := \begin{pmatrix} k(\boldsymbol{x}_1, \boldsymbol{x}_1) & \dots & k(\boldsymbol{x}_1, \boldsymbol{x}_t) \\ \dots & & \\ k(\boldsymbol{x}_t, \boldsymbol{x}_1) & \dots & k(\boldsymbol{x}_t, \boldsymbol{x}_t) \end{pmatrix}, \tag{4.27}$$

$\mathbf{k}_{\boldsymbol{x}_{t+1}, S_t} := [k(\boldsymbol{x}_{t+1}, \boldsymbol{x}_1) \dots k(\boldsymbol{x}_{t+1}, \boldsymbol{x}_t)]$ and $\boldsymbol{y} := [y_1, \dots, y_t]$ [99]. To predict the value of the function g at $t+1$, we need to compute the conditional probability of $y_{t+1} = g(\boldsymbol{x}_{t+1})$ under the observation x_{t+1}. From [98], it can be shown that:

$$y_{t+1} | (\boldsymbol{x}_1, y_1), \dots, (\boldsymbol{x}_t, y_t), \boldsymbol{x}_{t+1} \sim \mathcal{N}\left(\mathbf{k}_{\boldsymbol{x}_{t+1}, \mathcal{S}_t} \mathbf{K}_{\mathcal{S}_t}^{-1} \boldsymbol{y}, k(\boldsymbol{x}_{t+1}, \boldsymbol{x}_{t+1}) - \mathbf{k}_{\boldsymbol{x}_{t+1}, \mathcal{S}_t} \mathbf{K}_{\mathcal{S}_t}^{-1} \mathbf{k}_{\mathcal{S}_t, \boldsymbol{x}_{t+1}}\right), \tag{4.28}$$

where the covariance structure is the Schur-complement of the matrix $[K]_{i,j} = k(\boldsymbol{x}_i, \boldsymbol{x}_j)$ for $\boldsymbol{x}_i \in \mathcal{S}_t \cup \boldsymbol{x}_{t+1}$. Then, the prediction involves sampling from the above conditional density function. The Gaussian random variables are concentrated around their mean, therefore, we take the mean of the conditional as the prediction:

$$\check{y}_{t+1} = \check{g}(\boldsymbol{x}_{t+1}) = \mathbf{k}_{\boldsymbol{x}_{t+1}, \mathcal{S}_t} \mathbf{K}_{\mathcal{S}_t}^{-1} \boldsymbol{y}, \tag{4.29}$$

which will be used for predicting the observations of the subcarriers. The variance term given in (4.28) is an indication of how good is this prediction statistically.

GP regression-based learning method

In order to apply GP regression to learn the bidding behavior of other CRs, it is very important to select proper values for y_i and $\boldsymbol{x}_i$. Let us recall that the observation for all subcarriers at time t are stored in vector $\boldsymbol{o}^t \in \mathbb{R}^N$, and $\boldsymbol{o}^1, \ldots, \boldsymbol{o}^t$ are available, where N denotes the number of subcarriers. The goal is to predict the observations for all subcarriers ($\check{\boldsymbol{o}}^{t+1}$), using GP regression. Implicitly, we assume that o_n^{t+1}, the highest bid of other CRs for subcarrier n at time $t+1$, depends on $\boldsymbol{o}^1, \ldots, \boldsymbol{o}^t$ for all $n = 1, \ldots, N$.

In order to use GP regression, we construct the covariates vector of size $L = lN$

$$\boldsymbol{x}_{t+1} = \left[o_1^t - o_1^{t-1}, \ldots, o_1^{t-l+1} - o_1^{t-l}, \quad \ldots \quad , o_N^t - o_N^{t-1}, \ldots o_N^{t-l+1} - o_N^{t-l}\right], \quad (4.30)$$

and the response variable $y_{n,t+1} = \check{o}_n^{t+1}$, $n = 1, \ldots, N$. The length of time samples is shown by l, which is arbitrary selected. The covariates vector is defined to track the changes of observations. In GP regressive learning method we do not consider subcarriers independent of each other, and therefore, the covariates vector consists of values from all subcarriers observations.

Now, let us define sample sets $S_{n,t} := \{(\boldsymbol{x}_i, y_{n,i})_{i=1}^t\}$ for all $n = 1, \ldots, N$. By applying (4.29), we obtain

$$\check{o}_n^{t+1} = \check{c_n} = \mathbf{k}_{\boldsymbol{x}_{t+1}, \mathcal{S}_{n,t}} \mathbf{K}_{\mathcal{S}_{n,t}}^{-1} [y_{n,1} \ldots y_{n,t}]^\top, n = 1, \ldots, N. \quad (4.31)$$

From (4.31), each CR computes its predicted cost for every subcarrier. In practice in order to avoid complex computations, we can restrict the sample size and set $S_{n,t} := \{(\boldsymbol{x}_i, y_{n,i})_{i=t-\tau}^t\}$.

4.3.3 Iterative steps of the proposed scheme

Now, we summarize all the bidding and the utility maximization procedure for the k^{th} CR at time t. The required steps are as follows:

(1) The CR computes the predicted cost of each subcarrier either using DP-based learning method from (4.24), or using GP regression-based learning from (4.31).

(2) The CR computes the bids using either (4.5), or (4.14) in auctions without and with entry fee, respectively.

(3) The CR submits its bid vector to the CSM.

(4) The CSM performs the auction, and informs each CR about its assigned subcarriers and their cost.

(5) The CR pays the cost to the CSM, and maximizes its utility using either (4.8) or (4.17) in auctions without and with entry fee, respectively.

(6) The CR updates its observation matrix using (4.18).

Each CR goes through the above process at each time slot. In practice the CR can perform the first step right after the last step of the previous time slot, because at that time all the required information for cost prediction is available.

4.4 Numerical results

In this section, we present and discuss our simulation results. We consider a coverage area of 100 square meters. The propagation model consists of path

Table 4.1: Comparison of average utility between CR pairs using learning and Myopic algorithms

CR pair 1, CR pair 2	DP learning	Myopic
DP learning	1.6106, 1.7730	1.7270, 1.7084
Myopic	1.5391,1.8764	1.5540, 1.7082

loss, shadowing effect and fast fading (similar to the previous chapters). In the DP-based learning method, we begin with a uniform prior distribution, and set $M = 100$ and $\alpha = 1$. In GP regression-based learning method we set $l = 5$.

The utility of the CRs equipped with our proposed nonparametric learning schemes is compared with CRs using a Myopic algorithm as their bidding policy. The only difference of Myopic-based and learning-based CRs is the way that they bid for the subcarriers. Myopic-based CRs make no prediction for the costs, therefore, they bid for subcarriers based on their maximum achievable capacity given by a water-filling algorithm. After the announcement of the auction results both Myopic-based and learning-based CRs recalculate their utility following the procedures described in Section.4.2.1 or Section.4.2.2.

4.4.1 Auction without entry fee

Initially, we consider a simple system with two CR pairs ($K = 2$) and two subcarriers ($N = 2$). We randomly place the two CR pairs, and investigate their bidding behavior in 2000 time slots. Table 4.1 presents a comparison between the average utility of CRs, when they are using DP-based learning method and Myopic. When both CRs use DP-based learning method to bid for the subcarriers, we observe that both CR pairs have an average utility which is higher than the case where both using Myopic. For the cases that either of them applies DP-based learning method, the DP-based CR can achieve higher utility than the case when it uses Myopic. In other words, applying DP-based learning method gives

an improvement over applying a Myopic strategy.

In Fig.4.2, we illustrate and compare the bidding procedure of Myopic, DP-based, and GP regression-based CRs in a system with two subcarriers and two CRs. At the 130^{th} time slot ($t = 130$), CR 1 has a much better channel gain than CR 2 on subcarrier 1, while none of them experiences high channel gain on subcarrier 2. As it is shown in the figure, only GP regression-based CR 2 intelligently divides its power and wins the subcarrier 2. At the time slot 135, both CRs do not experience high channel gain on both subcarriers. Learning helps DP-based and GP regression-based CRs to concentrate their bids on the subcarrier that is predicted to have higher utility, but Myopic CRs bid on both subcarriers. As a result, all learning based CRs won a subcarrier, while Myopic CRs could not even satisfy the base price and no subcarrier is assigned to them. At the 141^{th} time slot, subcarrier 2 had a better channel gain for both CRs, but the cost prediction led the DP-based and GP regression-based CR 2 to bid only on subcarrier 1, and win it. On the other hand, Myopic CR 2 bid on subcarrier 2 where the CR 1 has a higher bid. Therefore, at this time slot Myopic CR 2 could not get any subcarrier. This illustration shows that how learning based cost prediction increases the success probability in bidding.

In Fig.4.3, we assumed a system with two subcarriers and two CR pairs. Fig.4.3 provides a comparison of the average utility as a function of time for the cases where both CRs are using Myopic, DP-based learning method and GP regressive learning method as their bidding policy. As the number of time slots increases, the difference between the learning-based CRs and Myopic CRs slightly increases. The increase diminishes after 1000 time slots, which shows that the learning algorithms converged to a stable state. Moreover, the results also indicate that both learning algorithms have achieved the same performance.

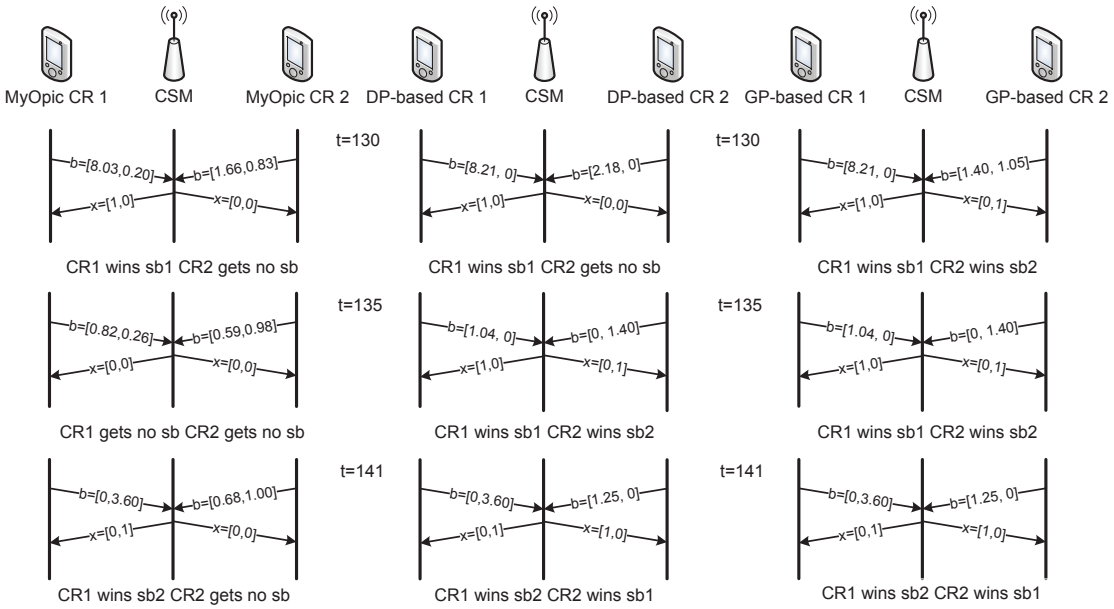

Figure 4.2: Illustration of bidding process for Myopic and learning based CRs at $t = 130, 135, 141$ time slots. $\mathbf{b}$ is the bidding vector, and $\mathbf{x}$ is the subcarrier assignment vector

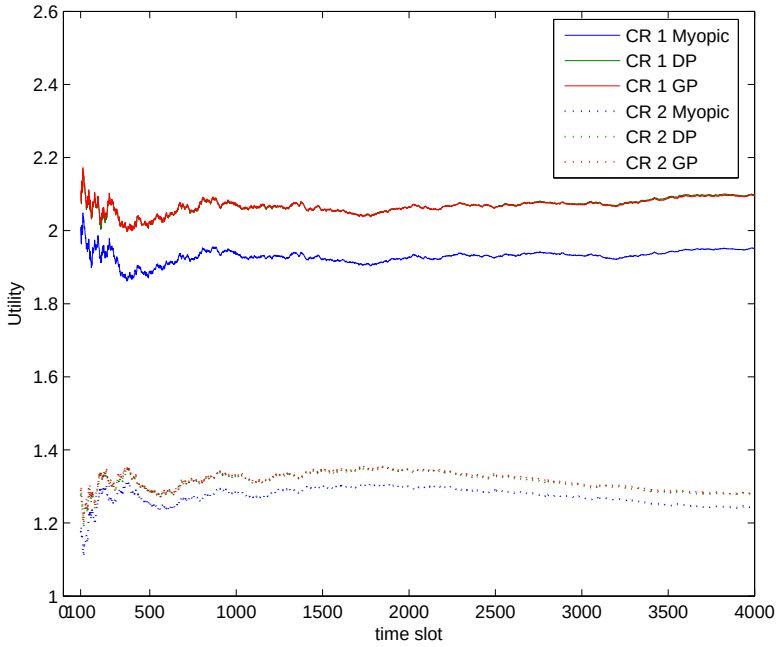

Figure 4.3: Average total utility in different time slots

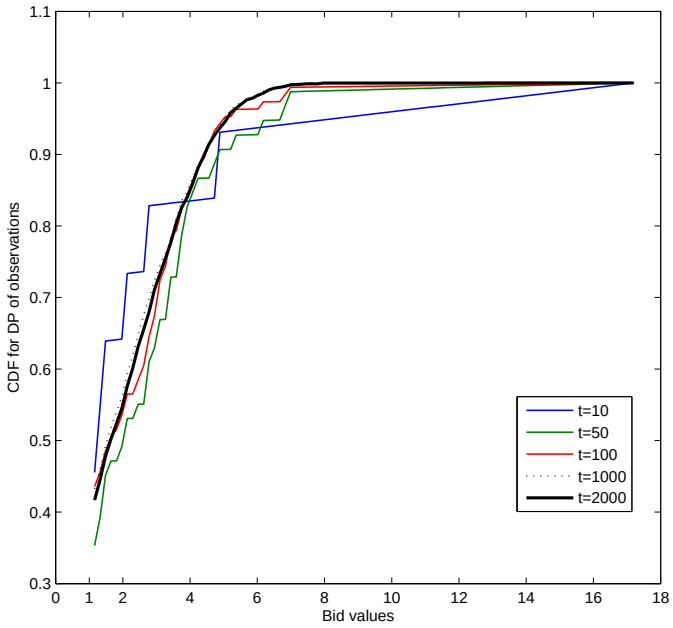

Figure 4.4: The convergence of learning the bidding behavior of competitors over time for CR 1 on subcarrier 1

The learning evolution of DP could be illustrated by the changes of the CDF for DP of observations over time. Fig.4.4 shows the CDF for DP of observations curve for CR 1 on subcarrier 1 in the aforementioned system for Fig.4.3 at different time slots. The curve initially has sharp changes, but after receiving more samples the curve becomes smooth, and has little changes in subsequent updates. This shows that the learning algorithm converged after 1000 auctions. We set the base price (R_0) to unity and due to the channel conditions and prediction about the opponents, it is possible that a CR does not bid on a subcarrier. As a result, it is possible that the other CR wins the subcarrier by only bidding at the base price. Thus, Fig.4.4 shows that CR 1 believes that the probability of the cost being the same as the base price on subcarrier 1 is 0.4.

To ensure that applying the proposed learning methods helps the CRs to improve their utility in all possible locations, we randomly relocated two CR pairs in a system with two subcarriers for 100 times, and computed their average utility

Table 4.2: Comparison the average utility of CRs over 100 different locations

CRs	Myopic	DP	GP
CR 1	1.4418	1.5387	1.5355
CR 2	1.2036	1.2736	1.2718
Total	2.6454	2.8123	2.8073

on each location. In this study, the average utility of each location is taken over 2000 time slots. Table 4.2 shows the average utility over 100 locations. From the table we can conclude that applying the DP-based learning method and/or GP regression-based learning method significantly increases the utility.

Fig.4.5 presents the overall average utility of 16 CRs. In this scenario, we considered a system with 16 CR pairs, competing for 8 subcarriers initially. Then, we increased the number of subcarriers to 16 and 32 to compare the average utility of CRs under different competition schemes. When the number of subcarriers is lower, the competition among CRs will be higher. The figure shows that the overall utility of the system is higher when the CRs are equipped with the learning algorithms, and the difference increases as the number of available subcarriers increases.

In order to statistically investigate the performance of the learning method in the aforementioned system, we provide the box plots of the achieved utilities of Myopic, DP and GP regression-based CRs in Fig.4.6. Although the difference between the performance of Myopic and learning methods is not high when there are 8 subcarriers available, the learning algorithms perform much better when the number of subcarriers increases. The box plots illustrate that the DP-based learning method and the GP regression-based learning method performed statistically similarly.

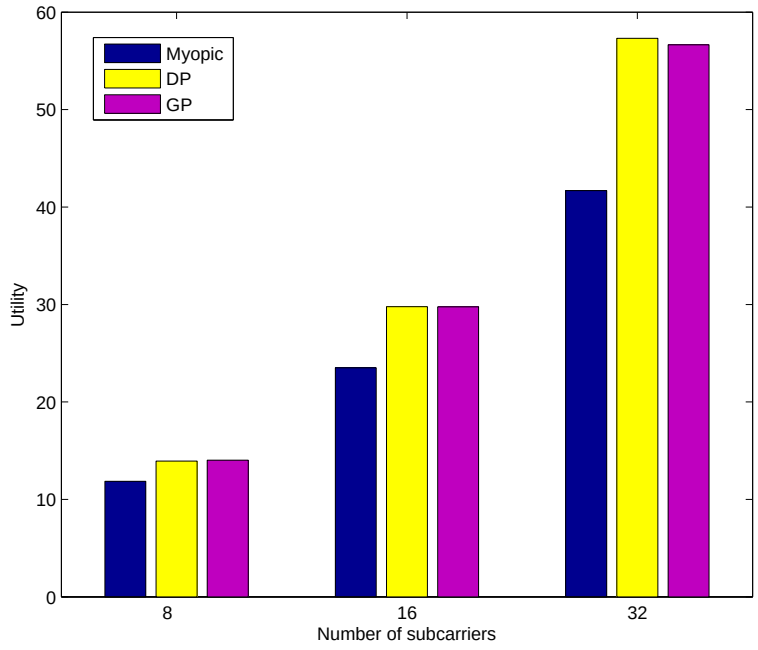

Figure 4.5: Comparison of the proposed methods with Myopic method for 16 CRs in systems with different number of subcarriers.

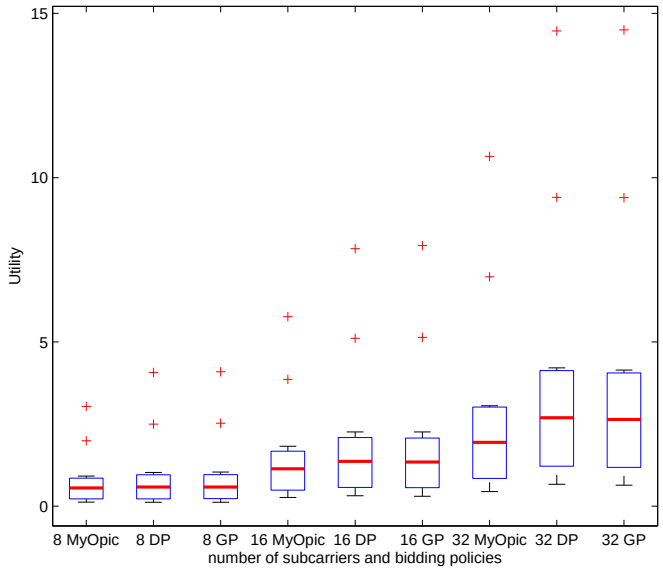

Figure 4.6: Comparison of the utility in systems without entry fee using box plots. The thick red lines denote the median of achieved utility, the lower and upper sides of the box represent the 25% and 75% quantiles and the black line stands for the outliers.

4.4.2 Auction with entry fee

An Auction with entry fee has the additional cost of participation in the auction. Therefore, focusing on the subcarriers which have a higher chance of winning becomes more important for CRs.

We consider an entry fee of 1 for a system with 8 subcarriers and 16 CRs. Later, we increase the number of available subcarriers in the system to 16 and 32. Fig.4.7 shows the overall average utility of CRs adopting Myopic, DP-based learning method and GP regression-based learning method for their bidding policies on the aforementioned scenario over 2000 time slots. The overall average achieved utilities of CRs adopting learning methods are significantly higher than the Myopic CRs, regardless of the number of available subcarriers. Fig.4.8 gives the box plots of the aforementioned simulations. The box plots statistically illustrate that adopting learning algorithms significantly improves the average utility of CRs regardless of the number of subcarriers in the system. Similar to Fig.4.6, Fig.4.8 shows that statistically neither of the learning algorithms outperforms the other one. In addition, Fig.4.8 shows that by adopting learning algorithms the CRs with lower utility also significantly improve their utility.

To investigate the effect of entry fee on utility of CRs, we compared the utility of the CRs which are applying different bidding policies in systems with different entry fees. Fig.4.9 presents the changes in average utility of the CRs when the entry fee increases. As expected, the increase in the entry fee reduces the average utility. It also slightly reduces the difference between the utility of CRs. Fig.4.9 also shows that even with different entry fees, the learning-based CRs still achieve higher utility than the Myopic CRs and an increase/decrease of the entry fee will not affect it.

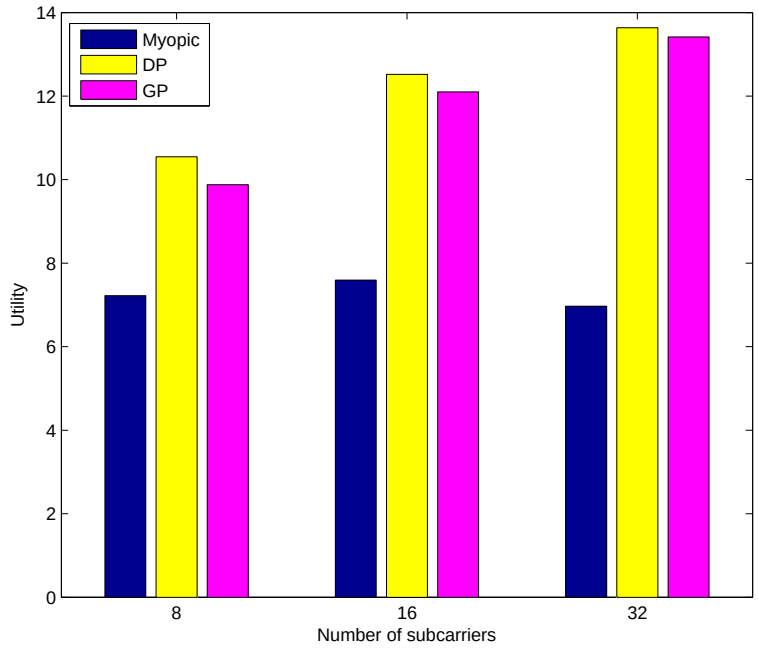

Figure 4.7: Comparison of the proposed methods with Myopic method for 16 CRs in systems with different number of subcarriers and having entry fee.

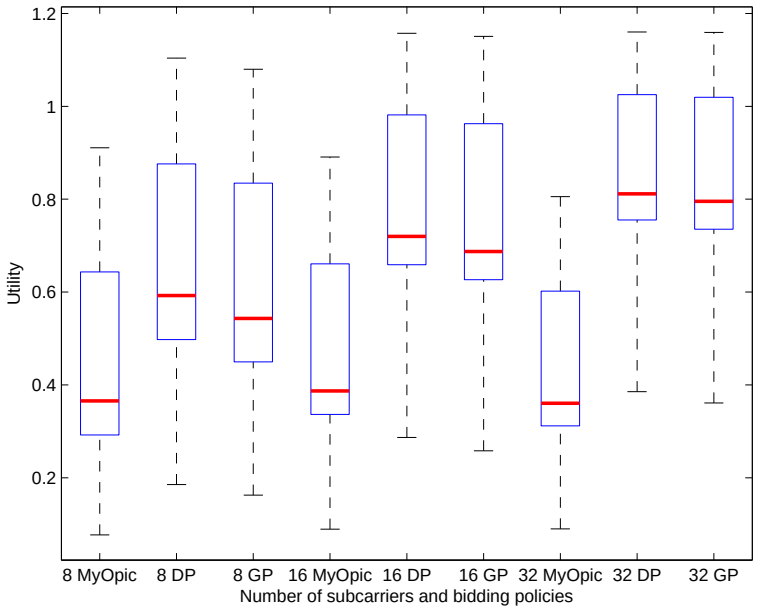

Figure 4.8: A comparison of the utility in systems with entry fee using box plots. The thick red lines denote the median of achieved utility, the lower and upper sides of the box represent the 25% and 75% quantiles and the black line stands for the outliers.

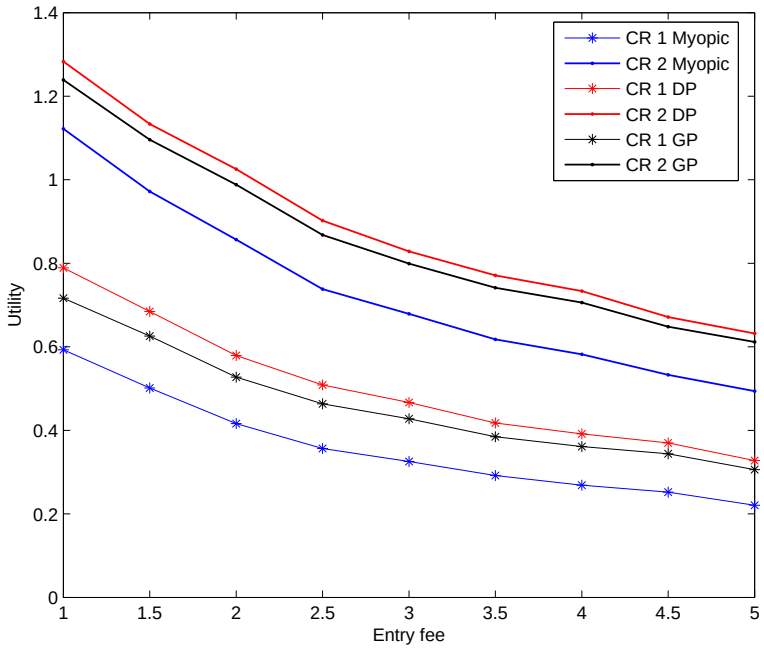

Figure 4.9: Utility of learning based CRs compared with Myopic CR having different values for entry fees.

4.5 Conclusions

In this chapter, we modeled DSA as repeated auctions, where CRs were bidding for multiple subcarriers to transmit their data. The CRs were free to manage their bid on every subcarrier by dynamically changing their power assigned to each subcarrier. We proposed DP-based and GP regression-based learning methods to learn the bidding behaviors of other CRs. Both learning methods significantly improved the utility, and the improvement in the utility was more significant in auctions with entry fee. We simulated the proposed schemes for a multiple-carrier CR system, and also investigated the performance of our proposed learning methods in systems with different competition scenarios. Both proposed nonparametric learning algorithms achieved similar maximum utility performance.

Chapter 5

Hidden Markov model-based learning algorithm for distributed dynamic spectrum access

In an OSA model, to detect white spaces, CRs have to frequently sense the channels in the spectrum band under consideration. Some commonly known sensing techniques include energy detection, matched filter and the cyclostationary feature detection [7].

Although the CR can have two interfaces to support concurrent data transmission and spectrum sensing [88], unfortunately, most CRs are unable to sense all the targeted subcarriers concurrently [100]. If the CRs need to sequentially sense all the subcarriers before a decision is made on which subcarrier to use, spectrum sensing can waste a significant amount of the scarce spectrum resources. For example, compare an algorithm which on average needs to sense four subcarriers before it can find a subcarrier to transmit, to one which on average needs to sense only two subcarriers: the latter has the advantage that the transmission can begin

earlier, whilst in the earlier case, white spaces remain unused for four sensing durations. The authors of [100] extensively discussed this matter, and have proven that the throughput increases, with having a prediction of PUs' activity. In [101], the authors have collected real data, and by analyzing these data they have shown that the wireless activity in real channels is predictable.

These findings motivate the idea to search for an intelligent predictive method so that CRs can learn from the past subcarrier utilization, and predict which subcarrier is likely to be available for transmission. By prioritizing the order in which subcarriers are sensed according to the likelihood that the subcarriers are available, the probability that a CR gets a subcarrier upon its first attempt increases significantly. In other words being able to learn from the previous experiences helps to find the appropriate time and frequency bands to sense, and the predicted knowledge of the subcarrier status helps the CR to exploit the spectrum more efficiently.

For the first time, Clancy et.al. proposed a Markov chain approach to model the channel occupancy in [102]. The authors model the channel usage from one time period to another using HMM in a manner similar to that used in speech processing [103]. Later, the authors of [104] discuss applying machine learning methods for prediction of white spaces in OSA. Further studies employ HMM or other prediction methods to either sense the most probable idle channel first, or reduce frequency switching by predicting the longest white space.

In [50], the authors employ an HMM to predict the occupancy and availability of a channel. They assume 4 channels with 4 PUs, with the activity durations of each channel to be modeled by Poisson distributions. An HMM is trained for each channel. The trained HMM predicts the presence of PUs to avoid transmission collision. The CR will occupy a channel until it predicts that the PU will become

active, and then it will switch to an idle channel. Simulation results show that the probability of collision with the PU is reduced, compared to the random selection case. However, the accuracy of the HMM predictions is not presented. The authors in [105] apply prediction to reduce the number of channel sensings to be performed. They propose a novel artificial neural network (ANN) to predict the channel state and to reduce the sensing energy. The paper also presents the ANN's prediction accuracy. The ANN accuracy is compared with the accuracy of HMM in [106].

An entropy-based prediction method is introduced in [107]. The authors find the correlated channels to optimize the sensing strategy. In [108], the authors applied maximum likelihood to predict the length of the idle period of each channel. By selecting the channel with the longest predicted idle time, they achieved a reduction in the number of channel switchings needed.

In this chapter, we present an HMM-based method to learn the behavior of PUs on a subcarrier and predict their activity in the next time slot. The number of states in our proposed HMM is not fixed and grows as the training proceeds. We demonstrate that our model can avoid propagation of error if an error occurs. The accuracy of the proposed HMM is studied through simulation. We use a 4-channel system to illustrate the average number of sensings to be performed by a CR, before it can successfully obtain a white space.

5.1 Hidden Markov processes

The spectrum under consideration is divided into N subcarriers and each PU, if it transmits, will occupy at least one of the subcarriers. The presence of PUs on a subcarrier is represented with a "1" and the absence of PUs is shown with a "0". Some simplifications are made in our learning model. We assume that spectrum

sensing is performed periodically (which is known as the time stamp), and the sensing is ideal, i.e., the effects of noise, missed detection and false alarm errors are negligible. A CR uses an HMM-based approach to learn about the PU's usage pattern on each subcarrier through observing the outcomes of the sensing. Using the trained HMM, the CRs predict the availability of the subcarriers for possible usage in the next time slot through the algorithm to be introduced shortly.

A Hidden Markov Process (HMP) is a doubly stochastic process with hidden states which generate observations [103]. It is denoted mathematically as $\{\mathbf{x}_t, \mathbf{y}_t; t \in \mathbb{N}\}$, where t denotes the time stamp index which take an integer number. $\mathbf{x}_t$ is the J-state hidden stochastic process, and $x(t) \in \mathcal{S}$, where $\mathcal{S}$ is the finite set of J possible states whose transition probabilities is described by the $J \times J$ matrix denoted by $\mathbf{A}$. The $\mathbf{y}_t$ is the stochastic process of the observations, and $y(t) \in \mathcal{O}$, where $\mathcal{O}$ is the finite set of possible observations with M possible outcomes. The distribution of the observation outcomes at each state is described by the respective column vector of the $J \times M$ emission matrix $\mathbf{B}$. The mathematical model that can generate an HMP is called an HMM [103]. The compact notation of $\lambda = \{\mathbf{A}, \mathbf{B}, \pi\}$ is usually used to represent an HMM. In this notation, the initial state distribution is shown by π.

There are some challenges in applying HMM; examples are model selection and parameter adjustment. Moreover, we should care about the overfitting and underfitting of the model as well [109]. By model selection we mean selecting the number of states and/or their possible transitions in a way that they describe the data in the best way. Parameter adjustment refers to adjusting the parameters, e.g. state transition probabilities and/or emission probabilities in the way that maximizes the likelihood of the data from the selected model. Overfitting and underfitting are more related to the training data. Various reasons may cause overfitting and underfitting, and one of the most common reasons is insufficient

amount of training data.

5.1.1 Conventional hidden Markov model

Given a sequence of observations, the Baum-Welch algorithm (BWA) [103] is the most commonly used method to compute the optimum λ. The BWA is an optimization technique that computes the maximum likelihood for HMM. In channel state prediction there are only two possible observations: idle or occupied channel, which means $\mathcal{O} = \{0,1\}$. To be able to predict, we have to gather the information from the channel behavior in the past time slots. We therefore need to observe the channel for T time slots, and save it as our observation sequence Y_T. Having sufficient observations, the HMM (λ) channel state for next time slot can be predicted by

$$\hat{y}(t+T+1) = \begin{cases} 1 & P(\zeta,1|\lambda) \geq P(\zeta,0|\lambda) \\ 0 & P(\zeta,1|\lambda) < P(\zeta,0|\lambda), \end{cases} \tag{5.1}$$

where $\zeta = \{y(t), y(t+1), ..., y(t+T)\}$.

Here, we only know the observations and their sequence, while the number of states, their transitions probabilities, and the initial state distribution are unknown. Therefore, we select the number of states (J) based on our experience, and apply BWA to achieve the optimum λ. Before applying BWA, we set the values of π arbitrarily. Since there is no information about the current state and previous states at the time when parameters are estimated by BWA, hereafter we shall refer to this type of HMM as an unknown-state sequence HMM (USS-HMM). The USS-HMM needs an online training for each prediction, because the optimum λ needs to be computed for ζ with different initiation time slots (t).

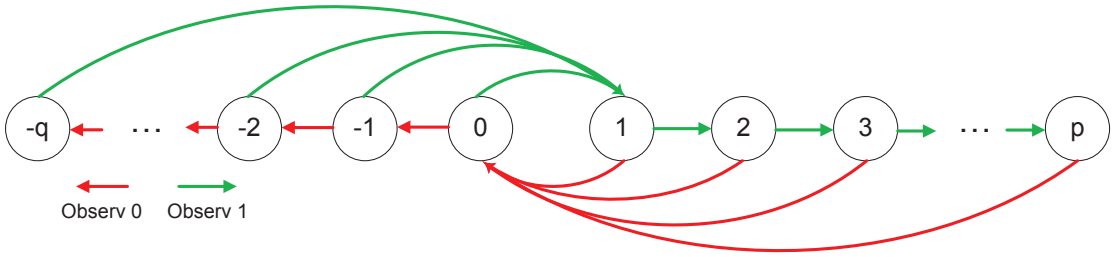

Figure 5.1: Proposed HMM state transition

5.1.2 Proposed hidden Markov model

In this work, we propose an HMM which can be trained offline and without a predefined number of states. In other words, we let the proposed HMM learn the number of its states from the training data. The proposed HMM knows the state sequence as well as the observation sequence. Thus, we call the proposed HMM known state sequence HMM (KSS-HMM). Given the current observation, the states sequence, and the HMM (λ), the channel state for the next time slot will be predicted by

$$\hat{y}(t+1) = \begin{cases} 1 & P(S(t),1|\lambda) \geq P(S(t),0|\lambda) \\ 0 & P(S(t),1|\lambda) < P(S(t),0|\lambda), \end{cases} \tag{5.2}$$

where $S(t)$ is the HMM state at time slot t. The actual state of the HMM is hidden, and the observation symbols are the only observable that the system has. Thus, to have the knowledge of states, we define the state transition in our model based on the run-length of each observed symbol as it is shown in Fig.5.1. The negative states represent that the subcarrier is unoccupied, and the positive states represent that the subcarrier is occupied by the PU. By observing a one, the run length increases and the system moves to the next state, and we go back to the state zero after observing a zero. The system will sequentially move to a more negative state by observing a zero, and will jump forward to the state one immediately after observing a one. If there are insufficient positive or negative states which

correspond to a higher run length, the system will expand itself on the fly by adding in new states. So, as we previously argued, we initially do not specify the number of states in KSS-HMM. By applying this method on training observation sequences, we will get the desired state sequence.

Having observation and state sequences, we will calculate the optimum λ applying BWA with a known state sequence [110]. In KSS-HMM, the π value for states zero and one is equal to $\frac{1}{2}$ and for all other states is zero. Moreover, $M = 2$ and $J = q + p + 1$ where q and p are shown in Fig.5.1, and they represent the maximum run-length of negative and positive states respectively. When all of the paths are known, then it is possible to count the number of times that each particular transition is visited in a set of training data. It has been proven in [110], that counting functions, say $\Phi_{ij}(\mathbf{x}_T)$ for the state transition and $\Phi_{mj}(\mathbf{y}_T)$, for the output observations provide maximum likelihood estimates for the desired model parameters, and they are given by

$$\hat{a}_{mj} = \frac{\Phi_{ij}(\mathbf{x}_T)}{\sum_j \Phi_{ij}(\mathbf{x}_T)} \tag{5.3}$$

$$\hat{b}_{nj} = \frac{\Phi_{mj}(\mathbf{y}_T)}{\sum_j \Phi_{mj}(\mathbf{y}_T)}, \tag{5.4}$$

where $\Phi_{ij}(\mathbf{x}_T)$ counts the number of transitions from state i to state j in the states sequence with length of T, and $\Phi_{mj}(\mathbf{y}_T)$ counts the number of observing m at state j. The basis of the proposed HMM is therefore to account for the probabilities of occurrence of different run-lengths of ones (or zeros). Clearly, the number of states J depends on how long the algorithm is trained, and hence will also affect the accuracy of the training. Although a disadvantage of the algorithm is that we had to deal with a situation where the number of states dynamically grows during the training, there is a nice property about the transition and emission matrices

in this model. Since the HMM adopted in the algorithm has only two possible transitions from one state, we therefore expect that transition matrix ($\mathbf{A}$) is a sparse matrix. It is not difficult to figure out that the non-zero elements in $\mathbf{A}$ are actually identical to the elements in the emission matrix ($\mathbf{B}$). In the following, we shall see this simplifies the prediction process, and enables corrective action to be taken if a prediction is in error.

The proposed method is given in the function block diagram which is shown in Fig.5.2. The HMM is trained with a certain number of observations. After training, the HMM only needs the current observation to predict the next channel state. This is in contrast with USS-HMM, where there is a need to use a sequence of observations to iteratively compute the next prediction. In our algorithm, the re-training is needed only if the channel statistics change.

The transition probability between any two states is denoted by

$$a_{ij} = Pr(x(t) = s_i | x(t-1) = s_j), \tag{5.5}$$

where s_i and s_j are the states at time t and $t-1$, respectively, and a_{ij} denotes the transition probability which is the (i, j) element of the matrix $\mathbf{A}$.

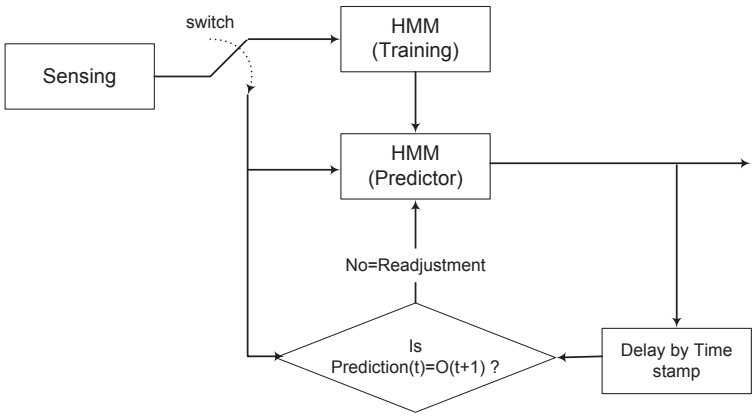

Figure 5.2: The proposed HMM system model

During the learning or training process, the computation of transition and emission probability over T observations can be easily calculated by (5.3) and (5.4). As there are only two possible observation states, the HMM is designed in a way that only two states are reachable from the current state. Moreover the probability of transition from the current state to either of the two states is equal to the probability of observing either a zero or a one. Thus, having knowledge of the emission matrix ($\mathbf{B}$) means that we have knowledge of the probability of the next state as well as the distribution of observations,

$$\begin{cases} b_{1,i} = a_{i,i+1}, b_{0,i} = a_{i,0} & i > 0 \\ b_{0,i} = a_{i,i-1}, b_{1,i} = a_{i,1} & i \leq 0. \end{cases} \tag{5.6}$$

This property makes the states sequence trackable. With this property, the proposed method does not need to compute the maximum likelihood over a long sequence of observations for each prediction.

A minimum separation factor ($0 \leq \delta < 1$) can be added to the decision criterion, so it will look like:

$$P(S(t), 0|\lambda) - P(S(t), 1|\lambda) > \delta \tag{5.7}$$

If (5.7) is satisfied, the CR will sense the subcarrier and in case of correct prediction, it will transmit its data over the subcarrier. On the other hand, if (5.7) is not satisfied, the CR will decide that the subcarrier is occupied on $t+1$. It is obvious that if $\delta = 0$, (5.7) will act as same as (5.2). In case, if we have an incorrect prediction, the observation gives us to the correct state. Therefore, the correct current state would be known at each state, and (5.7) will be computed with correct inputs for next time slot.

The purpose of prediction is to prioritize the subcarriers to be sensed, and

before the CR transmits, the sensing is still needed. This provides feedback to the predictor. In the case in which the prediction is wrong, our algorithm can make corrective action by changing its current state for the next prediction.

5.2 Simulation results

This section presents some simulation results of KSS-HMM and USS-HMM.

5.2.1 Accuracy of channel prediction

To evaluate the prediction accuracy by simulation, the statistics of PU activities on each subcarrier are assumed to remain unchanged over the simulation period. A subcarrier with Poisson arrival and Geometric ON duration is considered. We compute the average traffic intensity (γ) by

$$\gamma = \frac{\text{Mean ON Time}}{\text{Mean Arrival Time}}. \tag{5.8}$$

We also assume that the average traffic intensity (γ) is equal to 0.5, which means that the means of the ON period and the OFF period are considered equal. Moreover, we set $\delta = 0$ for our current simulations.

Initially, we investigate the importance of training sequence length on the prediction accuracy. As KSS-HMM is trained offline, the prediction accuracy will be tested on both training and test data sets. Training data are the data that KSS-HMM is created based on (the training phase in Fig.5.2). In other words, we use the training data to create KSS-HMM, and then, we compute the prediction accuracy of KSS-HMM for them. The test data are the new data that KSS-HMM has not seen before. On the other hand, USS-HMM must be trained online, so the

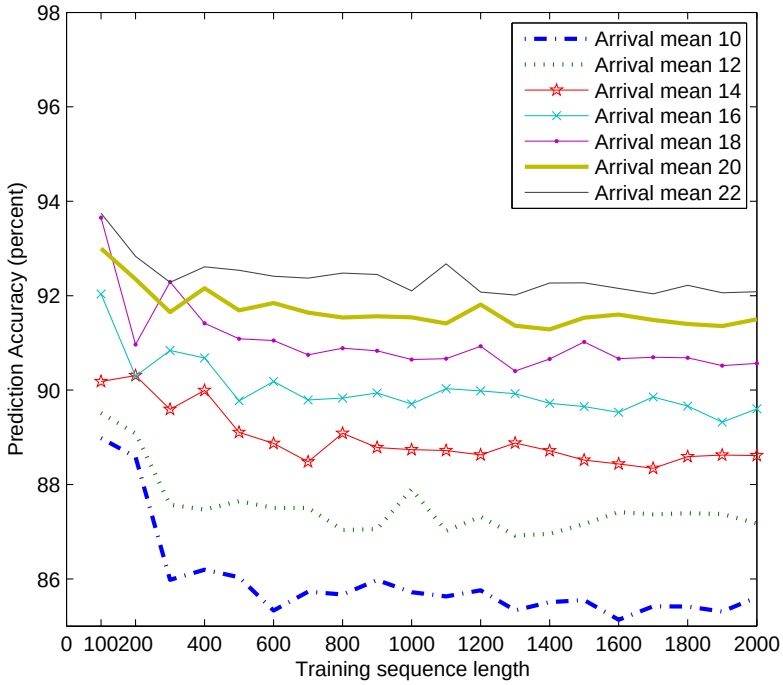

Figure 5.3: KSS-HMM prediction accuracy on training data set

training and test data are not separated.

Fig.5.3 and Fig.5.4 show the KSS-HMM prediction accuracy on training and test data for different mean arrival (Poisson) values, respectively. The prediction accuracy is given by

$$accuracy = \frac{\text{Correctly predicted}}{\text{Total predictions}} \tag{5.9}$$

It is visible that as the training sequence length increases, the prediction accuracy of training and test data are becoming closer to each other. On the other hand, for shorter sequence lengths, we see the high prediction accuracy on training data and low accuracy for test data (especially when the training sequence length is 100), which shows KSS-HMM is overfitted to the training data. In the above simulation the test set has 10000 time slots.

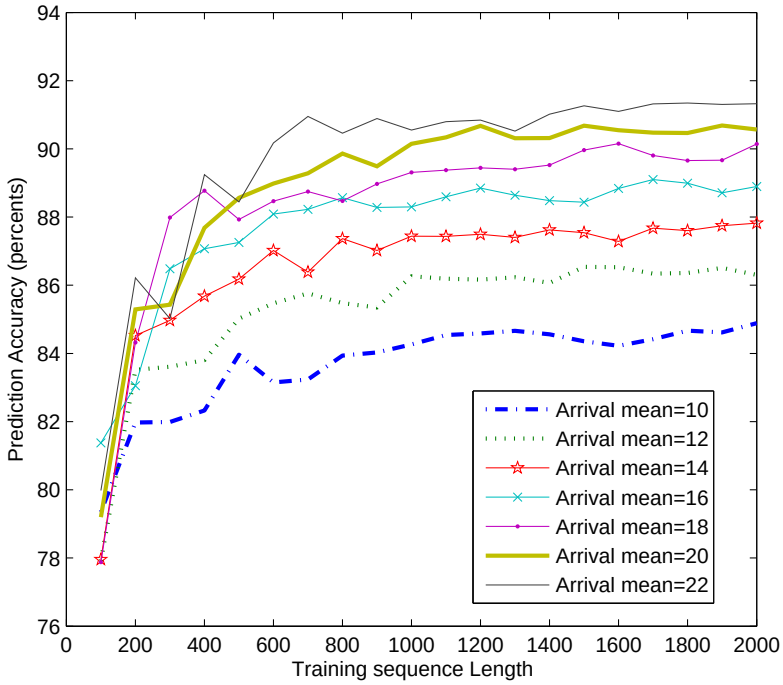

Figure 5.4: KSS-HMM prediction accuracy on test data set

Table 5.1: USS-HMM channel prediction accuracy with different number of states for different mean values of arrivals

Number of states	Arrival mean						
	10	12	14	16	18	20	22
2	0.8426	0.7140	0.8752	0.8968	0.6644	0.7828	0.9172
3	0.8422	0.8622	0.8768	0.8966	0.9014	0.9136	0.9184
4	0.8438	0.8610	0.8760	0.8952	0.9002	0.9080	0.9184
5	0.8406	0.8616	0.8710	0.8918	0.9018	0.9116	0.9186
6	0.8426	0.8606	0.8758	0.8934	0.8996	0.9132	0.9180
7	0.8408	0.8564	0.8680	0.8946	0.8986	0.9100	0.9170
8	0.8308	0.8546	0.8728	0.8904	0.8998	0.9096	0.9174
9	0.8306	0.8578	0.8690	0.8932	0.8996	0.9112	0.9146
10	0.8306	0.8516	0.8668	0.8910	0.8936	0.9080	0.9164

Table 5.2: USS-HMM channel prediction accuracy with different training sequence lengths for different mean values of arrivals

Training length	Arrival mean						
	10	12	14	16	18	20	22
50	0.8338	0.8596	0.8768	0.8910	0.9004	0.9104	0.9068
80	0.8344	0.8692	0.8802	0.8940	0.9042	0.9144	0.9182
100	0.8414	0.8692	0.8808	0.8924	0.9032	0.9162	0.9196
150	0.8416	0.8710	0.8802	0.8976	0.9062	0.9164	0.9202
200	0.8448	0.8712	0.8812	0.8978	0.9066	0.7196	0.9204
400	0.8464	0.8720	0.8818	0.8978	0.9070	0.9168	0.9204
600	0.8462	0.7378	0.8820	0.8978	0.7240	0.9168	0.6830
1000	0.8464	0.8724	0.8820	0.8978	0.9070	0.9168	0.9204

For USS-HMM we need to know both the training length and the number of states. Initially, we set the training length equal to 100 samples, and test the prediction accuracy for different number of states. The length of the test sequence for online prediction of USS-HMM is 5000 samples. We train the USS-HMM over its 100 previous samples once for each prediction (online training). Table.5.1 shows the USS-HMM prediction accuracy for different numbers of states and different mean arrival times. The table shows that the increase in number of states does not necessarily lead to an increase in accuracy, hence USS-HMM with 3 states has the best performance on the average. In Table.5.2, we investigated the effect of training sequence length on prediction accuracy of 3 states USS-HMM. Table.5.2 shows that too short and too long training sequences may cause lower accuracy in predictions. Moreover, longer training sequences increase the training time which is undesirable in many cases, especially in real time channel predictions.

In Fig. 5.5, the total error percentage, the error percentage in the prediction of the idle state and the error percentage in the prediction of the busy state, are illustrated for different mean values of arrivals. P_e(busy) represents the situations that the channel is busy, but the HMM mistakenly predicted the idle state. On

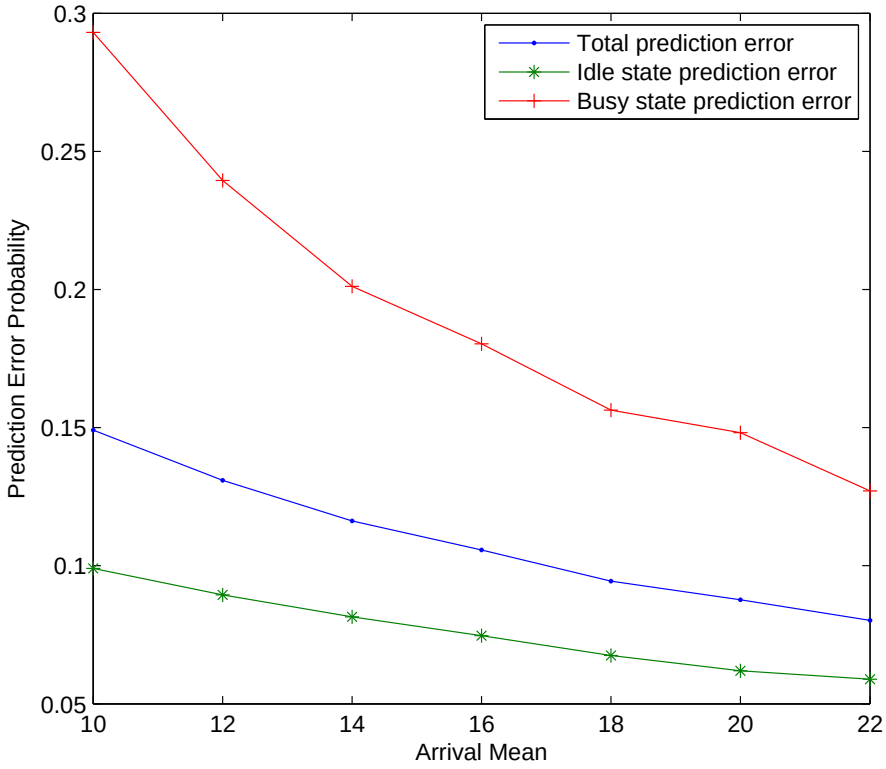

Figure 5.5: Prediction accuracy for a channel

the other hand, P_e(Idle) shows the cases that a busy state is predicted, but the actual state of the channel is idle. It is as expected that by increasing the arrival mean, the accuracy increases. In these simulations the KSS-HMM is trained with 1000 samples, and tested on the sequence of 30,000 samples.

5.2.2 Channel selection

In [50], the authors investigated the performance of their developed HMM in locating spectrum opportunities among four channels. In the considered system model, PUs activities on each channel followed a Poisson distribution with equal mean for the ON and OFF durations. We developed a similar scenario to investigate the performance of our proposed HMM. In this scenario, we trained a

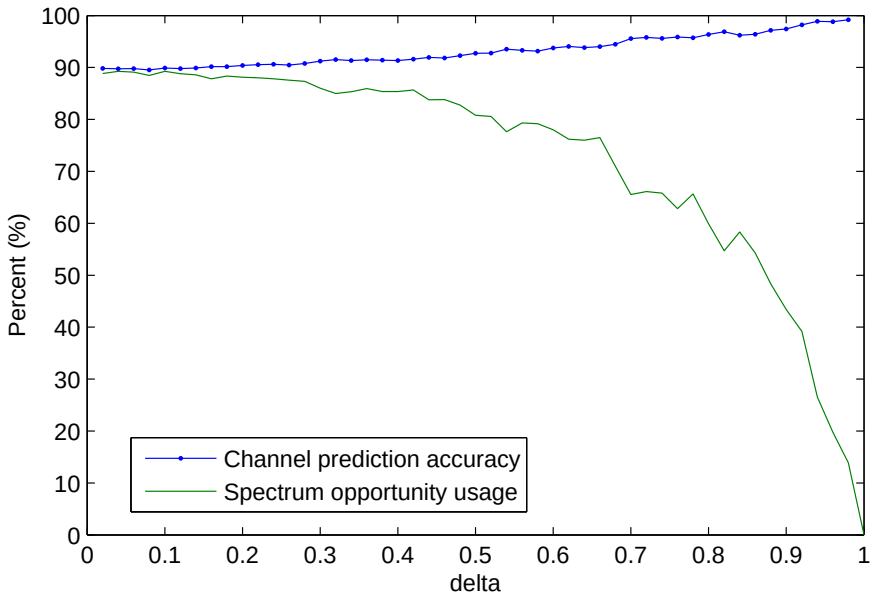

Figure 5.6: Effect of δ value on channel prediction accuracy and spectrum opportunity usage

KSS-HMM for each subcarrier with 1000 samples and tested over 30,000 samples. The effect of different values for δ on subcarrier prediction accuracy and the percentage of white spaces that are properly made use of is shown in Fig. 5.6. In this simulation, a prediction is said to be accurate if we successfully predict an empty subcarrier for transmission among the four subcarriers. As it can be seen, the increase of δ leads to an increase in accuracy, but it reduces the number of opportunities that are caught by the CR.

Another issue which must be mentioned is the acceptable accuracy of predicting an idle subcarrier in a time slot as well as taking most of the available opportunities (over 90%). Table 5.3 shows the mean of Poisson distribution for both ON and OFF periods on each subcarrier. Fig. 5.7 compares the learning based and random subcarrier selection approaches for the aforementioned scenario. As it was expected the random selection succeeds only about 50% of time, while the learning based approach succeeds in its first attempt with the probability of 0.9. In learning based approach, only less than 0.02% of attempts were not successful

Table 5.3: ON/OFF period mean values for different subcarriers

Channel	1	2	3	4
ON period mean	5	7	4	8
OFF period mean	5	7	4	8

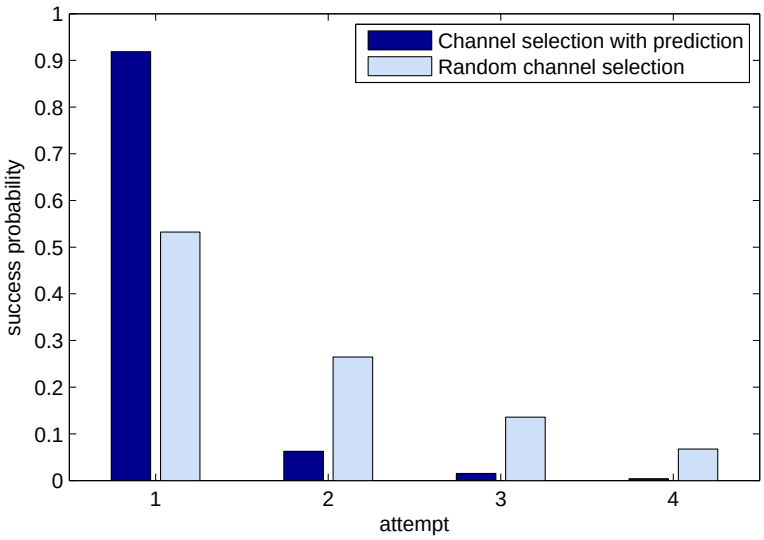

Figure 5.7: Comparison of subcarrier selection with prediction and random subcarrier selection

until sensing the last subcarrier, while about 7% of random subcarrier selection attempts were unsuccessful till the last channel is sensed.

Fig.5.8 illustrates the simulation results of the channel selection for data transmission among 4 channels based on HMM predictions for channels with the Poisson PU arrivals and Geometric distributed ON period. Channels are having the traffic intensity of 50% on average, and the mean arrival time for each of the channel 1 to 4 is 10, 14 ,18 and 22, respectively. Similar to the previous simulations, based on HMM predictions, the most probable channel to be idle is selected for sensing and data transmission. As it can be seen, both subcarrier usage and accuracy are having higher values, comparing to Fig.5.6 for lower δ values. Moreover, the increase in the accuracy and the decrease in subcarrier usage is not starting as early as in

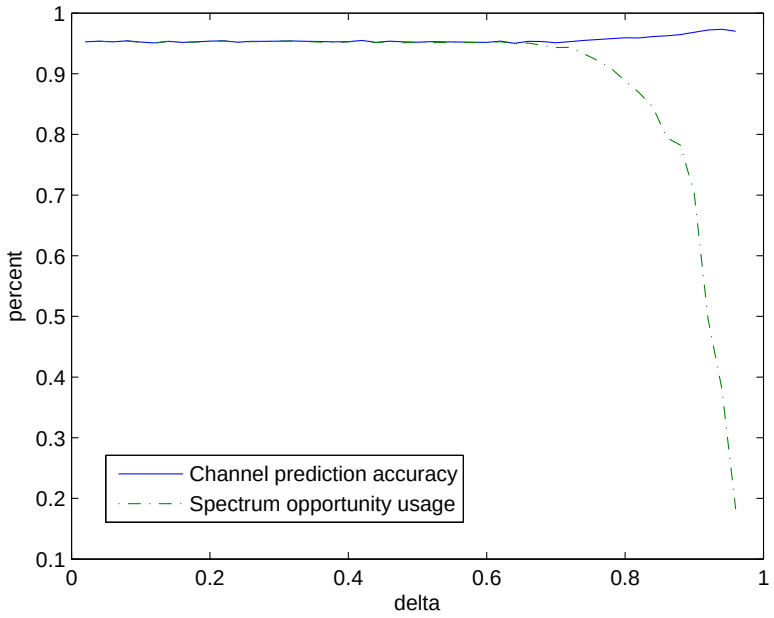

Figure 5.8: Effect of δ value on prediction accuracy and spectrum opportunity usage for Geometric On period and Poisson arrival

the case of having subcarriers with Poisson ON/OFF distributions. The difference between these two figures shows the effect of the transmitted signal statistics on its predictability.

5.2.3 Comparison on KSS-HMM and USS-HMM

The complexity of USS-HMM is higher than the complexity of KSS-HMM. KSS-HMM training complexity is $2.(T+1) \times J$ to create λ, and its decision is made by only checking either (5.2) or (5.7), where T is the training sequence length and J is the number of states. On the other hand, USS-HMM has J^2T calculations after the training [106], and it must be retrained after each prediction, while each iteration of training needs MJ^2T calculations, and it usually needs a minimum of 100 iterations to converge. M is the number of observation symbols (here $M=2$). KSS-HMM training is done once at the time and after that whenever

Table 5.4: Comparison of KSS-HMM and USS-HMM prediction accuracy for different mean values of arrivals

HMM type	Arrival mean						
	10	12	14	16	18	20	22
KSS-HMM	0.8388	0.8524	0.8830	0.8936	0.9016	0.9088	0.9192
USS-HMM	0.8478	0.8588	0.8858	0.8918	0.9076	0.9124	0.9184

it is required. The accuracy comparison of KSS-HMM and USS-HMM, over 5000 time slots is presented in Table.5.4. The KSS-HMM is trained offline over 1000 time slots, while the 3 state USS-HMM is trained online with 150 time slots. The results show that USS-HMM works slightly better on average, but there are cases that KSS-HMM has higher accuracy. However, the difference in accuracy is less than 1%, while the computation complexity of USS-HMM and KSS-HMM has a great difference.

5.3 Conclusions

In this chapter, we presented an HMM-based algorithm which can be used for channel activity prediction with a very simple prediction principle and with self-corrective capability if errors occur. We gave simulations for different scenarios. Our HMM is accurate, and the predictions can be made without the need to perform sophisticated optimization to obtain the next prediction. Furthermore, only the correct current observation is involved in the prediction. In this chapter, we extensively discussed the USS-HMM, and presented its prediction results having different numbers of states and different training lengths. Finally, it must be noted that prediction is not used to remove the need to perform channel sensing completely, but rather to produce a smart algorithm to reduce the need to sense for all subcarriers before a decision is made.

Chapter 6

Conclusions and future works

6.1 Conclusions

In this thesis, we studied optimization and learning algorithms for OFDM-based DSA. The first part of the thesis investigated the centralized DSA, and proposed efficient and low complexity optimization algorithms for it. We considered a centralized OFDM-based CR system, and formulated the joint subcarrier, power and bit assignment problem as a MINLP problem which is inherently NP-hard. To minimize the total power consumption, we fixed some parameters, and we transformed the problem into a mixed integer piecewise linear problem. The problem became easier to solve optimally. However, to perform in real time CR systems the optimization algorithm must have even less complexity, especially when the numbers of subcarriers under consideration and CR pairs are increasing. Therefore, we proposed GA and ACO heuristics, which have provided sufficiently good suboptimal solutions. Our simulations result show that ACO performs well, and reaches the global optimum in almost 70% of realizations. The proposed GA achieves acceptable results, which are not as good as ACO results. However, the

time complexity of the proposed GA is less than the proposed ACO.

Later, we extended the system model by enabling frequency reuse. In other words, the CSM is allowed to assign multiple CR pairs to any of the subcarriers. The CSM has to take into the account the interference that co-channel CRs impose on each other while assigning the subcarriers and power. We formulated the rate maximization problem of this system in the form of a MINLP problem. Then, we proposed a framework to convert this MINLP into a MBLP without making any assumption or approximation. The simulations results show that the CR system with frequency reuse outperforms the one without frequency reuse, and the difference becomes more significant when the CR pairs of the system have smaller distance between their transmitters and receivers.

In the second part of the thesis we studied auction-based and distributed DSA, and proposed learning algorithms to improve their spectrum utilization. We considered an auction-based system, where the CRs bid for the subcarriers, and the CSM assigns the subcarriers to their respective highest bid. The cost of each subcarrier in this system is the second highest bid. We formulated the auction systems with and without entry fee, and proposed DP-based and GP regressive-based learning algorithms which assist the CRs to learn their competitors bidding behaviors. By learning the bidding behavior of the other CRs, each CR is able to predict the cost of the subcarriers and improve its bidding efficiency. In the simulations results, we have shown that the CRs which are equipped with the learning algorithms achieve significantly higher capacity per unit of cost compared to the CRs which do not have any prediction of the costs.

We also considered a distributed CR system under an OSA model, where the CRs sense the subcarriers before they start the transmission. We proposed an HMM-based learning algorithm that learns the subcarrier availability pattern, and

prioritizes the subcarriers based on their probability of being unoccupied. The proposed HMM is trained offline, and then, for each prediction it only needs the subcarrier state of the last time slot. The simulations results show that it performs significantly faster than the conventional HMM while their accuracy in prediction of the white spaces is similar.

6.2 Future works

In this thesis, we proposed two evolutionary algorithms for centralized DSA. Although the proposed EAs have low complexity and achieve optimal or near optimal solutions, we believe that it is still possible to reduce the complexity or improve the optimality of the achieved results. However, it is challenging to propose heuristic algorithms that can achieve near optimal solutions for the systems with frequency reuse. We believe that for the centralized DSA problem, hybrid EAs [111] can be the desired heuristic methods. Moreover, our proposed EAs, with some modifications, can be applied to other cross-layer resource allocation problems. The linearization method that we proposed in Chapter 3, has a broad usage and can be applied to many resource allocation problems.

We presented a combination of optimization and learning in this thesis under a general auction scheme. This work has a great potential of extension in several directions. Here, we considered that all the CRs have a constant equal amount of power at each time slot. Another possible scenario will consider that the CRs are able to save their power for future use, and maintain a predefined average power consumption level. As a result, the utility maximization problem and its constraints will be different. Therefore, to be able to learn the bidding behavior of other CRs in such a system, we will have to modify the learning algorithms to

suit the new problem.

The auction mechanism in this thesis is a second-highest price auction where the winner is paying the bid value of the runner-up as the auction cost. The next step of this research will be investigating the effect of applying learning algorithms in the first price auctions [92]. In the first price auctions, the cost of each subcarrier will be equal to the winner's bid. Therefore, the learning algorithm must help the CR to maximize the difference of the subcarriers' valuation and the bid on them, while keeping the bid higher than the opponent CRs bids. This new auction mechanism also requires a well-designed combination of optimization and learning processes, which is very challenging.

Generally, the application of game and auction theory with incomplete information is very new in wireless communications. Our nonparametric learning approaches can be used in power games, SINR auctions and carrier aggregation games when all the required information are not available.

Finally, to the best of our knowledge, the effect of imperfect sensing on white space prediction has not been investigated. We need to apply Markov decision processes or dynamic programming, to address the uncertainty, and to evaluate the probability that a subcarrier is unoccupied with imperfect sensing. Investigating the prediction accuracy of the proposed HMM on real spectrum measurement data is a possible extension of this work. We can also analyze the prediction accuracy of our proposed HMM in relation with duty cycle and predictability measures like the string complexity [112].

Bibliography

[1] P. Leaves, K. Moessner, R. Tafazolli, D. Grandblaise, D. Bourse, R. Tonjes, and M. Breveglieri. Dynamic spectrum allocation in composite reconfigurable wireless networks. *IEEE Commun. Mag.*, 2004.

[2] Cisco Systems. Inc. Cisco Visual Networking Index: Global Mobile Data Traffic Forecast Update, 2011-2016. Feb 2012.

[3] F.C.C.S.P.T. Force. Report of the spectrum efficiency working group. *Tech. Report Federal Commun. Commision*, pages 02–155, 2002.

[4] M. Wellens and P. Mähönen. Lessons learned from an extensive spectrum occupancy measurement campaign and a stochastic duty cycle model. *Mobile Netw. App.*, 15(3):461–474, 2010.

[5] D. Chen, S. Yin, Q. Zhang, M. Liu, and S. Li. Mining spectrum usage data: a large-scale spectrum measurement study. In *ACM conf. on Mobile comput. netw.*, pages 13–24, 2009.

[6] M.H. Islam, C.L. Koh, S.W. Oh, X. Qing, Y.Y. Lai, C. Wang, Y.C. Liang, B.E. Toh, F. Chin, G.L. Tan, et al. Spectrum survey in singapore: Occupancy measurements and analyses. In *IEEE CrownCom'08*, pages 1–7, 2008.

[7] I.F. Akyildiz, W.Y. Lee, M.C. Vuran, and S. Mohanty. NeXt genera-

tion/dynamic spectrum access/cognitive radio wireless networks: a survey. *Comput. Netw.*, 50(13):2127–2159, 2006.

[8] Qing Zhao and B.M. Sadler. A survey of dynamic spectrum access. *IEEE Signal Process. Mag.*, 2007.

[9] D.N. Hatfield and P.J. Weiser. Property rights in spectrum: Taking the next step. In *IEEE DySPAN'05*, pages 43–55, 2005.

[10] L. Xu, R. Tonjes, T. Paila, W. Hansmann, M. Frank, and M. Albrecht. Driveing to the internet: Dynamic radio for ip services in vehicular environments. In *IEEE LCN'00*, pages 281–289, 2000.

[11] J. Zhao, H. Zheng, and G.H. Yang. Distributed coordination in dynamic spectrum allocation networks. In *IEEE DySPAN'05*, pages 259–268, 2005.

[12] I. Katzela and M. Naghshineh. Channel assignment schemes for cellular mobile telecommunication systems: A comprehensive survey. *IEEE Pers. Commun.*, 3(3):10–31, 1996.

[13] W. Lehr and J. Crowcroft. Managing shared access to a spectrum commons. In *IEEE DySPAN'05*, 2005.

[14] J.M. Peha. Approaches to spectrum sharing. *IEEE Commun. Mag.*, 2005.

[15] M. Cooper. The economics of collaborative production in the spectrum commons. In *IEEE DySPAN'05*, 2005.

[16] O. Ileri, D. Samardzija, and N.B. Mandayam. Demand responsive pricing and competitive spectrum allocation via a spectrum server. In *IEEE DySPAN'05*, 2005.

[17] R. Etkin, A. Parekh, and D. Tse. Spectrum sharing for unlicensed bands. *IEEE J. Sel. Areas Commun.*, 2007.

[18] Aamir Ghasemi and Elvino S. Sousa. Spectrum sensing in cognitive radio networks: requirements, challenges and design trade-offs. *IEEE Commun. Mag.*, 2008.

[19] Ying-Chang Liang, Yonghong Zeng, E.C.Y. Peh, and Anh Tuan Hoang. Sensing-throughput tradeoff for cognitive radio networks. *IEEE Trans. Wireless Commun.*, 2008.

[20] Z. Han, R. Fan, and H. Jiang. Replacement of spectrum sensing in cognitive radio. *IEEE Trans. Wireless Commun.*, 8(6):2819–2826, 2009.

[21] G. Salami, O. Durowoju, A. Attar, O. Holland, R. Tafazolli, and H. Aghvami. A comparison between the centralized and distributed approaches for spectrum management. *IEEE Commun. Surveys & Tuts. J.*, (99):1–17, 2010.

[22] IEEE 802.22. Working group on wireless regional area networks (wran).

[23] S. Haykin. Cognitive radio: brain-empowered wireless communications. *IEEE J. Sel. Areas Commun*, 23(2):201–220, 2005.

[24] III Mitola, J. and Jr. Maguire, G.Q. Cognitive radio: making software radios more personal. *IEEE Pers. Commun.*, 1999.

[25] R.W. Thomas, L.A. DaSilva, and A.B. MacKenzie. Cognitive networks. In *IEEE DySPAN'05*, 2005.

[26] K.C. Chen, Y.J. Peng, N. Prasad, Y.C. Liang, and S. Sun. Cognitive radio network architecture: part i–general structure. In *ACM Conf. Ubiquitous information management and commun.*, pages 114–119, 2008.

[27] T. Hwang, C. Yang, G. Wu, S. Li, and G. Ye Li. OFDM and its wireless applications: a survey. *IEEE Trans. Vehicular Tech.*, 58(4):1673–1694, 2009.

[28] E. Dahlman. *3G evolution: HSPA and LTE for mobile broadband*. Academic Press, 2008.

[29] H. Mahmoud, T. Yucek, and H. Arslan. OFDM for cognitive radio: merits and challenges. *IEEE Wireless Commun.*, 2009.

[30] J.G. Proakis. Digital communications. 1995.

[31] Yonghong Zhang and C. Leung. Resource allocation in an OFDM-based cognitive radio system. *IEEE Trans. Commun.*, 2009.

[32] C. Lacatus, D. Akopian, P. Yaddanapudi, and M. Shadaram. Flexible spectrum and power allocation for OFDM unlicensed wireless systems. *IEEE Systems J.*, 2009.

[33] Tao Qin and C. Leung. A cost minimization algorithm for a multiuser OFDM cognitive radio system. In *IEEE PacRim'07.*, 2007.

[34] Yao Ma, Dong In Kim, and Zhiqiang Wu. Optimization of ofdma-based cellular cognitive radio networks. *IEEE Trans. Commun.*, 2010.

[35] Jiho Jang and Kwang Bok Lee. Transmit power adaptation for multiuser OFDM systems. *IEEE J. Sel. Areas Commun.*, 2003.

[36] Zukang Shen, J.G. Andrews, and B.L. Evans. Optimal power allocation in multiuser ofdm systems. In *IEEE GLOBECOM '03*, volume 1, pages 337 – 341 Vol.1, dec. 2003.

[37] T.M. Cover and J.A. Thomas. *Elements of information theory*, volume 6. Wiley Online Library, 1991.

[38] Bo Liu, Mingyan Jiang, and Dongfeng Yuan. Adaptive resource allocation in multiuser OFDM system based on genetic algorithm. In *CMC'09*, 2009.

[39] Yenumula B. Reddy and Nandigam Gajendar. Evolutionary approach for efficient resource allocation in multi-user OFDM systems. *J. of Commun.*, 2007.

[40] C. Mohanram and S. Bhashyam. A sub-optimal joint subcarrier and power allocation algorithm for multiuser ofdm. *IEEE Commun. Lett.*, 9(8):685 – 687, aug. 2005.

[41] Zhenyu Liang, Yong Huat Chew, and Chi Chung Ko. A linear programming solution to subcarrier, bit and power allocation for multicell ofdma systems. In *IEEE WCNC'08*, 2008.

[42] G. Iosifidis and I. Koutsopoulos. Challenges in auction theory driven spectrum management. *IEEE Commun. Mag.*, 49(8):128–135, 2011.

[43] Fangwen Fu and M. van der Schaar. Learning to compete for resources in wireless stochastic games. *IEEE Trans. Vehicular Tech.*, 2009.

[44] Mikko A. Uusitalo Kimmo Berg and Carl Wijting. Spectrum access models and auction mechanisms. In *IEEE DySPAN'12*, 2012.

[45] K. Akkarajitsakul, E. Hossain, and D. Niyato. Distributed resource allocation in wireless networks under uncertainty and application of bayesian game. *IEEE Commun. Mag.*, 49(8):120–127, 2011.

[46] L. Rose, S. Lasaulce, S.M. Perlaza, and M. Debbah. Learning equilibria with partial information in decentralized wireless networks. *IEEE Commun. Mag.*, 49(8):136–142, 2011.

[47] R.S. Sutton and A.G. Barto. *Reinforcement learning: An introduction*, volume 1. Cambridge Univ Press, 1998.

[48] M. Zinkevich, M. Johanson, M. Bowling, and C. Piccione. Regret minimization in games with incomplete information. *Adv. Neural Inform. Process. Syst.*, 20:1729–1736, 2008.

[49] S. Lasaulce, M. Debbah, and E. Altman. Methodologies for analyzing equilibria in wireless games. *IEEE Signal Process. Mag.*, 26(5):41–52, 2009.

[50] I.A. Akbar and W.H. Tranter. Dynamic spectrum allocation in cognitive radio using hidden markov models: Poisson distributed case. In *IEEE SoutheastCon.'07*, 2007.

[51] Chengqi Song and Qian Zhang. Intelligent dynamic spectrum access assisted by channel usage prediction. In *IEEE INFOCOM'10*, 2010.

[52] Kae Won Choi, E. Hossain, and Dong In Kim. Downlink subchannel and power allocation in multi-cell ofdma cognitive radio networks. *IEEE Trans. Wireless Commun.*, 2011.

[53] H. Ahmadi, Y. H. Chew, and C. C. Chai. Multicell multiuser ofdma dynamic resource allocation using ant colony optimization. In *IEEE VTC'11-Spring*, pages 1–5. IEEE, 2011.

[54] I. Macaluso, T.K. Forde, L. DaSilva, and L. Doyle. Impact of cognitive radio: Recognition and informed exploitation of grey spectrum opportunities. *IEEE Vehicular Tech. Mag.*, 7(2):85 –90, june 2012.

[55] S. Chieochan and E. Hossain. Adaptive radio resource allocation in OFDMA systems: a survey of the state-of-the-art approaches. *Wireless Commun. and Mobile Comput.*, 9(4):513–527, 2009.

[56] Zhenyu Liang, Yong Huat Chew, and Chi Chung Ko. A linear programming solution to the subcarrier-and-bit allocation of multiclass multiuser OFDM systems. In *IEEE VTC'07-Spring.*, 2007.

[57] Kainan Zhou and Yong Huat Chew. Heuristic algorithms to adaptive subcarrier-and-bit allocation in multiclass multiuser OFDM systems. In *IEEE VTC'06-Spring*, 2006.

[58] Cheong Yui Wong, Roger S. Cheng, Khaled Ben Letaief, and Ross D. Murch. Multiuser OFDM with adaptive subcarrier, bit, and power allocation. *IEEE J. Sel. Areas in Commun.*, 17(10), 1999.

[59] J. Liu, W. Chen, Z. Cao, and KB Letaief. Dynamic power and sub-carrier allocation for OFDMA-based wireless multicast systems. In *IEEE ICC'08*, pages 2607–2611, 2008.

[60] A. He, Kyung Kyoon Bae, T.R. Newman, J. Gaeddert, Kyouwoong Kim, R. Menon, L. Morales-Tirado, J.J. Neel, Youping Zhao, J.H. Reed, and W.H. Tranter. A survey of artificial intelligence for cognitive radios. *IEEE Trans. Vehicular Tech.*, 2010.

[61] D.T. Ngo, C. Tellambura, and H.H. Nguyen. Efficient resource allocation for ofdma multicast systems with spectrum-sharing control. *IEEE Trans. Vehicular Tech.*, 2009.

[62] N. Sharma, A. Rao, A. Dewan, and M. Safdari. Rate adaptive resource allocation for multiuser OFDM using nsga - ii. In *WCSN'08.*, 2008.

[63] P. Mitran, Long Le, C. Rosenberg, and A. Girard. Resource allocation for downlink spectrum sharing in cognitive radio networks. In *IEEE VTC'08-Fall.*, 2008.

[64] Zhijin Zhao, Zhen Peng, Shilian Zheng, and Junna Shang. Cognitive radio spectrum allocation using evolutionary algorithms. *IEEE Trans. Wireless Commun.*, 2009.

[65] M. Sahin, I. Guvenc, and H. Arslan. Opportunity detection for ofdma-based cognitive radio systems with timing misalignment. *IEEE Trans. Wireless Commun.*, 2009.

[66] Stephen Boyd and Lieven Vandenberghe. *Convex Optimization*. Cambridge University Press, 2004.

[67] Dimitris Bertsimas and John N. Tsitsiklis. *Introduction to linear optimization*. Athena Scientific, 1997.

[68] Kenneth Holmström. The TOMLAB Optimization Environment in Matlab. *Advanced Modeling and Optimization*, 1(1):47–69, 1999.

[69] Melanie Mitchell. *An Introduction to Genetic Algorithms*. The MIT press, 1998.

[70] Randy L. Haupt and Sue Ellen Haupt. *Practical Genetic Algorithms*. Wiley Interscience, 2004.

[71] J. Robinson and Y. Rahmat-Samii. Particle swarm optimization in electromagnetics. *IEEE Trans. Antennas and Propag.*, 2004.

[72] David.E Goldberg. *Genetic algorithms in search, optimization and machine learning*. Addison-Wesley, 1989.

[73] M. Dorigo, V. Maniezzo, and A. Colorni. Ant system: optimization by a colony of cooperating agents. *IEEE Trans. on Systems, Man, and Cybernt.-Part B*, 1996.

[74] M. Dorigo, M. Birattari, and T. Stutzle. Ant colony optimization. *IEEE Comput. Intel. Mag.*, 2006.

[75] P.C. Pinto, A. Giorgetti, M.Z. Win, and M. Chiani. A stochastic geometry approach to coexistence in heterogeneous wireless networks. *IEEE J. Sel. Areas Commun.*, 27(7):1268–1282, 2009.

[76] Y.S. Cho, J. Kim, W.Y. Yang, and C.G. Kang. *MIMO-OFDM wireless communications with MATLAB*. Wiley, 2010.

[77] Inhyoung Kim, In-Soon Park, and Y.H. Lee. Use of linear programming for dynamic subcarrier and bit allocation in multiuser OFDM. *IEEE Trans. Vehicular Tech.*, 2006.

[78] M.T. Jensen. Reducing the run-time complexity of multiobjective eas: The nsga-ii and other algorithms. *IEEE Trans. Evol. Comput.*, 2003.

[79] Guoqing Li and Hui Liu. Downlink radio resource allocation for multi-cell ofdma system. *IEEE Trans. Wireless Commun.*, 2006.

[80] Yu-Jung Chang, Zhifeng Tao, Jinyun Zhang, and C.-C.J. Kuo. A graph-based approach to multi-cell ofdma downlink resource allocation. In *IEEE Globcom'08*, 2008.

[81] Xin Wang and G.B. Giannakis. Resource allocation for wireless multiuser OFDM networks. *IEEE Trans. Inform. Theory*, 2011.

[82] A.G. Armada and J.M. Cioffi. Multi-user constant-energy bit loading for m-psk-modulated orthogonal frequency division multiplexing. In *IEEE WCNC'02.*, volume 2, pages 526–530. IEEE, 2002.

[83] K.W. Choi and E. Hossain. Opportunistic access to spectrum holes between packet bursts: A learning-based approach. *IEEE Trans. wireless Commun.*, 10(8):2497–2509, 2011.

[84] H. Ahmadi, Y.H. Chew, P.K. Tang, and Y.A. Nijsure. Predictive opportunistic spectrum access using learning based hidden markov models. In *IEEE PIMRC'11*, 2011.

[85] J. Unnikrishnan and V.V. Veeravalli. Algorithms for dynamic spectrum access with learning for cognitive radio. *IEEE Trans. Signal Process.*, 58(2):750–760, 2010.

[86] A.B. MacKenzie and L.A. DaSilva. Game theory for wireless engineers. *Synthesis Lectures on Communications*, 1(1):1–86, 2006.

[87] G. Iosifidis and I. Koutsopoulos. Challenges in auction theory driven spectrum management. *IEEE Commun. Mag.*, 49(8):128–135, 2011.

[88] D. Niyato, E. Hossain, and Z. Han. Dynamic spectrum access in ieee 802.22-based cognitive wireless networks: a game theoretic model for competitive spectrum bidding and pricing. *IEEE Wireless Commun.*, 16(2):16–23, 2009.

[89] J. Sun, E. Modiano, and L. Zheng. Wireless channel allocation using an auction algorithm. *IEEE J. Sel. Areas Commun.*, 24(5):1085–1096, 2006.

[90] X. Wang, Z. Li, P. Xu, Y. Xu, X. Gao, and H.H. Chen. Spectrum sharing in cognitive radio networks-an auction-based approach. *IEEE Trans. Systems, Man, and Cybernetics, Part-B*, 40(3):587–596, 2010.

[91] J. Bae, E. Beigman, R. Berry, M. Honig, and R. Vohra. Sequential bandwidth and power auctions for distributed spectrum sharing. *IEEE J. Sel. Areas Commun.*, 26(7):1193–1203, 2008.

[92] B. Eraslan, D. Gözüpek, and F. Alagöz. An auction theory based algorithm for throughput maximizing scheduling in centralized cognitive radio networks. *IEEE Commun. Lett.*, 15(7), 2011.

[93] Z. Han, R. Zheng, and H.V. Poor. Repeated auctions with bayesian nonparametric learning for spectrum access in cognitive radio networks. *IEEE Trans. Wireless Commun.*, 10(3):890–900, 2011.

[94] Paul Klemperer. Auction theory: A guide to the literature. *J. Economic Surveys*, 1999.

[95] A. Danak and S. Mannor. A robust learning approach to repeated auctions with monitoring and entry fees. *IEEE Trans. Comput. Intel. AI Games*, (99):1–1, 2011.

[96] Y. W. Teh. Dirichlet processes. In *Encyclopedia of Machine Learning*. Springer, 2010.

[97] D.J.C. MacKay. Introduction to gaussian processes. *NATO ASI Series For Computer and Systems Sciences*, 168:133–166, 1998.

[98] CKI Williams and CE Rasmussen. *Gaussian processes for machine learning*. MIT Press, 2006.

[99] C. Rasmussen. Gaussian processes in machine learning. *Advanced Lectures on Machine Learning*, pages 63–71, 2004.

[100] Guangxiang Yuan, R.C. Grammenos, Yang Yang, and Wenbo Wang. Performance analysis of selective opportunistic spectrum access with traffic prediction. *IEEE Trans. Vehicular Tech.*, 2010.

[101] Chengqi Song, Dawei Chen, and Qian Zhang. Understand the predictability of wireless spectrum: A large-scale empirical study. In *IEEE ICC'10*, 2010.

[102] T. Clancy and B. Walker. Predictive dynamic spectrum access. In *SDR forum tech. conf.*, 2006.

[103] L. Rabiner and B. Juang. An introduction to hidden markov models. *IEEE ASSP Mag.*, 1986.

[104] C. Clancy, J. Hecker, E. Stuntebeck, and T. O'Shea. Applications of machine learning to cognitive radio networks. *IEEE Wireless Commun.*, 2007.

[105] V.K. Tumuluru, Ping Wang, and D. Niyato. A neural network based spectrum prediction scheme for cognitive radio. In *IEEE ICC'10*, 2010.

[106] V.K. Tumuluru, P. Wang, and D. Niyato. Channel status prediction for cognitive radio networks. *Wireless Commun. and Mobile Comput.*

[107] S. Yin, D. Chen, Q. Zhang, and S. Li. Prediction-based throughput optimization for dynamic spectrum access. *IEEE Trans. Vehicular Tech.*, 2010.

[108] M. Hoyhtya, S. Pollin, and A. Mammela. Classification-based predictive channel selection for cognitive radios. In *IEEE ICC'10*, 2010.

[109] M.J. Beal, Z. Ghahramani, and C.E. Rasmussen. The infinite hidden markov model. *Advances in neural information process. systems*, 1:577–584, 2002.

[110] J.V. Candy. *Bayesian signal processing: classical, modern, and particle filtering methods*. Wiley-Interscience, 2009.

[111] Y. Wang, Z. Cai, G. Guo, and Y. Zhou. Multiobjective optimization and hybrid evolutionary algorithm to solve constrained optimization problems. *IEEE Trans. Systems, Man, and Cybernetics, Part-B*, 37(3):560–575, 2007.

[112] A. Lempel and J. Ziv. On the complexity of finite sequences. *IEEE Trans. Inform. Theory*, 22(1):75–81, 1976.

List of publications

Here, we summarized the list of publications. The content of Chapter 2 covers the following four papers:

(1) Ahmadi H, Chew Y. H, Evolutionary Algorithms for Orthogonal Frequency Division Muntiplexing-based Dynamic Spectrum Access Systems, *Accepted to be published in Computer Networks.*

(2) Ahmadi H, Chew Y.H, Adaptive Subcarrier-and-Bit Allocation in Multiclass Multiuser OFDM Systems using Genetic Algorithm, *IEEE PIMRC'09, Tokyo, Japan, September 2009.*

(3) Ahmadi H, Chew Y.H, Subcarrier-and-Bit Allocation in Multiclass Multiuser Single-cell OFDMA Systems Using an Ant Colony Optimization based Evolutionary Algorithm, *IEEE WCNC'10, Sydney Australia, April 2010.*

(4) Ahmadi H, Chew Y. H, Arvaneh M, Performance Comparison of Two Evolutionary Algorithms and the Piecewise Linear Optimum Solution of Downlink Multi-service Single-cell OFDMA Systems, *IEEE APWCS'10, May 2010. Kaohsiung. Taiwan.*

The content of Chapter 3 contain the following three papers:

(1) Ahmadi H, Chew Y. H, Chai C. C, A Framework to Optimize OFDM-based Multiuser Dynamic Spectrum Access Networks with Frequency Reuse, *Accepted to be published in Wireless Personal Communications.*

(2) Ahmadi H, Chew Y. H, Chai C. C, Multicell Multiuser OFDMA Dynamic Resource Allocation Using Ant Colony Optimization, *IEEE VTC'11-Spring, May 2011, Budapest, Hungary.*

(3) Ahmadi H, Chew Y. H, Chai C. C, Genetic Algorithm Approach for Dynamic Resource Allocation in Multicell OFDMA Networks, *IEEE APWCS'11, August 2011. Singapore.*

The contents of Chapters 4 and 5 cover the following papers:

(1) Ahmadi H, Chew Y. H, Reyhani N, Chai C. C, Nonparametric learning for auction-based dynamic spectrum access in multicarrier systems, *submitted to IEEE Journal on Selected Areas in Communications.*

(2) Ahmadi H, Chew Y. H, Tang P. K, Nijsure Y.A, Predictive Opportunistic Spectrum Access using Learning based Hidden Markov Models, *IEEE PIMRC'11, September 2011, Toronto, Canada.*